A Mathematical Study on the Emergence of Collective Differences from Individual Variation: The Complex Adaptive Dynamics of Eusocial-insect Colonies

by

Maria Gabriela Navas Zuloaga

A Dissertation Presented in Partial Fulfillment
of the Requirements for the Degree
Doctor of Philosophy

Approved November 2022 by the
Graduate Supervisory Committee:

Yun Kang, Co-Chair
Brian H. Smith, Co-Chair
Theodore P. Pavlic

ARIZONA STATE UNIVERSITY

December 2022

ABSTRACT

Variation in living systems and how it cascades across organizational levels is central to biology. To understand the constraints and amplifications of variation in collective systems, I mathematically study how group-level differences emerge from individual variation in eusocial-insect colonies, which are inherently diverse and easily observable individually and collectively. Considering collective processes in three species where increasing degrees of heterogeneity are relevant, I address how individual variation scales to colony-level variation and to what degree it is adaptive. In Chapter 2, I introduce a Markov-chain decision model for stochastic individual quorum-based recruitment decisions of rock-ant workers during house hunting, and how they determine collective speed–accuracy balance. Differences in the average threshold-dependent response characteristics of workers between colonies cause collective differences in decision-making. Moreover, noisy behavior may prevent drastic collective cascading into poor nests. In Chapter 3, I develop an ordinary differential equation (ODE) model to study how cognitive diversity among honey-bee foragers influences collective attention allocation between novel and familiar resources. Results provide a mechanistic basis for changes in foraging activity and preference with group composition. Moreover, sensitivity analysis reveals that the main individual driver for foraging allocation shifts from recruitment (communication) to persistence (independent effort) as colony composition changes. This might favor specific degrees of heterogeneity that best amplify communication in wild colonies. Lastly, in Chapter 4, I consider diversity in size, age, and task for nest defense in stingless bees. To better understand how these dimensions of diversity interact to balance defensive demands with other colony needs, I study their effect on colony size and task allocation through a demographic Filippov ODE model. Along each dimension, variation is beneficial in a certain range, outside of which colony adaptation and survival are compromised. This work elucidates how variation in

collective properties emerges from nonlinear interactions between varying components in eusocial insects, but it can be generalized to other biological systems with similar fundamental characteristics but less empirical tractability. Moreover, it has the potential of inspiring algorithms that capitalize on heterogeneity in engineered systems where simple components with limited information and no central control must solve complex tasks.

ACKNOWLEDGMENTS

My PhD position was supported by the Simon A. Levin Mathematical, Computational and Modeling Sciences Center (SAL MCMSC), the School of Human Evolution and Social Change (SHESC) and the Graduate Completion Fellowship from the Graduate College at Arizona State University. The research for Chapter 4 was partially supported by contract number W31P4Q18-C-0054 from the United States Defense Advanced Research Projects Agency (DARPA).

TABLE OF CONTENTS

CHAPTER Page

LIST OF TABLES

LIST OF FIGURES

Figure Page

Chapter 1

INTRODUCTION

1.1 Colonies as Models for Variation

All biological systems, from genes to organisms, populations and ecosystems, exhibit variation. Variation in nature underlies evolutionary change and allows biological systems to adapt and persist in dynamic environments. Therefore, understanding the drivers of variation is fundamental to study living systems. However, most biological research focuses only on the average properties of populations, thus overlooking the effects of variation (McEntire et al. 2022). Despite an increasing interest across biological disciplines in studying variation and its consequences, most research considering variation focuses on a single level of biological organization. Nonetheless, the effects of variation may cascade across scales of biological organization (Mancinelli and Lodato 2018; Lemanski et al. 2019), like genetic variation manifesting in phenotypic differences between individuals.

Given the multi-scale nature of living systems, determining the drivers of variation and how it scales across levels of organization is central to all disciplines in biology. This is especially true for collective systems where interactions between tightly interconnected heterogeneous components give rise to highly nonlinear effects at the group level, like gene regulatory networks, bacterial colonies or neural circuits. To account for these complex cascading effects, the collection of empirical data must necessarily be complemented with predictive quantitative models applicable to systems or levels that might be unfeasible to observe experimentally (McEntire et al. 2022). To this end, this Dissertation undertakes a mathematical study of how individual variation scales to collective variation using a

biological model system that, while sharing fundamental characteristics with other collective systems that are considerably difficult to manipulate, provide unique empirical tractability at both the individual and collective levels: Eusocial-insects colonies.

Suzanne Batra introduced the term 'eusocial', or truly social, in 1966 (Batra 1966) to describe the nesting behavior of certain bees. Today, the term includes all insect colonies that share three characteristics (Wilson 1971):

- Reproductive division of labor: not all individuals are reproductive.
- Overlapping generations: multiple generations live together.
- Cooperative care of juveniles: individuals care for brood that is not their own.

All ants and termites, and some species of bees and wasps, are eusocial insects. Natural selection acts on colony-level variation, since reproduction is hierarchical within groups. Thus, the phenotypes of individual insects in colonies, freed from direct selective pressures, can diverge and enable colony-level adaptive function.

Collectively, colonies acquire, store, process, and respond to environmental information (learning, memory, decision-making), and they also become familiar with, value, and interact productively with environmental features (exploring, exploiting) to meet existential needs (survival, growth) (Navas-Zuloaga, Pavlic, and Smith 2022). In neuroscience, organisms with such information-processing abilities are denoted "cognitive" (Shettleworth 2009; Mazza et al. 2018). Thus, eusocial-insect colonies may be considered "collective brains" emerging from interaction networks to process complex and dynamic environmental information (Feinerman and Korman 2017; Sasaki and Pratt 2018; Couzin 2009; Solé, Moses, and Forrest 2019). In fact, models developed to describe neural systems have been used to understand the colony dynamics of decision making (Sasaki and Pratt 2018; Sasaki, Pratt, and Kacelnik 2018; Marshall et al. 2009), foraging (Davidson et al. 2016), house-hunting (Borofsky et al. 2020), task allocation (Gordon, Goodwin, and Trainor 1992), and activity

propagation (Couzin 2009; Piñero et al. 2019). As this common framework suggests, the benefits of studying the drivers of variation in eusocial-insect colonies extend beyond these organisms to a variety of biological systems that comprise multiple units exchanging signals to collectively acquire, store, and process information (Solé, Moses, and Forrest 2019). For example, social bacteria (Dinet et al. 2021), slime molds (Vallverdú et al. 2018; Latty and Beekman 2011), or immune systems (Piñero et al. 2019; Varela et al. 1988), which have been classified as "liquid brains" because of their display of memory, search, or decision making abilities (Solé, Moses, and Forrest 2019; Moses et al. 2019). Results from eusocial insects may elucidate how variation in the collective information processing properties of these systems emerges from the nonlinear interactions between their varying components.

1.2 Mathematical Models of Eusocial-Insect Behavior at Multiple Scales

Eusocial-insect colonies, like the other collective systems mentioned above, are complex adaptive systems (Holland 2014; Mitchell 2009): The properties of their individual components in isolation cannot describe their system dynamics, which are instead a product of the non-linear interactions between units the properties that emerge from them (Solé, Moses, and Forrest 2019; Camazine et al. 2003). Thus, understanding complex biological systems requires both experimental biology, collecting measurements of system properties at different scales in controlled conditions, and theoretical and computational models that integrate these measurements into generalizable system descriptions allowing the identification of emergent patterns that might be counterintuitive to predict a priori (Navas-Zuloaga, Pavlic, and Smith 2022).

Models of eusocial-insect behavior cover a wide range of scales, from detailed brain dynamics to colony-level population dynamics. At the level neural circuits, the same neural

network models used for human brains (Abbott and Kepler 2008) can be adapted to describe sensory processing and decision making in the insect brain (Bazhenov, Huerta, and Smith 2013). These models provide insights about the neural mechanisms that drive behavioral observations. However, this level of detail is not always fundamental to answer cognitive questions or to predict behavior, which can be achieved by coarser models. For example, drift–diffusion models, where brain dynamics are aggregated into a single decision variable, are widely used for decision-making in human and non-human primates (Ratcliff et al. 2016), and similar models have been applied to describe decisions by individual insects (Pavlic et al. 2021; Robinson et al. 2011; Davidson et al. 2016). In these models, the decision variable moves between decision thresholds as the subject accumulates evidence in favor of each alternative, and a choice is made when a decision threshold is surpassed. Evidence may be sampled directly from the environment, like honey bees or rock ants that only initiate recruitment to a food source or potential nest if the quality of the site is high enough (Robinson et al. 2011; Pratt 2019). Evidence might also come from interactions with other insects, like harvester ants that start foraging only after enough encounters with other incoming foragers (Pinter-Wollman et al. 2013), or rock ants that switch from slow to fast recruitment after encountering enough nestmates evaluating a candidate nest (Pratt 2005b). Thus, not unlike neurons in brains, insects in colonies integrate a variety of sensory inputs to produce threshold-dependent signals, and individuals may differ in their thresholds and sensitivities to stimuli (Navas-Zuloaga, Pavlic, and Smith 2022).

The exchange of signals within colonies generates networks of excitatory and inhibitory interactions, which have been described through network models (Gordon, Goodwin, and Trainor 1992; Miramontes, Sole, and Goodwin 2001) or agent-based models (Guo et al. 2020; Mosqueiro et al. 2017; Pratt et al. 2005; Pavlic et al. 2021). While both approaches describe colony dynamics at similar levels, modeling the characteristics and interactions

of each individual in the group, the former incorporate no explicit representation of space, while the latter facilitate the inclusion of spatial movement when relevant.

A coarser approach to modeling colony behavior is to divide the population into compartments (e.g. workers of a specific age, task or cast Kang and Theraulaz 2016) and describe changes in the average number of individuals in each compartment through mean-field differential equations. These models generally offer analytical tractability compared to agent-based models, which are computationally expensive to implement. Foraging and house-hunting models of eusocial insects usually divide the colony into categories of workers that are recruiting to a specific food source or candidate nest, or uncommitted and available for recruitment (Marshall et al. 2009; Britton et al. 2002). Additional categories include "searching" the environment or "following" a recruiter (Camazine and Sneyd 1991; Sumpter and Pratt 2003; Pratt and Sumpter 2006). For binary decisions (e.g. between two nest candidates), mean-field models of colony-level dynamics share the structure computational neuroscience models of neural population activities in brains making two-alternative choices. In both cases, two mutually inhibiting populations (either neural populations activated by competing evidence (Usher and McClelland 2001) or groups of scouts recruiting for different nests (Britton et al. 2002)) accumulate evidence for each option over time until some threshold is reached (Marshall et al. 2009; Navas-Zuloaga, Pavlic, and Smith 2022). Thus, similar decision models may be implemented at the level of single insects, as described earlier in this section, or at the level of whole colonies as superorganismic decision-making entities (Sasaki and Pratt 2018; Sasaki, Stott, and Pratt 2019; Sasaki, Pratt, and Kacelnik 2018).

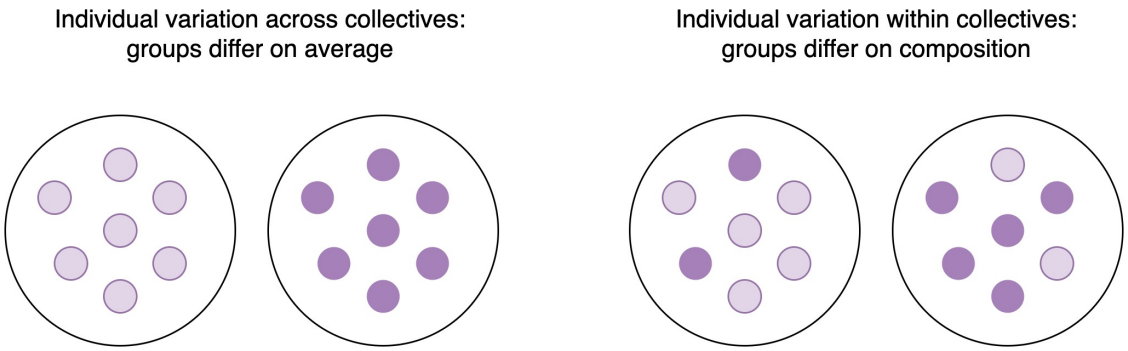

Figure 1. Variation between collectives may arise from differences in the average properties of their members (*left*) or from different mixtures of individuals belonging to different types (*right*). Taken from (Navas-Zuloaga, Pavlic, and Smith 2022), with permission.

1.3 Individual Variation

The origins of variation between colonies and the mechanisms that maintain it are at the basis of evolutionary change for eusocial insects (Pinter-Wollman 2012) because selection acts at the level of the colony. Differences in the collective properties of colonies emerge from the individual characteristics of their members in two broad ways: either the average properties of workers vary between groups (Figure 1, left), or the mixture of different types of individuals in the group (composition) changes between colonies (Figure 1, right) (Pinter-Wollman 2012; Dussutour et al. 2009).

The first case, where colonies differ because of variation in the average properties of their members, can be illustrated with two-alternative forced choice tasks in different species of ants. Studies demonstrated that certain ant species have better decision-making performance in dynamic environments than others, and this ability may arise from workers having a relatively more random behavior regarding whether or not to follow the recruitment trail (Dussutour et al. 2009). Thus, a higher level of behavioral noise in the workers of these colonies compared to others can benefit species that exploit ephemeral food sources. In

contrast, lower levels of noise are characteristic from species that exploit more permanent food sources, and that also exhibit a decreased collective decision-making performance in changing environments.

Similarly, differences in the average decision-making characteristics of rock-ant workers between colonies affects collective decision performance during house-hunting. When searching for a new nest, scouts will initiate a slow type of recruitment (tandem run) to alternatives of high enough quality. However, if a scout encounters enough nestmates evaluating a candidate nest, it switches to a fast type of recruitment (transport) (Pratt 2005b) that quickly increases the quorum in the site and triggers further transports. Thus, a colony where scouts have a very low quorum threshold to initiate transport might rush into a fast migration to a nest that has not been evaluated by enough scouts, and might therefore be a poor alternative. Evidence suggests that colonies decrease their recruitment quorum if the migration is urgent and that colonies of different species have different prioritization of speed and accuracy (Pratt 2005a; Franks et al. 2003). Thus, variation in the individual decision parameters of workers across colonies determine collective success in different environments where risks and nest availability are dynamic.

Individual variation within colonies is readily observable in terms of age, task or morphology, but also present in less evident forms, like cognitive diversity between workers. While heterogeneity might bring benefits to colonies (O'shea-Wheller et al. 2017), there are tradeoffs associated with it. For example, theoretical models show that group modularity regarding interactions, which inherently causes information loss, may improve decision accuracy in complex environments (Kao and Couzin 2019). Similarly, a model of contact-based information spread in ants shows that a well-mixed population has the best information transmission, but a heterogeneous spatial distribution prevents the transmission of pathogens and other deleterious elements (Guo et al. 2020).

Colonies with different mixtures of individuals differ in their collective properties. In honey bees, there is cognitive diversity between workers in the form of "high-attention" and "low-attention" profiles (Smith and Cook 2020). Colony composition regarding the relative presence of these cognitive phenotypes affects group-level attention patterns (i.e. allocation of foragers across potential food sources) (Lemanski et al. 2019). In fact, prevalently low-attention colonies dedicate equal attention to novel and familiar sources, while colonies with more high-attention foragers preferentially exploit familiar sources (Cook et al. 2020). Thus, group composition shifts the balance between collective exploration (attention distributed over multiple sources) and exploitation (foraging form a single source), which determines foraging success in different environments.

While cognitive diversity is one possible dimension of heterogeneity, group composition may vary in multiple dimensions. The allocation of workers to defense in stingless bees provides an example of how multiple dimensions of diversity within a colony can shape collective adaptation to the environment. Some species of stingless bees produce a minority of large-bodied workers (*majors*) that are more efficient at nest defense than their smaller nestmates (*minors*) but also require more resources (Grüter et al. 2012; Jones et al. 2012; Zweden et al. 2011). The size of new workers depends on the amount of food that they receive as brood (Segers et al. 2015), so the proportion of majors in the colony can be regulated by the nurse bees. In fact, colonies exposed to a higher frequency of threats produce a larger proportion of majors (Segers, Zuben, and Grüter 2016). While the size of majors remains fixed through their lifetime, they exhibit some degree of behavioral flexibility: they perform mostly nest maintenance and brood care for the first part of their lives and then transition to guarding tasks as older bees (about two weeks old). However, crisis situations require a response within minutes. This need is addressed by minors rapidly switching from their regular foraging tasks to guarding positions that they would not

take under regular circumstances. Thus, heterogeneity over the timescales of reproduction (morphological specialization), development (maturation of majors into guards) and behavior (task switching by minors) all contribute to collective defense against threats, and variation in group composition along any of those dimensions affects colony survival in a dynamic environment.

1.4 Document Structure

Understanding the causes and consequences of variation within and between living systems is central to biology because variation (1) is ubiquitous across biological disciplines; (2) drives evolutionary change; (3) allows acclimation to dynamic environmental conditions; and (4) may cascade across levels of biological organization (McEntire et al. 2022). The degree to which heterogeneity is adaptive in a system can control how variation scales from individuals to collectives and quantitative models are a valuable tool to study how much variation a system requires or can tolerate (Scheiner and Holt 2012; Mosqueiro et al. 2017). In this Dissertation, I present a mathematical approach for understanding the constraints and amplifications of variation in collective systems as it cascades across organizational levels. Specifically, I model how collective differences emerge from variation at the individual level in eusocial-insect colonies, which are ideal biological model systems because they (1) exhibit high inherent diversity between workers and (2) can be easily observed and manipulated at the individual and colony levels. In the following chapters, I model the behavior of three species of eusocial insects as they engage in different collective processes where increasing degrees of heterogeneity are relevant (see Figure 2). For each case, I address the following questions:

- How does colony-level variation emerge from individual variation?

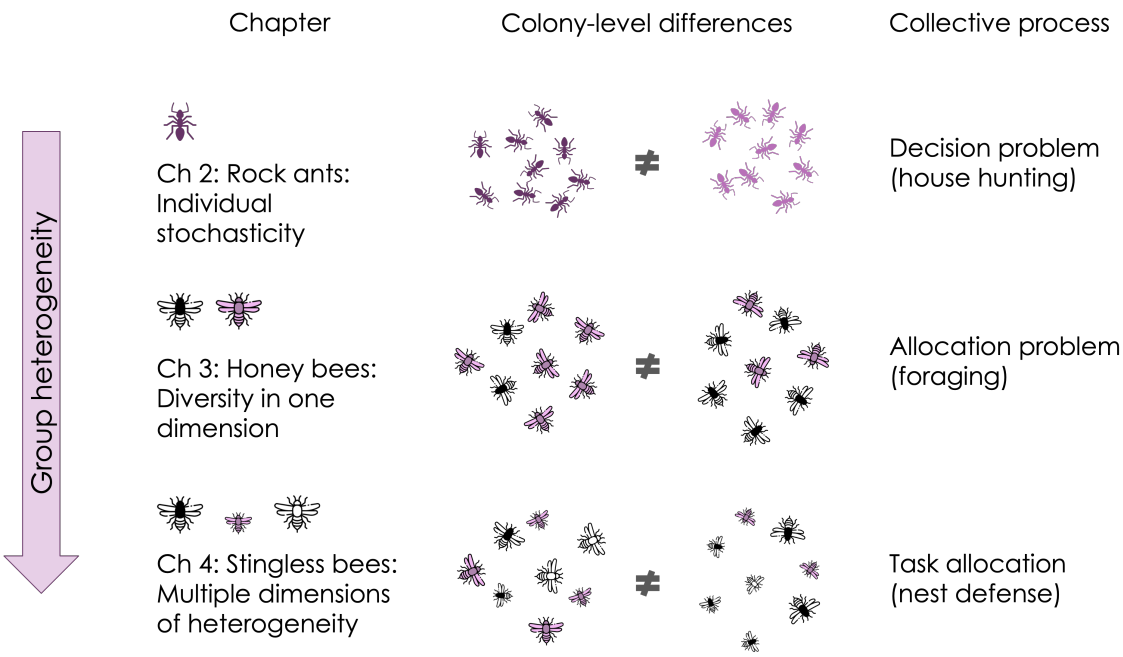

Figure 2. Document structure: This work comprises three projects where increasing levels of heterogeneity are relevant. Chapter 2 illustrates how, during house-hunting in rock ants, differences in the average threshold-dependent response characteristics of workers between colonies cause collective differences in decision-making. In Chapter 3, the mixture of cognitive phenotypes in honey bee colonies affects collective attention allocation between novel and familiar resources. In Chapter 4, multiple dimensions of group heterogeneity in stingless-bee colonies have collective impacts on task allocation and colony survival.

- To what degree is individual variation adaptive for the colony?

Chapter 2 regards collective decision-making during house-hunting in rock ants where, despite low within-group heterogeneity, differences in the average threshold-dependent response characteristics of workers between colonies cause collective differences in decision-making. In *Temnothorax* ants, colony migration to the best available nest relies on scouts switching between recruitment behaviors based on the number of nestmates encountered in a candidate site. How scouts sense quorum attainment and what determines when they stop acquiring encounter information remains unclear. Phenomenological drift–diffusion models from cognitive psychology are a good qualitative match to ant dynamics, but these

models also predict unbounded decision latency when evidence is ambiguous. Furthermore, these models do not explicitly incorporate the discrete encounter events experienced by ants and instead assume information arrives continuously over time. I propose a more mathematically tractable finite-state model of evidence accumulation by a mobile ant that explicitly accounts for discrete ant-to-ant interactions and predicts finite deliberation times. This approach provides a new lens for examining how cognitive processes in ants under different conditions balance speed and accuracy at the individual and collective levels.

In Chapter 3, I study how group composition in regard to cognitive phenotypes in honey bee colonies affects collective attention allocation between novel and familiar resources. Recent studies have shown that discrete heritable attention phenotypes in individual honey-bee foragers drive their foraging decisions, thus affecting colony fitness. In particular, individual and collective preference for familiar or novel resources is dependent on the relative presence of high and low attention individuals in the colony. Previous models of honey-bee foraging have not included this phenotype-dependent preference. In order to understand how colony-level preferential exploitation of novel and familiar resources emerges from the interaction of individuals with different preferences and behavioral tendencies, I develop an ordinary differential equation model of self-organized foraging based on the two different phenotypes found among honey-bee foragers and identify the individual processes that have the most impact on collective preference. Thus, the model can guide future experiments focusing on the collective implications of heterogeneity in social insect colonies by determining the individual behaviors that most heavily impact collective decisions in the context of group diversity.

In Chapter 4, I consider group heterogeneity in multiple dimensions using stingless bees as model organisms in the context of nest defense allocation. For these colonies, several layers of worker diversity have collective consequences for labor division that determine

colony survival and adaptation in dynamic environments. *Tetragonisca angustula* stingless bees employ a combination of defensive strategies found across other social insects and colonial animals: 1) morphological specialization (distinct soldiers (majors) are produced over weeks); 2) age-based polyethism (young majors transition to guarding tasks over days); and 3) task switching (small workers (minors) replace soldiers within minutes under crisis). To better understand how these timescales of reproduction, development, and behavior integrate to balance defensive demands with other colony needs, I developed a demographic model using a Filippov ODE system to study the effect of these processes on task allocation and colony size. This work elucidates the demographic factors constraining collective defense regulation in social insects while also suggesting new explanations for variation at different timescales in the defensive dynamics of other biological systems that are more difficult to observe.

Chapter 2

A MODEL FOR ANT QUORUM SENSING WITH BOUNDED LATENCY FOR HARD DECISIONS

2.1 Introduction

Collective decision making is a process that involves information processing acting at multiple scales. In the brain, decisions emerge from local interactions inside large populations of excitable neurons, which in turn are highly complex cells, sensitive to the concentrations of a range of neurotransmitters and their molecular dynamics. Other systems that function as collectives, such as insect societies, also rely on local interactions between group members—with their own complex intrinsic dynamics—to produce decentralized group decisions where no individual needs global information (Camazine et al. 2003). In all cases, adaptive properties observable at the level of the collective emerge from the non-trivial interactions of individuals in the group. Thus, understanding these complex group-level properties requires a study of both the networks of interacting individuals as well as the dynamics of the individuals themselves. However, scaling detailed models of complex individual behaviors to models of group-level behavior often becomes mathematically or computationally intractable as the group size increases (Dada and Mendes 2011; Chopard et al. 2018). Thus, the study of how cognition emerges from collectives benefits from simplified, coarse-grained models of individual behavior (such as models of neurons as binary elements in neural networks) that allow the exploration of richer dynamics at higher levels of integration.

In the context of analyzing how individual decisions scale up to group-level decisions,

social insects lend themselves as an ideal model organism for collective cognition. They process information and act accordingly as a group relying only on the interactions between partially informed individuals (Sasaki and Pratt 2018; Marshall et al. 2009). Moreover, ants are known to exhibit neuron-like excitable dynamics, in the sense that their probability of engaging in an activity increases through accumulated contacts with other ants (Pinter-Wollman et al. 2013; Pratt 2005b; Davidson et al. 2016) like the probability of a neuron firing increasing with excitatory synaptic inputs. However, the relatively low level of integration of colonies compared to brains (Sasaki and Pratt 2018) makes the observation of individual components much easier in the former. Thus, ants provide a tractable model system for studying how complex individual-level dynamics couple to generate cognition at higher levels of organization. This paper focuses on better understanding how collective cognition in ants could be built from excitable dynamics of individual ants akin to excitable neurons in the brain.

House hunting is a well-studied instance of collective decision making in ants, where brain-like colonies are capable of choosing the best-quality site among multiple candidates and then collectively migrating to it without splitting (Pratt 2005a; Marshall et al. 2009; Pratt 2019). In species of *Temnothorax* ants where nest-site selection has been studied in detail, this emergent ability relies on an individual-level quorum rule in which a scout assesses a candidate nest and switches, as in the onset of an activation potential in a neuron, from slow recruitment mode (*tandem run*) to fast nestmate transportation mode (*transport*) after experiencing a sufficiently high nestmate encounter rate in the candidate site (Pratt 2005b). Bio-inspired models of similar processes often depend on counting historical encounters to estimate encounter rate numerically (Pavlic and Passino 2010; Musco, Su, and Lynch 2017), but studies of counting in social hymenoptera suggest counting beyond four may be beyond the abilities of ants (Dacke and Srinivasan 2008). How scouts reliably determine

that the decision quorum has been reached without counting a large number of previous encounters remains unknown, and how the scout determines how much evidence is needed to be gathered to make such an inference is less clear.

The first unknown—how ants integrate sequential encounters to sense a quorum—could be addressed using drift–diffusion models (DDMs), a popular way to characterize individual decisions without the need of including the detailed neural activity of the subject (Ratcliff et al. 2016; Ratcliff 1978). For example, Davidson et al. (2016) used this approach to analyze how harvester ants use encounters with incoming foragers to determine whether to go out to forage or return to the nest. A DDM models the mental evidence-accumulation process of an individual facing a forced binary choice as a continuous 1D random walk—a diffusion process, equivalent to Brownian motion or a Wiener process—that starts between between two absorbing decision thresholds. Evidence in favor of one of the choices acts as a continuous drift that drives the process to the corresponding threshold while the randomness of diffusion can hasten or prolong the decision and even generate errors in decision making. Although diffusion models have classically been used to describe decision processes in humans and other primates, they have also been employed to describe the decision-making dynamics of social insects (including honeybees and ants) both at the level of the individual (Davidson et al. 2016) and in the aggregate dynamics of the colony (Marshall et al. 2009; Sasaki, Pratt, and Kacelnik 2018; Ayalon et al. 2021). In the case of colony-level DDMs, evidence typically accumulates not within some internal state of each individual but rather in some external physical variable or the spatial demographics of the colony itself. In fact, quorum sensing itself has been conceptualized as an absorbing threshold of such a physically embodied DDM where the number of individuals accumulating at a particular candidate site is analogous to a randomly walking decision variable (Sasaki and Pratt 2018).

The second unknown—how subjects determine when the accumulation of information

stops and the deliberative decision should be made—cannot be fully explained by diffusion processes. In most DDM cases, when the evidence is reasonably strong, a decision threshold will be reached after a finite expected latency. However, when the evidence is ambiguous (i.e., net drift is very low), the expected decision time (or hitting time) predicted by diffusion models tends to infinity. This is consistent with the classical, stereotyped paradox of Buridan's Donkey, which starves to death after being unable to decide between equally accessible food piles. Determinism has been said to be at the heart of the paradox because there is no rational, deterministic way to decide between equivalent choices (Weinstein and Pavlic 2017). However, even stochastic decision models like continuous random walks can take an indefinite time to break symmetric cases. Thus, in this paper, I propose an alternative to the classical DDM that retains the ability to explain decision-making accuracy while not also predicting unbounded decision latency for comparisons of equally desirable options.

Taking a more physical perspective implicates continuity as the source of the paradox of Burdian's Donkey. It is impossible to ensure that a discrete decision based on an input in a continuous range of values can be made in a bounded duration of time (Lamport 2012); even random walks facing near-symmetric conditions can, with some probability, fail to be absorbed by a decision boundary when evolving through a continuous space where the gap between the walker and the boundary can always be halved. However, random walks over discrete spaces (e.g., the classic Gambler's Ruin problem (Feller 1968), which predicts how many turns of a game of chance until a gambler will lose all her money) can be guaranteed to be absorbed in a finite amount of time. Motivated by this property of discrete random walks, I develop here a model of decision making in a mobile ant based on a Markov chain model (Papoulis and Pillai 2002) that is equivalent to a discrete random walk over a finite number of states. Although qualitatively similar in structure to the continuous DDM, this discrete model is simpler in form than the stochastic differential equations of a DDM and

has convenient closed-form analytical expressions for decision distributions and speed. Furthermore, it predicts bounded deliberation times and reproduces the accuracy and latency observed in real ants.

2.2 Two-Alternative Forced Choice Decisions in Ants

In laboratory assays of nest-emigration behavior of *Temnothorax* ant colonies, Pratt (2005b) observed that individual scout ants would sometimes leave a candidate nest site and perform one of two different recruitment behaviors – tandem running (where the recruited ant followed behind the scout) or transporting (where the recruited ant was carried by the scout). When either recruitment behavior was observed, the conditions within the candidate nest immediately before that decision were studied, and it was determined that scout decisions are well predicted by the encounter rate with ants in the candidate nest. The blue circles in Figure 3 show individual decisions by scouts with respect to the average encounter rate in the candidate nest at the time of the recording. The green triangles in Figure 3 represent the duration of time that each scout remained in the candidate nest before leaving to perform a recruitment behavior. It is clear that tandem running is more common at lower encounter rates and transporting becomes prevalent as the encounter rate increases. Intermediate encounter rates produce both recruitment types at higher latencies, which is consistent with the speed–accuracy trade-off apparent in decision-making processes in mammalian brains; when the evidence is ambiguous, subjects take longer to make decisions and make less accurate choices (Roitman and Shadlen 2002; Ratcliff et al. 2016).

I have reproduced the best-fit Hill function from Pratt (2005b) in the inset in Figure 3. This function, usually applied in biochemistry to describe ligand binding as a function of ligand density (Goutelle et al. 2008), was selected as a convenient two-parameter sigmoid

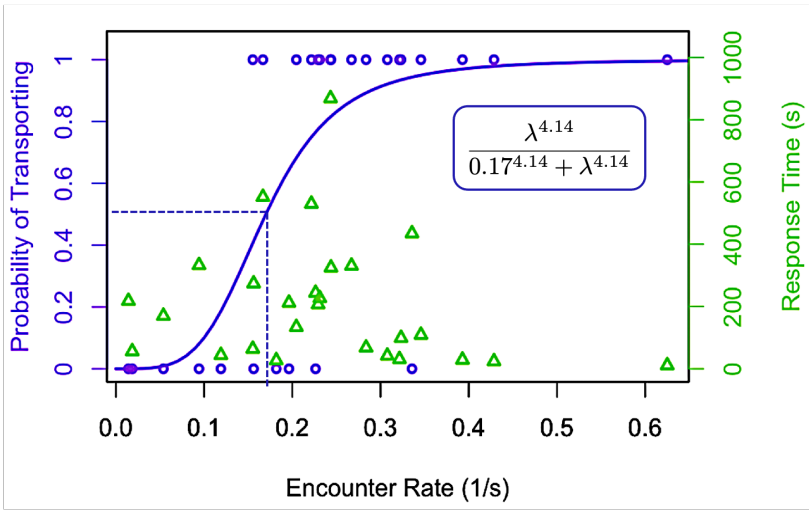

Figure 3. Decision probabilities and latencies for real ants. During a colony migration, scout ants were recorded as performing tandem runs (0) or transports (1) as the encounter rate at the new nest increased (*blue circles*). *Green triangles* represent decision latencies, measured as the time spent by the ant in the new nest before returning to the old nest and performing either type of recruitment. Data from Pratt (2005b).

with a built-in "half-saturation" threshold—in this case, 0.17 encounters per second—that could be interpreted as the critical encounter rate that separates the two forms of recruitment. Similar formulations have been used in social-insect models to describe the probability of a decision as a saturating function of evidence strength (Camazine et al. 2003; Detrain and Deneubourg 2008). However, beyond being a convenient two-parameter characterization, the choice of Hill function was essentially arbitrary. Here, I show that a simple finite-state Markov chain model for binary decisions coincidentally produces precisely this mathematical form for the curve predicting decision probabilities.

2.3 Markov-Chain Model of Decision-Making Dynamics

I focus on modeling the quorum-sensitive process of deciding between recruitment types that occurs *after* a scout has decided to recruit for a given candidate nest site (but

before the scout has committed to transport ants to it). Consequently, I only model evidence accumulated from social information about quorum attainment; I do not model the earlier process of deciding to recruit based on physical information about the candidate nest site. A similar model focused on the decision to start recruiting to a site has been developed by Robinson et al. (2011).

Consider a scout that has decided to start recruiting for a candidate nest. At time $t = 0$, she enters the chosen nest and starts exploring the space. After some time $t = T$, she will exit and return to her old nest and choose either to recruit another ant by tandem running or switch to transporting behavior. I assume that the tandem-run–transport decision is made inside the candidate nest and does not change after the ant exits. We refer to the duration T spent in the candidate site during the decision-making process as the *decision latency*.

I describe the mental state of an ant at time t using a discrete random variable X_t that can take integer values from $-n$ to n for some finite "radius" $n \in \{1, 2, \ldots\}$ of discrete states, as depicted by the line of $2n + 1$ states in Figure 4. That is, each random variable X_t has the range $\mathcal{R}_X = \{i \in \mathbb{Z} : |i| \leq n\}$. As I will describe below, this discrete (and finite) random variable will act analogously to the evidence variable in a DDM. That is, more evidence for a transport decision will lead to faster increases, and more evidence for a tandem-run decision will lead to faster decreases. An ant decision is modeled to occur at any time t^* when $|X_{t^*}| = n$; at that point, the ant will leave the candidate nest (ignoring any additional contacts along the way) and start transporting if $X_{t^*} = n$ or continue to recruit by tandem running if $X_{t^*} = -n$. Initially, at time $t = 0$, I configure the random process $\{X_t, t \geq 0\}$ such that $X_{t=0} = 0$ (i.e., the ant enters the nest without any bias toward either decision to transport or continue tandem running).

To incorporate the effect of encounters in the decision-making process, I model the mental state X_t of the ant as a continuous-time Markov-chain process with two opposing

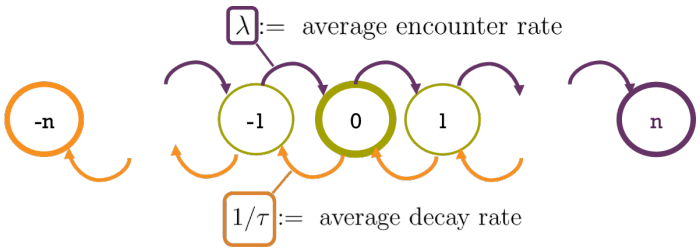

Figure 4. Diagram of decision process as a Markov chain model in continuous time. The mental state X_t is 0 when $t = 0$, then decays continuously by one at a constant rate $1/\tau$ and increases by one at a constant rate λ equal to the encounter rate.

rates and two absorbing states (Figure 4). The two rates are chosen based on the assumption that frequent encounters are a cue of quorum attainment and infrequent encounters are a cue that quorum has not been reached. In particular, the mental state X_t increases by one at a rate λ, equal in magnitude to the encounter rate (i.e., inter-encounter times are exponentially distributed with an average time between ant encounters of $1/\lambda$). This rate models the assumption that ant-to-ant encounters tend to increase an ant's motivation toward transporting. The mental state X_t decreases by one at a rate $1/\tau$, which I call a "decay" rate (with τ being the average of the exponentially distributed time between spontaneous decreases in the mental state X_t). This decay rate models the assumption that long waiting times will tend to decrease an ant's motivation toward transporting and increase her motivation toward tandem running. A decision has been made once $|X_t| = n$. Consequently, the range $\mathcal{R}_X$ of the mental state is divided among two absorbing states, n and $-n$, and $2n - 1$ transient states only accessed during in-nest deliberation. This is a discrete analog of a traditional DDM with two absorbing boundaries. However, whereas a continuous DDM has an unbounded hitting time when there is no net drift, I will show below that the analogous zero-drift case of $\tau = 1/\lambda$ will nevertheless have a bounded mean hitting time.

2.3.1 Master Equation of Deliberation by Discrete Random Walk

The model described above is effectively a random walk in continuous time over a finite set of discrete sets. Consider some time t and mental state X_t. For any $i \in \mathcal{R}_X$, I define $v_i^t \in [0,1]$ to be the probability that the mental state $X_t = i$. I collect these $2n+1$ probabilities into a state vector

$$\mathbf{v}^t \triangleq [v_{-n}^t, v_{-n+1}^t, \ldots, v_0^t, \ldots, v_{n-1}^t, v_n^t]^\top \in [0,1]^{2n+1}.$$

The continuous-time evolution of this state vector is governed by the master equation $\mathrm{d}\,\mathbf{v}^t/\,\mathrm{d}\,t = M\mathbf{v}^t$, where M is the transition rate matrix

$$M \triangleq \begin{bmatrix} 0 & 0 & 0 & 0 & ... & 0 \\ \frac{1}{\tau} & -(\frac{1}{\tau}+\lambda) & \lambda & 0 & ... & 0 \\ 0 & \frac{1}{\tau} & -(\frac{1}{\tau}+\lambda) & \lambda & \vdots & 0 \\ 0 & \ddots & \ddots & \ddots & \ddots & 0 \\ 0 & ... & 0 & \frac{1}{\tau} & -(\frac{1}{\tau}+\lambda) & \lambda \\ 0 & ... & 0 & 0 & 0 & 0 \end{bmatrix},$$

and the initial probability vector $\mathbf{v}^0$ is such that

$$v_i^0 \equiv \begin{cases} 1 & \text{if } i = 0 \\ 0 & \text{if } i \in \mathcal{R}_X \setminus \{0\} \end{cases}.$$

Furthermore, if I focus only on the times of the discrete events where the state transitions (i.e., due to an encounter or a decay), the corresponding embedded discrete-time jump

Markov chain $\mathbf{v}^{k+1} = P^\top \mathbf{v}^k$ has a transition probability matrix

$$P \triangleq \begin{bmatrix} 1 & 0 & 0 & 0 & ... & 0 \\ q & 0 & p & 0 & ... & 0 \\ 0 & q & 0 & p & \vdots & 0 \\ 0 & \ddots & \ddots & \ddots & \ddots & 0 \\ 0 & ... & 0 & q & 0 & p \\ 0 & ... & 0 & 0 & 0 & 1 \end{bmatrix} \quad \text{with} \quad p \triangleq \frac{\lambda}{1/\tau + \lambda} \quad \text{and} \quad q \triangleq 1 - p = \frac{1/\tau}{1/\tau + \lambda}, \tag{2.1}$$

where P_{ij} gives the probability of going from state i to state j at the transition instances (i.e., disregarding the holding time in state i).

2.3.2 Decision Probabilities (Limit Distribution)

To determine the probabilistic distribution of outcomes of the Markov-chain model of ant decision making, I utilize the embedded jump chain described by Equation (2.1). The jump-chain process is equivalent to a one-dimensional random walk in discrete time, where in each discrete-event time k, the mental state X_k will increase with probability p and decrease with probability $q \triangleq 1 - p$, where:

$$p = \frac{\lambda}{\lambda + 1/\tau} = \frac{\lambda\tau}{\lambda\tau + 1} \quad \text{and} \quad q \triangleq 1 - p = \frac{1/\tau}{\lambda + 1/\tau} = \frac{1}{\lambda\tau + 1}. \tag{2.2}$$

In the original continuous-time process, these steps are spaced apart by random, exponentially distributed time intervals (i.e., holding/dwell times in each discrete state), but the sequence of states in the original process and the discrete-time jump-chain processes is the same.

Finite-Time Convergence:

The discrete jump model described by Equation (2.1) effectively describes a classical gambler's ruin problem between two gamblers with a finite number of coins where, in each round of play, one gambler gives the other gambler one of their coins. In the gambler's ruin problem, there is zero probability that such a game will continue for an infinite number of rounds; there is unity probability that one gambler will be ruined. Similarly, in the discrete jump model, a decision is guaranteed with unity probability to eventually be reached (for details, see Supplementary Information).

Decision Distribution:

Given that the jump chain will reach an absorbing decision state (i.e., Tandem Run or Transport) with unity probability, I next determine the probability distribution of the jump chain reaching each of these two states. Using the jump chain, I can derive an expression for the probabilities P_i^T and P_i^R for the probabilities that an ant in an initial state $i \in \mathcal{R}_X$ decides to recruit by transporting or tandem running, respectively. Trivially, $P_n^T = 1$ and $P_{-n}^T = 0$ (and, likewise, $P_n^R = 0$ and $P_{-n}^R = 1$) because the ant starts in its terminal, deciding state. For the cases where the initial state i is a transient state (i.e., $|i| < n$), the probabilities can be expressed as the recurrence relationships:

$$P_i^T = qP_{i-1}^T + pP_{i+1}^T \qquad \text{and} \qquad P_i^R = qP_{i-1}^R + pP_{i+1}^R.$$

Consequently, a closed-form solution for P_i^T and P_i^R can be found (for details, see Supplementary Information). In particular, the probability that an ant starting in state $i = 0$ and

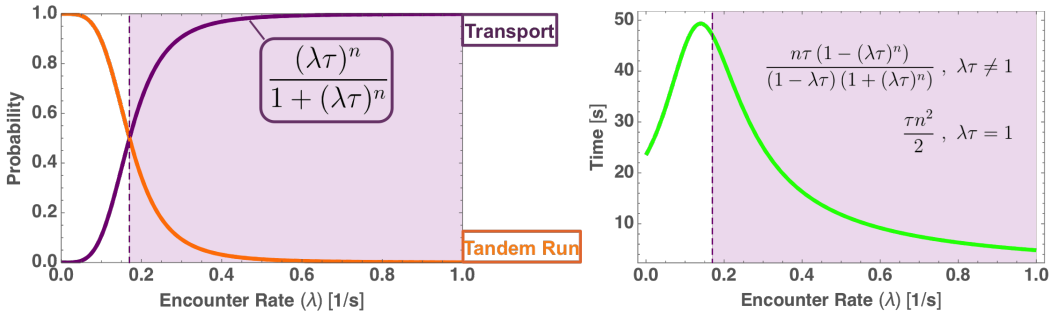

Figure 5. Decision curves (left) and latency (right) as a function of the encounter rate λ. In both graphs, $n = 4$ and $1/\tau = 0.17$.

then recruiting by transporting is:

$$P_0^T = \frac{(p/q)^n}{(p/q)^n + 1} = \frac{(\lambda\tau)^n}{1 + (\lambda\tau)^n} = \frac{\lambda^n}{(1/\tau)^n + \lambda^n}. \tag{2.3}$$

Thus, this Markov-chain model yields the expected Hill function for the decision probability curve identical to the one chosen to fit observations in Figure 3 with $1/\tau = 0.17$ and $n = 4.14$. In the model, the "radius" n of the $2n + 1$ states is a whole number; consequently, I plot Equation (2.3) with $1/\tau = 0.17$ and $n = 4$ in the left panel of Figure 5. For low encounter rates, the probability of performing transports is low (purple curve), but it approaches 1 as the encounter rate increases. When $\lambda = \lambda_c \triangleq 1/\tau$, there is an equal chance of performing either recruitment type; thus, the average decay duration τ acts to set the critical encounter rate while the number of states n shapes the sharpness of the decision curve.

2.3.3 Decision Latency (Hitting Time)

The decision latency is the time spent in deliberation before making a decision. In the ant data, I defined decision latency as the time an ant spends in the new nest before leaving and recruiting by either tandem running or transporting. In this Markov-chain model, decision

latency corresponds to the duration of time it takes for the system to reach an absorbing state (i.e., the length of time the random walk takes to hit a decision barrier). As I have described above, an infinite period of transience (i.e., avoiding an absorbing decision barrier) can only occur with zero probability. Thus, I seek to describe the average decision latency (which must itself be bounded).

Our approach to formulating the decision latency in the Markov-chain model is to scale the expected number of transient steps before absorption by the average duration of time between transitions. Let S_i be the number of steps until absorption when starting from state $i = X_0 \in \mathcal{R}_X$. For the two absorbing states, S_{-n} and S_n are both 0. After the first transition occurs, the conditional expectation of the number of steps is $S_{i+1} + 1$ if the state increased by one and $S_{i-1} + 1$ if it decreased. Consequently, expected value S_i follows the recurrence relation

$$S_i = pS_{i+1} + qS_{i-1} + 1.$$

A detailed solution to this recurrence relation can be found in the Supplementary Information. For the initial state $i = X_0 = 0$, I obtain

$$S_0 = \begin{cases} -\dfrac{n\left(\left(\frac{q}{p}\right)^n - 1\right)}{(p-q)\left(\left(\frac{q}{p}\right)^n + 1\right)} & \text{if } p \neq q, \\ n^2 & \text{if } p = q. \end{cases}$$

After substituting values for p and q and multiplying by the average holding time, $1/(\lambda + 1/\tau)$, the decision latency from an initial neutral state $i = X_0 = 0$ is

$$L_o \triangleq \frac{S_0}{\lambda + 1/\tau} = \begin{cases} \dfrac{n\tau\left(1 - (\lambda\tau)^n\right)}{(1-\lambda\tau)\left(1 + (\lambda\tau)^n\right)} & \text{if } \lambda\tau \neq 1, \\ \dfrac{\tau n^2}{2} & \text{if } \lambda\tau = 1. \end{cases}$$

The latency curve L_0 is a continuous function of the encounter rate, with a maximum near $\lambda_c \triangleq 1/\tau$ and lower values elsewhere (see Figure 5). In agreement with the finite

convergence result from above, this expression for the expected decision latency does not have infinite singularities; the expected latency value is always bounded. The shape matches the experimental observations in Figure 3, with the lowest latency values for very small or very large encounter rates and increased decision times near the threshold. Furthermore, if the decay time τ is held constant, the peak latency occurs at an encounter rate $\lambda_{max} \leq \lambda_c$. This effect results from the fact that reducing the encounter rate by a small amount while keeping the decay rate constant effectively increases the residence time $1/(\lambda_{max} + 1/\tau) \geq 1/(\lambda_c + 1/\tau)$ while keeping a similar number of steps.

2.4 Discussion: Counterbalancing Speed and Accuracy in Individuals and Collectives

The best-fit parameters shown in Figure 3 are taken from a colony of one particular species of *Temnothorax* ant during one migration event. However, the best-fit parameters may vary even for the same colony in a different decision context. For example, it is known that the population threshold required to trigger transport behavior (related to τ and λ_c) can vary between species as well as with the urgency of the emigration conditions (Pratt 2005a). Our discrete model provides novel insights into how speed–accuracy trade-offs at the level of these individual parameters (τ and n) scale to speed–accuracy trade-offs at the level of collectives.

2.4.1 Assessing Speed and Accuracy in Individuals

At the level of individuals, quorum-sensing speed is inverse to the decision latency. Individual-level quorum-sensing accuracy could be defined in a number of ways, but for my purposes I relate it to the *sensitivity* of the decision outcome to changes in the encounter

rate near the critical value. In the probability curve $P_0^T(\lambda)$ from Equation (2.3), the position of the inflection point depends solely on the average decay time τ. So every value of τ uniquely determines a critical encounter rate $\lambda_c \triangleq 1/\tau$ where the decision maker is the least accurate (i.e., the decision is most similar to random chance). Given a critical threshold λ_c, a steeper slope at the inflection point implies a higher sensitivity to changes in the encounter rate near the critical threshold. Decision makers that are more sensitive at this inflection point will require a smaller move away from the inflection point to restore the same amount of accuracy. In this sense, the decision process is more accurate when there is a sharper transition from tandem running to transporting. I define sensitivity as the derivative of the decision curve with respect to λ at the critical encounter rate $\lambda_c \triangleq 1/\tau$:

$$\left.\frac{dP_0^T(\lambda)}{d\lambda}\right|_{\lambda=\frac{1}{\tau}} = \frac{n\tau}{4}.$$

Figure 6 shows the effect of parameter variation on the decision characteristics.

The main role of the average decay time τ is to fix the critical encounter rate $\lambda_c \triangleq 1/\tau$ (vertical dashed line in Figure 6) that separates decisions to recruit by tandem running (encounter rates lower than λ_c) from decisions to begin transport behavior (encounter rates higher than λ_c). However, this decay-based tuning of the critical encounter rate has a side effect of also adjusting the mean decision latency for individuals at each encounter rate. In particular, a smaller decay duration τ (solid lines in the right panels of Figure 6) not only increases the encounter rate threshold λ_c, but it also reduces the peak latency for individual decisions. That is, when an ant's mental state intrinsically decays rapidly toward one decision boundary, reaching the opposite decision boundary requires very high encounter rates (and thus very high quorums in densely packed nest candidates). However, fast decay rates (and the very fast encounter rates necessary to compensate for them) also correspond

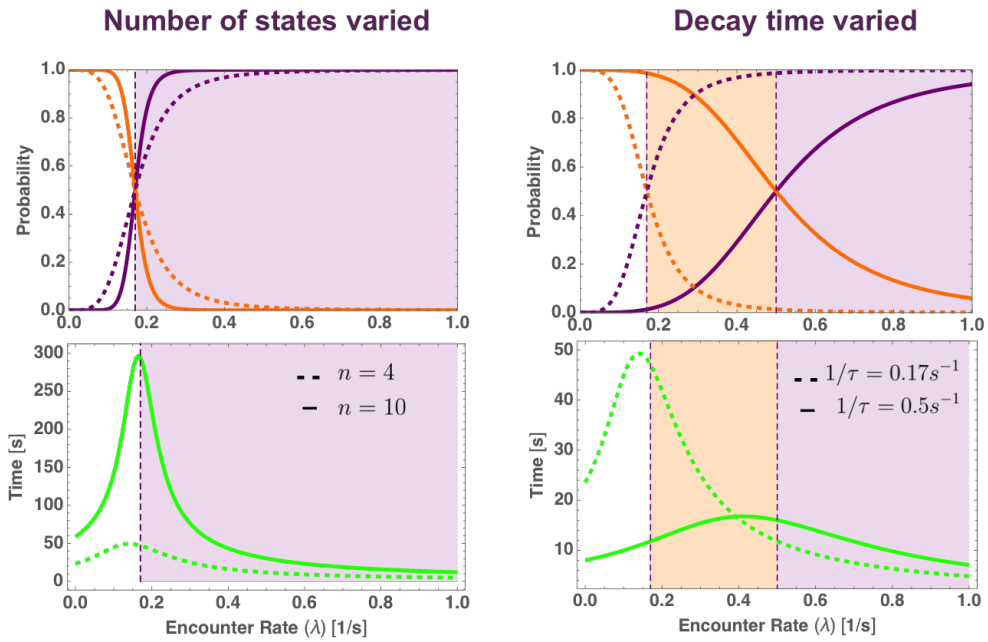

Figure 6. Effect of parameter variation on the decision outcomes (top) and latencies (bottom) when n is varied (left) or τ is varied (right).

to fast decisions. Similarly, a high decay duration τ associated with a low critical encounter rate λ_c also corresponds to longer decision times by individuals.

2.4.2 From Individual Performance to Collective Performance

The coupling between the critical encounter rate λ_c and the peak latency of individuals suggests that λ_c (and, correspondingly, decay duration τ) provides a potential mechanism for trading speed and accuracy at the level of collective decisions. Quorum detection with a high critical encounter rate λ_c requires the accumulation of many scouts in a candidate nest, but the corresponding short decay duration τ means that scouts will leave nests early. Because of the long time a tandem run takes to bring a new ant to a candidate nest, scouts will be unlikely to significantly accumulate in nests in the high-λ_c case until there are a large number of tandem-running ants recruiting to the same nest. Thus, as $\lambda_c \to \infty$,

collective decisions are resolved after longer periods of time and require a greater degree of consensus among ants. Similarly, a low λ_c corresponds to a high decay duration τ, meaning that ants will accumulate more readily. Furthermore, the low λ_c threshold only requires a small number of ants to accumulate before triggering to transport. So, as $\lambda_c \to 0$, colonies effectively pick randomly as transporters simultaneously triggered for different nests race to exhaust the supply of ants from the home nest to be transported. From this perspective, the individual-level decay duration τ is a parameter that tunes a colony-level speed–accuracy trade-off. That is, colonies made up of individuals with high critical encounter rates (low τ) have long collective deliberation periods that are more likely to achieve consensus (if they complete). Similarly, colonies made up of individuals with low critical encounter rates (high τ) effectively make random decisions among nest candidates.

Just as λ_c (or, equivalently, τ) may be viewed as a parameter that tunes the collective-level speed–accuracy trade-off, the "radius" n of the $2n + 1$ mental states can adjust the individual-level speed–accuracy trade-off and modulate the decision performance of the collective. In particular, for any given critical encounter rate, n has the ability to independently adjust the decision latency and accuracy. A larger n (solid lines in the left panels of Figure 6) produces more accurate (i.e., steeper P_0^T) but slower individual-level decisions (i.e., larger L_o peak) with no effect on critical encounter rate λ_c. Thus, although increasing critical encounter rate λ_c corresponds to decreased individual-level latency that may prevent accumulation of a sufficient number of recruits to ever reach the threshold λ_c, increasing n raises individual-level latencies, which increases both individual-level quorum-detection accuracy and the chance of accumulation toward quorum. So although individuals with high n spend longer deliberating in each nest at any encounter rate (Figure 7), the chances of individuals accumulating in a nest are higher, and so the deliberation time of the collective may be shorter. Similarly, because a small λ_c is generally associated with

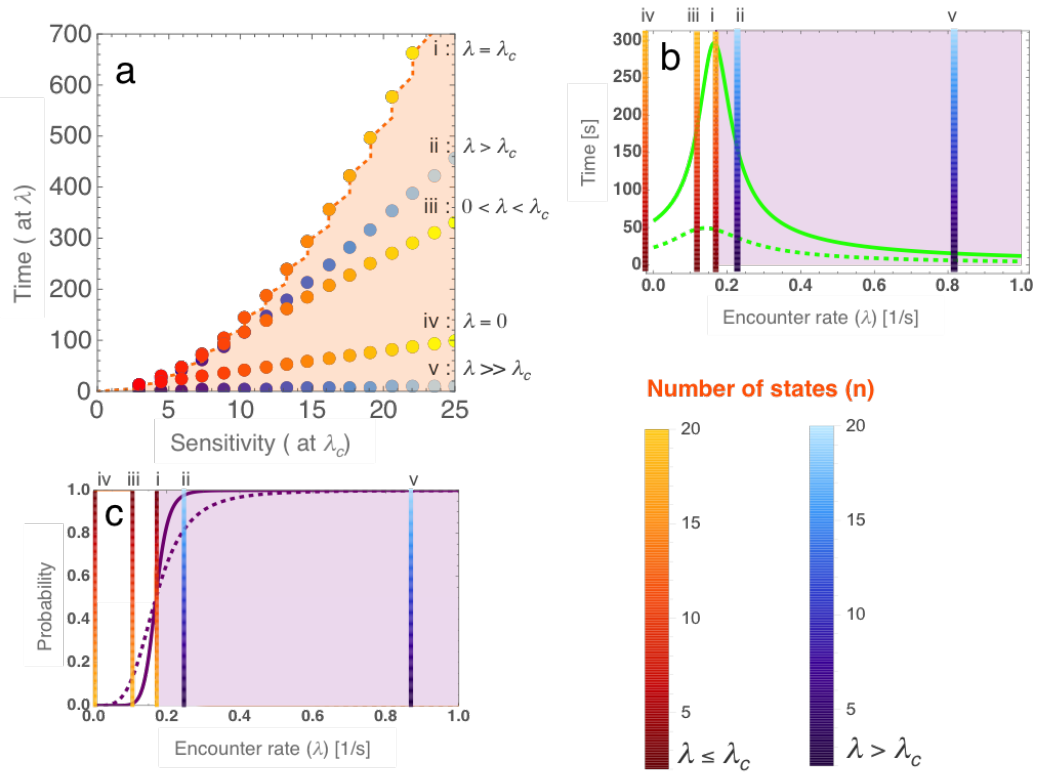

Figure 7. Characterization of the relation between latency and sensitivity of the decision curve when the number of states n changes. In **a**, different curves **i-v** correspond to different encounter rates λ, indicated as *vertical lines* **i-v** in panels **b** and **c**. *Darker* dots in **a** and *dotted* lines in **b** and **c** correspond to low n values. Increasing n (*ligther* dots in **a**) produces higher latencies and a sharper decision curve (solid lines in **b** and **c**). The trade-off between sensitivity and speed is stronger for encounter rates close to λ_c (**ii, iii**) and disappears for high values of λ (**v**).

a collective prioritization of speed and an individual prioritization of accuracy, n can be reduced while still maintaining high individual-level accuracy. Thus, if λ_c (or, equivalently, τ) is viewed as a parameter that can be changed over short time scales to tune colony speed–accuracy balance, then n may be viewed as a parameter that can be changed over longer time scales to optimize performance for normal ranges of λ_c.

2.5 Summary, Conclusions, and Future Work

In this paper, I proposed a simple discrete Markov-chain model for sequential evidence accumulation during individual binary decisions and applied it to describe the choice between recruitment types in *Temnothorax* ants. The model reproduced core features of the latency and outcome characteristics from experimental observations of real ants while providing a framework for examining how cognitive processes in ants under different conditions balance speed and accuracy. Furthermore, because the model predicts bounded decision latencies, it is the first, to my knowledge, to predict a logical connection between critical encounter rate and worst-case decision latency. For small colonies, high critical encounter rates may effectively eliminate transport as a plausible recruitment mode because the concomitant low decision latencies will prevent those high encounter rates from ever being met. Thus, this model helps to better understand the colony-level implications of individual-level cognitive parameters of decision making. More generally, the finite-state approach in this model suggests a novel path for characterizing neuron-like excitable elements interacting in a group in order to understand collective cognition in multi-scale cognitive systems.

The model's discrete representation of the decision state space in continuous time enabled the formulation of a bounded latency curve even for ambiguous evidence, where previous continuous sequential-sampling models would predict infinite expected decision times. This constraint on deliberation time regardless of the difficulty of the decision allows the characterization of the trade-off between speed and accuracy for any possible level of evidence (encounter rate) in the ant's environment. The fact that only a region of the Time–Sensitivity space in Figure 7 can be explored by the model is a representation of the latency bound, and the shape of the region boundary describes the trade-off for hard problems.

Optimality models have been proposed that suggest that apparent impulsiveness (i.e., a favoring of rewards after shorter waiting times regardless of eventual rewards) can actually be the outcome of behaviors that minimize opportunity costs in ecologically relevant contexts (Pavlic and Passino 2010). The bounded latencies predicted by our model may also be able to be viewed as heuristics for opportunity-cost minimization – forcing decision makers to reach a decision quickly in order to avoid accumulating opportunity costs from long-term deliberation.

2.5.1 Contribution Relative to Related Work

Our model is not the only one that can describe the features of the dataset in Figure 3. In fact, there is a wide range of successful applications of continuous sequential-sampling models to binary decisions in insects (Clemens, Krämer, and Ronacher 2014; DasGupta, Ferreira, and Miesenböck 2014), colonies (Marshall et al. 2009), birds (Kacelnik et al. 2011) and primates (Usher and McClelland 2001), among others (Ratcliff et al. 2016). My choice of a discrete state space is based on the fact that encounters are discrete events that are experienced in continuous time, but it also allows a characterization of symmetric cases that are unbreakable by continuous-state methods. A commonly studied aspect of sequential-sampling methods is their relation to the formulation of optimal decision-making behavior. However, this model represents an individual decision process that is to be integrated with a large number of other individual processes to produce an appropriate collective decision. Furthermore, I demonstrate that patterns at the individual level can, when combined with other ants in the same colony, counter-intuitively lead to qualitatively different patterns in colony-level decision making. Thus, I have not characterized our model in terms of

individual-level decision-making optimality because the net effect of setting individual-level parameters on the cognitive characteristics of the colony is non-trivial.

The same *Temnothorax* nest-site selection data that inspired this study also recently inspired a different quorum sensing model that incorporated excitable ants with finite internal states (Pavlic et al. 2021). In that temporally discounted quorum sensing (TD-QS) approach, ants are assumed to have only two states (quiescent or excited). Similar to our model, encounter events move ants into the excited state, and long durations without an encounter move ants back into the quiescent state. However, in that TD-QS model, there are not absorbing decision states per ant. Instead, an ant's random encounter with the exit of the cavity forces a decision based on which of the two irreducible states is occupied. Hypothetical ants whose decisions are described by this approach have finite decision latencies (because of the certainty of an ant in a two-dimensional random walk in the planar nest cavity encountering the exit of the cavity) and decision accuracy described by a Hill function $\frac{\lambda}{1/\tau+\lambda}$ where λ is the encounter rate and τ is the average dwell time in the excited state. This accuracy is equivalent to the decision probability P_0^T when $n = 1$. In this case in the model, an ant makes a decision after the first transition away from the initial state. However, the parameter n available in my model allows for tuning of the steepness of the transition region of the Hill function around the critical, half-saturation encounter rate. Furthermore, unlike the TD-QS model, my approach provides analytical expressions for average latency that explicitly depend upon the encounter rate within the cavity. Thus, this analytically tractable model provides a better description (with $n = 4$) of the ant data from Pratt (2005b) while also being able to mimic (with $n = 1$) the computational simplicity of the event-triggered decision making of the other approach.

2.5.2 Caveats and Future Work

Although the latency curves derived here have the desirable property of boundedness, there are simple ways in which their quantitative estimation could be improved. On the one hand, I did not account for an actuation time between decision and implementation, which in this case corresponds to the gap between cognitively making a recruitment choice and physically finding the nest exit. This could be estimated from the nest size and ant walking speed and added to the predicted latency. On the other hand, I assumed a neutral initial state between the two alternatives, whereas real ant scouts may have a bias towards a specific recruitment modality. In fact, results from Pratt (2005a) suggest an initial bias toward tandem running, given that ants seem to require a higher quorum for their first recruitment act than they do for later ones. In the future, the effect of including asymmetric decision boundaries could be analyzed by considering the initial mental state as an additional model parameter.

While the model's flexible structure allows straightforward modifications for improvement, it also provides, in its present form, a simple framework to analyze how variation at the individual level may cause groups to differ from one another. Variation across colonies of social insects, arising from differences in the behavioral traits of their members, is at the basis of evolutionary change (Jandt and Gordon 2016). There is evidence of interspecific differences in the way that *Temnothorax* ant colonies balance speed and accuracy when choosing a new nest, and there is also evidence that ant colonies may reduce their quorum size under urgent emigration circumstances (Pratt 2005a; Franks et al. 2003). In the light of the model, such observed collective differences can be mapped to individual decision parameters, which can be verified experimentally by tracking the behavior of single ants from different colonies. The model then provides a method to identify individual traits that

are plastic enough to shift in response to unexpected environmental circumstances as well as parameters that must be acted on by natural selection at evolutionary time scales.

This model is especially useful in the context of collective behavior, given its simple structure and the fact that it provides a closed analytical formulation of individual decision characteristics. The expressions for decision probability and latency can be readily implemented in colony-level mean-field or agent-based models as functions of the current interaction rate without the need to simulate the complete Markovian process for single decisions. Therefore, the accuracy and latency characteristics predicted by this model provide a path toward building new models of multi-scale phenomena that integrate individual behaviors into collective decisions. Complex models of the brain are built from connecting individual neuronal units that are modeled as coarse-grained switches that respond to rates of interactions with other switches. Similarly, I have proposed a simple discrete-state model of individual-level excitation that could be used as the basis for understanding the brain-like collective cognition of interacting mobile ants.

Chapter 3

FROM INDIVIDUAL PHENOTYPES TO COLLECTIVE BEHAVIOR IN HONEYBEE FORAGERS: A MATHEMATICAL MODEL

3.1 Introduction

The emergence of collective behavior from local interactions between individuals is common to a wide range of biological systems at many levels of organization, from bacteria to superorganismic social-insect colonies (Piñero et al. 2019; Couzin 2007, 2009). Members of such collectives can differ in many aspects, like their age, reproductive ability, or the way they interact with others and the environment. However, quantitative models of collective behavior generally assume a homogeneous population where every individual follows the same behavioral rules (Seeley and Buhrman 1999; Couzin et al. 2002; Britton et al. 2002; Marshall et al. 2009; Sumpter and Pratt 2003; Camazine and Sneyd 1991), largely overlooking individual variation and its collective effects (Kao and Couzin 2019; Valentini et al. 2020; Cook et al. 2020; Cook et al. 2019; Richardson et al. 2018; Delgado et al. 2018; Mosqueiro et al. 2017; O'shea-Wheller et al. 2017; Pinter-Wollman 2012).

Social-insect colonies are exceptional model organisms to study how individual variation scales up to collective behavior. Each colony can be conceived as a superorganism (Sasaki and Pratt 2018; T. D. Seeley 1989; Behmer 2009), where local interactions between individual insects and their environments produce a self–organized, decentralized system with tasks distributed across different workers (Camazine et al. 2003; Beshers and Fewell 2001; Borofsky et al. 2020). In these collectives, reproductive hierarchies cause natural selection to act on the group level rather than the individual level (T. D. Seeley 1989; Thomas D. Seeley

1997). Without direct individual selective pressures, there are more degrees of freedom for individual phenotypes to diverge while maintaining group fitness, which enables the emergence of heterogeneous social architectures. Moreover, colonies provide high empirical tractability, where both individual and collective behavior can be experimentally observed and manipulated. Thus, social-insect colonies constitute tractable collective systems of naturally varying individuals (e.g. in age, genetics, morphology or cognitive properties) that are experimentally accessible at multiple scales.

Particularly well studied among social insects are honey bees, which collectively perform different tasks like brood care, nest maintenance or foraging. Empirical work has covered multiple levels of organization, from the genetic basis of individual behavior to colony-level function (Smith and Cook 2020; Lemanski et al. 2019). Recent studies have revealed distinct heritable attention phenotypes among foragers, which manifest in their ability to learn to ignore familiar, previously unrewarded stimuli (Bhagavan et al. 1994; Chandra, Hosler, and Smith 2000; Chandra, Wright, and Smith 2010; Brandes 1991; Chandra et al. 2001). Furthermore, the interaction between workers with different cognitive phenotypes drives the division of labor in the colony (Cook et al. 2019). I focus on the effect of individual cognitive variations on collective foraging and take a mathematical modeling approach to guide future experimentation towards the most relevant individual processes regulating collective decisions.

During collective foraging, colonies must allocate individuals to sample the environment and exploit it in a way that guarantees sufficient resource intake (Thomas D Seeley 1995; Hills et al. 2015). In honey bees, a small number of bees (called scouts) spontaneously leave the hive in search for food and, once they find a source, they fly back to the hive and may perform waggle dances to recruit other foragers to the patch they visited (T. D. Seeley 1989). In general, models of collective foraging dynamics assume that the population is

homogeneous - every bee behaves according to the same rules, on average (Sumpter and Pratt 2003; Camazine and Sneyd 1991). However, it is known that bees present behavioral differences, and those impact the group foraging patterns. For example, individuals vary in their tendency to collect nectar, pollen or both, as well as their propensity to explore independently (scout) for new resources or follow the dance communication from other bees that leads to already discovered resources.

Closely related to this task division are variations in the cognitive characteristics of foragers. Cook et al. (Cook et al. 2019) found that scouting (independently leaving the nest to search for food) is associated with high attention. Moreover, since attention profiles are heritable in honey bees (Brandes 1991; Chandra, Hosler, and Smith 2000; Chandra et al. 2001; Bhagavan et al. 1994), genetic lines for high- and low-attention bees can be selected in the laboratory and functioning colonies can be assembled with arbitrary mixtures of individuals from each line. These genotypes have been shown to have high penetrance, that is, a bee genetically selected for high attention manifests high attention behavior even when immersed in a social environment where the low attention phenotype is predominant (and vice-versa) (Cook et al. 2020). This means that the distribution of attention-related behaviors in the colony can be manipulated by altering the proportion of bees from each line that constitute it, and thus the collective effects of individual phenotypic variation can be observed. In fact, recent data (Cook et al. 2020) show that colonies display preferential exploitation of familiar or novel resources according to their composition in attention phenotypes. This poses the question of how genetically determined differences in the attention profile of individual honey-bee forgers give rise to different collective foraging preferences of the colony.

Previous models of honey-bee foraging have not included this phenotype-dependent preference. Camazine, Seeley and Sneyd (Camazine and Sneyd 1991; Seeley, Camazine,

and Sneyd 1991) proposed a model where every forager may initiate recruitment with some probability dependent on the quality of the food source it found, and thus the colony can keep track of variations in the profitability of known resources. The model matches experimental data on visitation to different feeders, although it doesn't include a mechanism for the discovery of new resources or any form of individual heterogeneity. Later work expanded on this model to include scouting (individual exploration for food sources), but still considered a homogeneous population (Sumpter and Pratt 2003). The same holds for models of honey-bee recruitment dynamics during house-hunting Britton et al. 2002; Marshall et al. 2009 and recent work on collective foraging (Borofsky et al. 2020): in general, all bees are modeled as behaviorally identical. A recent model of honey bee foraging by Mosqueiro et al. (2017) included individual variation in the form of task fidelity, or persistence. However, the focus of the model is colony performance in terms of overall resource collection, rather than collective preference for certain resources in the form of forager allocation.

In this paper, I study the effect of individual differences in the cognitive phenotypes of honey-bee foragers on the colony tendency to exploit familiar resources or novel ones, using a mathematical model of self-organized foraging based on attention profiles. I include the new findings in characterizing individuals of different attention profiles and colonies with different compositions of them. In particular, I study the following questions:

- How do colony-level differences in collective attention allocation (i.e. forager allocation) to novel and familiar resources emerge from different group compositions in relation to cognitive phenotypes?
- What are the individual processes that have the most impact on collective preference for familiar or novel food sources?

In addressing these questions, the model suggest future research avenues for experimental

methods focusing on the collective implications of heterogeneity in social insect colonies by determining the individual behaviors that most heavily impact collective decisions in the context of group diversity.

The paper is organized as follows. In Section 3.2, I provide a detailed derivation of the differential equation model of honey bee foraging. In Section 3.3 I analyze the properties of the model and provide theoretical results about its dynamics. In Section 3.4, I describe the results from fitting the model to data to obtain parameter values, obtaining bifurcation diagrams of forager allocation with respect to group composition, and performing sensitivity analysis to determine which parameters have the most prominent impact on colony preference for novel or familiar sources. Lastly, I summarize the results and indicate directions for future work in Section 3.5.

3.2 Model Derivation

3.2.1 Previous Empirical Work

I base my model on the experiments conducted by Cook et al. (2020) regarding forager allocation to Novel and Familiar feeders for different group compositions. Genetically selected High and Low attention worker honey bees were grouped in different proportions to form three types of colonies of 1300 individuals. In all colonies, half of the workers were control bees that were not selected or tested for attention profiles. In "High" and "Low" colonies, the other half consisted entirely of High and Low attention individuals, respectively. In "Mix" colonies, the remaining bees were High and Low in equal portions. Control colonies of equal size were used for comparison. Colonies were put in separate flight cages and given two feeders to forage from each day: a "Familiar" one, and a "Novel" one. Visits

to each feeder were recorded over time every day for three weeks. High colonies were found to forage more than Low colonies and to preferentially visit the Familiar source, whereas Low colonies exhibited no feeder preference. Low attention individuals within Low colonies showed no preference, but those in Mix colonies preferentially visited the the Familiar source. The data are publicly available (https://doi.org/10.6084/m9.figshare.9775955.v6).

3.2.2 Model Equations

Suppose that a colony has two sources available: one that is familiar (some foragers have visited it before) and one that is novel, like the experimental setting in (Cook et al. 2020). I assume that all foragers in the colony can be in one of three possible states: Waiting in the hive (W), exploiting the Novel source (N) or exploiting the Familiar source (F). Every forager has a "High attention" or "Low attention" profile that is genetically determined, and that is indicated for each of the thee categories by the subscript h or l, respectively. Thus, I have the six state variables shown in Table 1.

Consider a colony with P foragers, where a fraction α of them has a "High attention" profile and the remaining $(1 - \alpha)$ is "Low attention". I assume that the forager group size remains fixed during the foraging day, so I have a closed population. Similarly, the proportion α does not change over time since it is genetically determined.

I begin with a pool of W available foragers waiting in the hive. I denote W_h and W_l the number of High and Low attention bees respectively, so that $W = W_h + W_l$.

Scouting: Available bees may spontaneously leave the nest to *scout* for new food sources. Some of these searching bees might get lost and go back to waiting in the hive (Sumpter and Pratt 2003). However, some of them will successfully find food and begin foraging. I denote σ_h or σ_l the average rates at which High and Low attention bees scout

and find resources, respectively. A fraction q_i of the successful scouts of attention type $i \in \{h, l\}$ will exploit the familiar source, and the remaining $(1 - q_i)$ will exploit the novel one.

Recruiting: Bees that find a source may go back to the hive and recruit more foragers to that source. I denote by N and F the number of bees committed to the Novel and Familiar feeders respectively. In this model, all foragers committed to a source are recruiting for it. This is not always the case: bees may exploit a source without performing recruitment waggle dances (T. D. Seeley 1989)). Modeling this would require an additional "Dancing" or "Recruiting" state (see (Seeley, Camazine, and Sneyd 1991; Sumpter and Pratt 2003)). However, I stick to the simplest possible model of collective worker allocation (similar to Marshall et al. (2009) and Britton et al. (2002)) to gain some insight about the interaction of the two phenotypic groups. In an approach similar to Britton et al. (2002) model of recruitment for house-hunting, foragers of type i committed to source X recruit waiting foragers of type j at a rate

$$\beta_{ix} X_i W_j$$

where β_{ix} is the per capita rate of recruitment for type i bees.

Abandoning: Foragers exploiting a source will visit it repeatedly for some time before abandoning it to go back to the hive. The rate at which foragers of type i leave source X is δ_{ix}, with $1/\delta_{ix}$ being the average time that the bee stays committed to the source.

A diagram of the resulting model can be observed in Figure 8 and is governed by the equations in System (3.1)

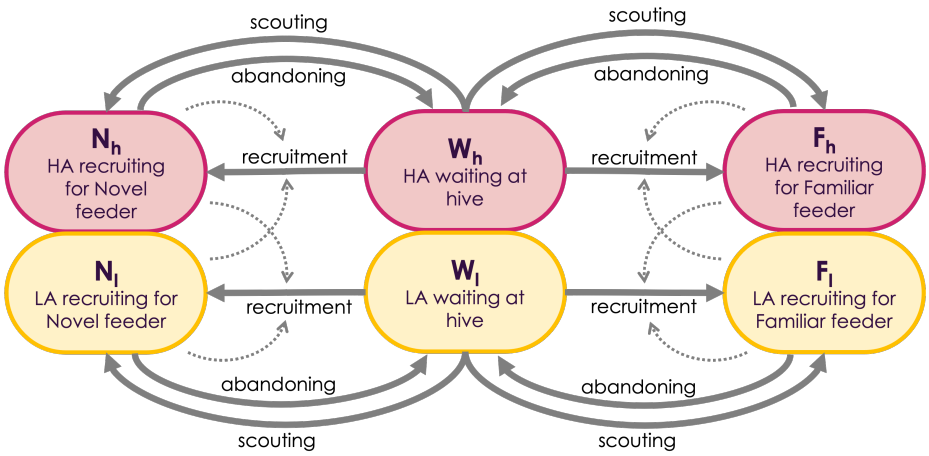

Figure 8. Diagram of the model transitions. Foragers become committed to a source by either independent discovery (scouting) or recruitment, and eventually abandon the source to go back to the hive.

High attention

$$\frac{dW_h}{dt} = \underbrace{\delta_{hn}N_h + \delta_{hf}F_h}_{\text{abandoning}} - \underbrace{W_h(\beta_{hn}N_h + \beta_{ln}N_l + \beta_{hf}F_h + \beta_{lf}F_l)}_{\text{recruiting}} - \underbrace{\sigma_h W_h}_{\text{scouting}} \tag{3.1a}$$

$$\frac{dN_h}{dt} = \underbrace{W_h(\beta_{hn}N_h + \beta_{ln}N_l)}_{\text{recruiting}} + \underbrace{\sigma_h(1-q_h)W_h}_{\text{scouting}} - \underbrace{\delta_{hn}N_h}_{\text{abandoning}} \tag{3.1b}$$

$$\frac{dF_h}{dt} = \underbrace{W_h(\beta_{hf}F_h + \beta_{lf}F_l)}_{\text{recruiting}} + \underbrace{\sigma_h q_h W_h}_{\text{scouting}} - \underbrace{\delta_{hf}F_h}_{\text{abandoning}} \tag{3.1c}$$

Low attention

$$\frac{dW_l}{dt} = \underbrace{\delta_{ln}N_l + \delta_{lf}F_l}_{\text{abandoning}} - \underbrace{W_l(\beta_{ln}N_l + \beta_{hn}N_h + \beta_{lf}F_l + \beta_{hf}F_h)}_{\text{recruiting}} - \underbrace{\sigma_l W_l}_{\text{scouting}} \tag{3.1d}$$

$$\frac{dN_l}{dt} = \underbrace{W_l(\beta_{ln}N_l + \beta_{hn}N_h)}_{\text{recruiting}} + \underbrace{\sigma_l(1-q_l)W_l}_{\text{scouting}} - \underbrace{\delta_{ln}N_l}_{\text{abandoning}} \tag{3.1e}$$

$$\frac{dF_l}{dt} = \underbrace{W_l(\beta_{lf}F_l + \beta_{hf}F_h)}_{\text{recruiting}} + \underbrace{\sigma_l q_l W_l}_{\text{scouting}} - \underbrace{\delta_{lf}F_l}_{\text{abandoning}} \tag{3.1f}$$

Name	Definition	Units
	State Variables	
W_h	Number of waiting High attention bees	ind.
N_h	Number of High attention bees at novel feeder	ind.
F_h	Number of High attention bees at familiar feeder	ind.
W_l	Number of waiting Low attention bees	ind.
N_l	Number of Low attention bees at novel feeder	ind.
F_l	Number of Low attention bees at familiar feeder	ind.
	Parameters	
α	Proportion of High attention bees	unitless
δ_{hf}	Abandoning rate of the familiar source by High attention bees	min^{-1}
δ_{hn}	Abandoning rate of the novel source by High attention bees	min^{-1}
δ_{lf}	Abandoning rate of the familiar source by Low attention bees	min^{-1}
δ_{ln}	Abandoning rate of the novel source by Low attention bees	min^{-1}
σ_h	Rate of successful scouting for High attention bees	min^{-1}
σ_l	Rate of successful scouting for Low attention bees	min^{-1}
q_h	Fraction of successful High attention scouts going to familiar source	min^{-1}
q_l	Fraction of successful Low attention scouts going to familiar source	min^{-1}
β_{hf}	Recruiting rate by High attention bees to familiar source	(ind. min) $^{-1}$
β_{lf}	Recruiting rate by Low attention bees to familiar source	(ind. min) $^{-1}$
β_{hn}	Recruiting rate by High attention bees to novel source	(ind. min) $^{-1}$
β_{ln}	Recruiting rate by Low attention bees to novel source	(ind. min) $^{-1}$

Table 1. Parameter definitions and dimensions for System ((3.1)). "ind."= number of individuals

In the following sections, I will perform mathematical analysis and simulations on this model to address the following questions: (1) What is the effect of group composition (α) on colony preference for novel or familiar sources? (2) What process in the foraging dynamics (scouting, recruiting, abandoning) most heavily impacts colony preference?

3.3 Mathematical Analysis

I start by analyzing basic properties about Model ((3.1)) to ensure that it is biologically meaningful. That is, all populations remain positive and finite. I will then analytically study

the long-term behavior of the model in specific cases to understand how forager allocation depends on the model's parameters. This analysis will be complemented with numerical simulations of the whole system under biologically realistic scenarios in Section 3.4.

Theorem 3.3.1. (Basic Dynamical Properties) *Model* (3.1) *is positive invariant and bounded in* $\mathbb{R}^6_+$. *Moreover, the population size* $P = \sum_{i=h,l} W_i + F_i + N_i$ *is constant over time.*

Proof. Let $(W_h, N_h, F_h, W_l, N_l, F_l) \in \mathbb{R}^6_+$. Then for $i, j \in \{h, l\}, i \neq j$

$$\begin{aligned}
\frac{dW_i}{dt}\Big|_{W_i=0} &= \delta_{in} N_i + \delta_{if} F_i \geq 0 \\
\frac{dN_i}{dt}\Big|_{N_i=0} &= W_h(\beta_{jn} N_j) + \sigma_i(1 - q_i) W_i \geq 0 \\
\frac{dF_i}{dt}\Big|_{F_i=0} &= W_i(\beta_{jf} F_j) + \sigma_i q_i W_i \geq 0
\end{aligned}$$

since all parameter values are nonnegative and $0 \leq q_i \leq 1$. It follows that Model (3.1) is positive invariant in $\mathbb{R}^4_+$ by Theorem A.4. in Thieme (2018).

Also note that the population P size remains constant over time, since

$$\frac{dW_i}{dt} + \frac{dF_i}{dt} + \frac{dN_i}{dt} = 0,$$

and therefore

$$\frac{dP}{dt} = \frac{d(\sum_{i=h,l} W_i + F_i + N_i)}{dt} = 0$$

In particular, since all group sizes are positive and their sum is constant, the model is bounded in $\mathbb{R}^6$. □

Theorem 3.3.1 guarantees that the equations in System (3.1) model the population in a biologically meaningful way, that is, no group size becomes negative or infinite. Moreover,

the fact that the derivatives in System ((3.1)) add up to 0 ensures that a constant population size P is maintained.

3.3.1 Homogeneous Population

First take a scenario where there is no phenotypic distinction inside the colony. This is qualitatively equivalent to taking $\alpha = 1$ in the model, thus virtually reducing it to the case studied by Britton et al. (2002). For simplicity, I remove the attention subindex from the variables and parameters. The equations are now

$$\begin{aligned}
\frac{dW}{dt} &= -W\beta_n N - W\beta_f F + \delta_f F - \sigma s W + \delta_n N_h \\
\frac{dN}{dt} &= W\beta_n N + \sigma s(1-q)W - \delta_n N_h \\
\frac{dF}{dt} &= W\beta_f F + \sigma s q W - \delta_f F
\end{aligned}$$

Since I assume that the colony size P does not change over time, then the system can be reduced to two dimensions. For convenience, define also

$$D_n := \sigma(1-q)\ ,\ D_f := \sigma q,$$

where D_n and D_f are the rates at which scouts discover the Novel and Familiar sources, respectively. Substituting,

$$\frac{dN}{dt} = (P-N-F)\beta_n N + D_n(P-N-F) - \delta_n N \tag{3.3a}$$

$$\frac{dF}{dt} = (P-N-F)\beta_f F + D_f(P-N-F) - \delta_f F. \tag{3.3b}$$

The system may also be normalized, dividing both sides of the equations by P. The resulting System (3.4) governs the change of the fractions $x = N/P$ and $y = F/P$ over time:

$$\frac{dx}{dt} = (1-x-y)\widetilde{\beta}_n x + D_n(1-x-y) - \delta_n x \tag{3.4a}$$
$$\frac{dy}{dt} = (1-x-y)\widetilde{\beta}_f y + D_f(1-x-y) - \delta_f y. \tag{3.4b}$$

where $\widetilde{\beta}_i = \beta_i P$ for $i \in \{x, y\}$.

Theorem 3.3.2. *The normalized System* (3.4) *for a homogeneous population with two sources has no periodic orbits in the region* $[0,1] \times [0,1]$

Proof. Let

$$\frac{dx}{dt} = f(x,y) = (1-x-y)\widetilde{\beta}_n x + D_n(1-x-y) - \delta_n x \tag{3.5}$$
$$\frac{dy}{dt} = g(x,y) = (1-x-y)\widetilde{\beta}_f y + D_f(1-x-y) - \delta_f y. \tag{3.6}$$

Now I use Bendixon-Dulac criterion to show that no periodic orbits exist. Let $\phi(x,y) = \frac{1}{xy} \in C^1$. It remains to show that $\dfrac{\partial(\phi f)}{\partial x} + \dfrac{\partial(\phi g)}{\partial y}$ does not change sign in the region $[0,1] \times [0,1]$:

$$f * \phi = \frac{(1-x-y)\widetilde{\beta}_n}{y} + \frac{D_n(1-x-y)}{xy} - \frac{\delta_n}{y}$$
$$g * \phi = \frac{(1-x-y)\widetilde{\beta}_n}{x} + \frac{D_f(1-x-y)}{xy} - \frac{\delta_f}{x}$$

which yields

$$\frac{\partial(\phi f)}{\partial x} = -\frac{\beta_n}{y} - \frac{D_n}{xy} - \frac{D_n(1-x-y))}{x^2 y} = -\frac{D_n + \beta_n x^2 - D_n y}{x^2 y}$$
$$\frac{\partial(\phi g)}{\partial y} = -\frac{D_f + \beta_f y^2 - D_f x}{y^2 x}$$

and lastly

$$\frac{\partial(\phi f)}{\partial x} + \frac{\partial(\phi g)}{\partial y} = D_f(-1+x)x + D_n(-1+y)y - xy(\beta_n x + \beta_f y)$$

which is 0 at $(0,0)$ and negative elsewhere in $[0,1]\times[0,1]$, since all parameters are non-negative. Thus, the existence of ϕ rules out the possibility of periodic orbits for System (3.4). □

Theorem 3.3.2 guarantees that a homogeneous population with two resource options, governed by System (3.4), will not oscillate stably between the two resources but rather assymptitically approach a stable allocation of foragers between resources. Simulations suggest that the full system ((3.1)) has equilibrium dynamics as well, i.e., no oscillations.

Theorem 3.3.3. *For identical sources ($\widetilde{\beta}_n = \widetilde{\beta}_f =: \widetilde{\beta}, D_n = D_f =: D, \delta_n = \delta_f =: \delta$), System* (3.4) *has a single equilibrium point*

$$x^* = y^* = \frac{1}{4}\left(1 - A - 2R - \sqrt{(1-A-2R)^2 + 8R}\right)$$

where $A = \delta/\widetilde{\beta}, R = D/\widetilde{\beta}$. This equilibrium is Locally Assymptotically Stable (LAS).

Proof. The nullclines of the system can be found by setting $\frac{dx}{dt} = 0$ and $\frac{dy}{dt} = 0$:

x nullcline:

$$y = -\frac{A_x x}{R_x + x} - x + 1$$

y nullcline:

$$x = -\frac{A_y y}{R_y + y} - y + 1$$

where

$$A_i = \frac{\delta_i}{\widetilde{\beta}_i}\ ,\ R_i = \frac{D_i}{\widetilde{\beta}_i}.$$

for $i \in \{x, y\}$. The equilibrium points of the system are at the intersections of the nullclines. When the sources are identical (the bees behave the same with respect to both), then I have

$$A_x = A_y = A\ ,\ R_x = R_y = R$$

and the nullclines are inverses. They intersect at a unique positive point along the line $y = x$, and the equilibrium value is

$$x^* = y^* = \frac{1}{4}\left(1 - A - 2R - \sqrt{(1 - A - 2R)^2 + 8R}\right)$$

The equilibrium is locally asymptotically stable. This can be seen by noting that the eigenvalues of the Jacobian matrix have the form

$$\lambda_1 = 1 - A - 2R - 4x^* \ , \ \lambda_2 = 1 - A - 2x^*$$

so they are both real for real values of x^*, and negative, since

$$\lambda_1 < \lambda_2 = \frac{1}{2}(1 - A + 2R - \sqrt{8R + (-1 + A + 2R)^2} < 0.$$

□

The phase portrait in Figure 9 summarizes the dynamics for the symmetric case. Since there is a unique equilibrium point in this case, Theorems 3.3.3 and 3.3.2 ensure that, for any positive population size, the allocation of foragers will converge to that point regardless of the initial conditions.

3.4 Numerical Results

The analysis in the previous section covered qualitative results about the general dynamics of the model. Now, in order to obtain quantitative conclusions about the system's behavior in realistic conditions, I perform parameter estimation using experimental data from Cook et al. (2020). With the resulting values, I perform numerical simulations, build

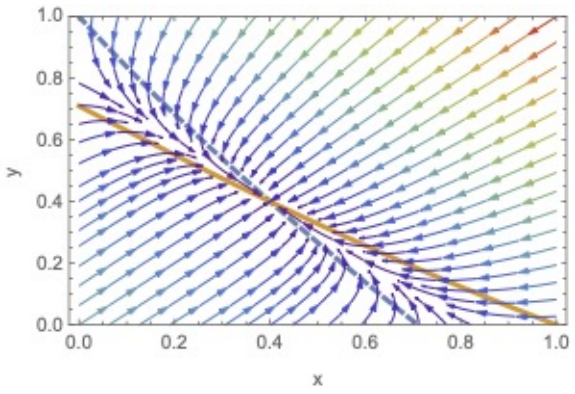

Figure 9. Phase diagram for the symmetric 2D system, with one stable equilibrium point. The *dashed* line is the y nullcline, while the solid orange line is the x nullcline. Since the system is symmetric, they are inverse functions and the equilibrium point lies in the line $x = y$. Darker arrow colors represent smaller magnitudes in the vector field. For this diagram, $A = 0.7$ and $R = 1$.

bifurcation diagrams of colony-level resource preference with respect to group composition, and perform sensitivity analysis to identify the main parameters that drive changes in colony-level foraging preferences.

3.4.1 Parameter Values and Experimental Data

In order to perform simulations and compare the model outcomes to experimental results, I determine parameter values by fitting the model to the time series data provided in Cook et al. (2020). The dataset is publicly available (https://doi.org/10.6084/m9.figshare.9775955.v6). To prevent over-fitting due to the large number of model degrees of freedom, I make some assumptions and reduce the number of parameters to fit. Namely,

- Population size: I estimate the foraging group size from the data in Cook et al. (2020), using an approach similar to Seeley, Camazine, and Sneyd (1991). I average the number of new visitors that go to the feeders every day, and thus get an estimate of

the number bees that participate in daily foraging. Based on this calculation, I set $P = 20$ foragers per day.

- Abandoning: I assume that all bees have the same rate of abandoning sources $\delta = \delta_{hf} = \delta_{hn} = \delta_{lf} = \delta_{ln}$. Mosqueiro et al. (2017) measured the average number of return trips to a feeder that a bee would perform before abandoning it (persistence), as well as the inter-visit time. From their values, I get

$$\delta = \frac{1}{(\text{Persistence})(\text{Inter-visit time})} \approx \frac{1}{2.86 \text{ trips} * 3.462 \text{ min}/ \text{ trip}} = 0.101 \text{ min}^{-1}$$

(see SI for more details). I fix δ at this reference value to perform the fitting.

- Scouting: Cook et al. (2019) showed that scouts in honey bee colonies have higher attention than other foragers. Since the population in the model is divided into two discrete "High" and "Low" types and I am interested in the collective results of this heterogeneity, I set $\sigma_l = 0$ and fit to the data for σ_h. This means that only High attention individuals scout in the model. A similar approach was taken in Mosqueiro et al. (2017), where a fixed proportion of bees performs scouting and recruiting, while the rest exclusively follow dances to discovered resources. I also fit for q_h, the proportion of successful scouts that commit to the Familiar feeder. This allows us to quantify individual bias or preference by High attention individuals towards the Familiar source. Note that, since I set $\sigma_l = 0$, the value of q_l is unused.
- Recruitment: I assume that all bees have the same rate of recruitment $\beta = \beta_{hf} = \beta_{hn} = \beta_{lf} = \beta_{ln}$ and estimate its value through model fitting. Cook et al. (2020) found that most recruitment and following acts are performed by Low attention individuals in colonies where there is an equal number of High and Low attention individuals. However, High attention bees dance more vigorously and more of their dances are followed. This does not clearly indicate a difference in the overall recruitment rates by High and Low individuals. Moreover, I don't expect a difference between recruitment

Name	Value	1 SD interval	Source
β	0.00576 (ind.min)$^{-1}$	[0.00567 , 0.00583]	Fitted
σ_h	0.00205 min^{-1}	[0.00171 , 0.00246]	Fitted
q_h	0.663	[0.643 , 0.685]	Fitted
δ	0.101 min^{-1}		(Mosqueiro et al. 2017)
P	20 ind.		Data from Cook et al. (2020)
α	62.5%, 37.5%, 12.5%, 25%		(Cook et al. 2020), expert elicitation

Table 2. Parameter values used in simulations. Note that I use $\delta = \delta_{hf} = \delta_{hn} = \delta_{lf} = \delta_{ln}$, and $\beta = \beta_{hf} = \beta_{hn} = \beta_{lf} = \beta_{ln}$. I also assume that only High attention scout, so $\sigma_l = 0$ and q_l is not needed.

rates to Novel and Familiar sources by Low attention individuals because they attend equally to novel and familiar information (Cook et al. 2019) and the feeders are identical in quality. While there could be a difference in recruitment by High attention bees to Novel and Familiar feeders, it has not been quantified in previous literature.

In order to fit the model to data, I first obtain the average daily time series of visits to the Novel and Familiar feeders from Cook et al. (2020). I obtain four datasets, one for each colony type: High, Mix, Low and Control. Each dataset stores two average time series, one for each feeder. I fit the model to all four datasets simultaneously using the Graphical Monte Carlo method. Since the observations are count data, I calculate the negative log-likelihood statistic for each dataset and minimize the sum of the four. For this, I run the model with the different α values corresponding to the estimated proportion of High attention individuals in each of the four colony types. These values are $\alpha = 62.5\%$, 37.5%, 12.5% and 25% for High, Mix, Low and Control colonies, respectively (see SI for details). The best-fit parameters are shown in Table 2. Details on the fitting process can be found in the SI.

The value of q_h quantifies the bias of individual High attention bees to commit to the Familiar source. The estimate shows that about 66% of successful scouts will commit to

the Familiar source instead of the Novel one. This might be interpreted as scouts finding both sources and choosing to initiate recruitment for the Familiar one more often, or by most scouts remembering the general location of the Familiar resource and flying straight to it to initiate recruitment (without comparing both sources). In any case, the fact that the estimate is multiple standard deviations away from random chance implies that scouts learn to recognize the Familiar feeder and biasedly commit to it.

The results of simulations with the best-fit model parameters are shown in Figure 10. Compared to High and Mix colonies, recruitment to both feeders is slower in Low and Control colonies and it takes more time for the system to reach equilibrium, that is, for distribution of foragers between the two feeders to stabilize. High and Mix colonies present a fast build-up of foragers in both feeders, population at Familiar grows and stabilizes quickly. Thus, the time for convergence increases with α. These transients suggests why it might be adaptive for colonies to maintain a High attention proportion that is close to the Control type (about 25%). Too many Low attention individuals can be disadvantageous if resources are ephemeral, since recruitment to floral patches would be slow and flowers may be available for only a portion of the day (Thomas D Seeley 1995). Conversely, too many High attention individuals can lead the colony to allocate too many foragers to exploitation of familiar resources too fast, and loose flexibility to explore novel resources that might be better in quality. In fact, High attention individuals are characterized by high attention and poor reversal learning, which is a liability for keeping track of quality changes. Thus, they may lock the colony on exploiting a relatively poor source by fixating recruitment to a site that is familiar but no longer profitable.

Figure 11 shows the time series of the cumulative number of visits to both feeders, as an indicator of the average foraging activity in a day. In line with the experiments, High colonies are more active than the others, and the foraging activity decreases when α does. It

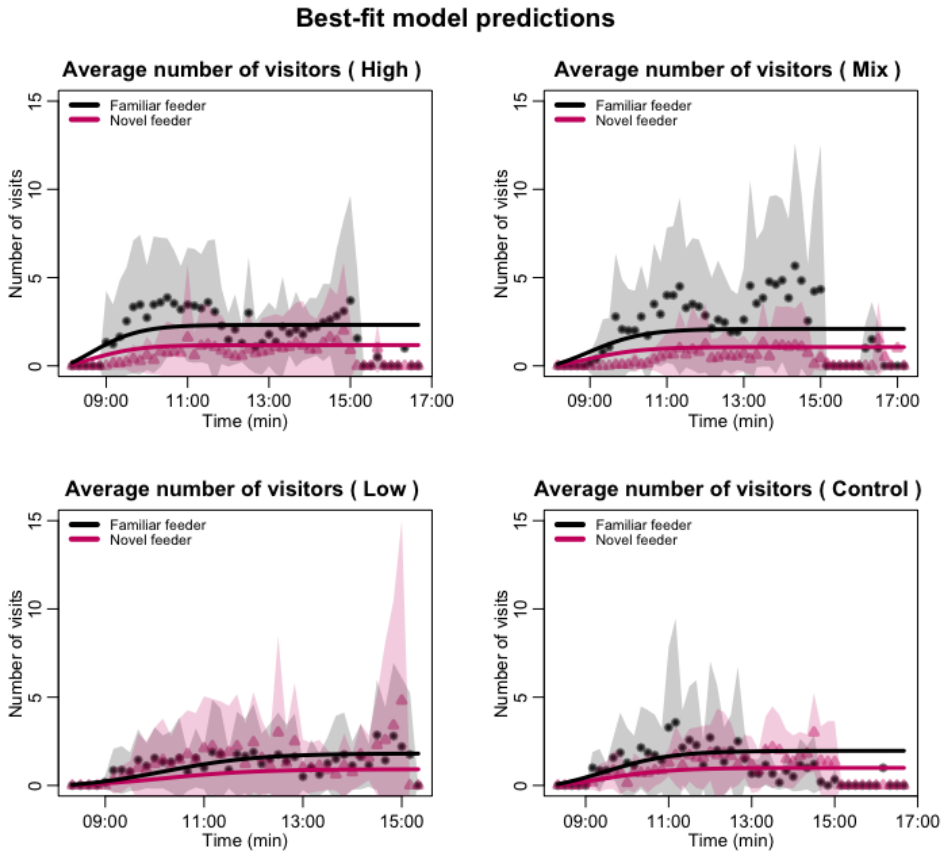

Figure 10. Best fit of the model to the four datasets for High, Mix, Low and Control colonies. *Circles* and *triangles* represent the average number of visits to the Familiar and Novel feeders, respectively, from the data in Cook et al. (2020). Bands represent one standard deviation from the average. *Solid lines* show the best-fit model simulation for each alpha value. The parameter values used are in Table 2

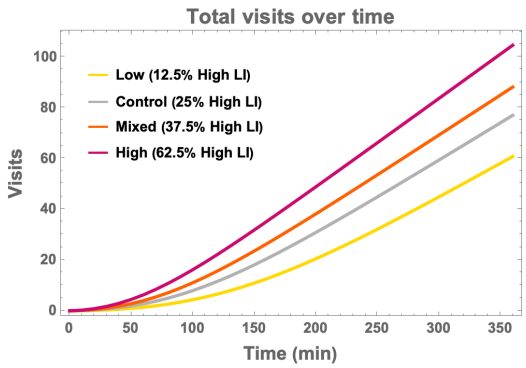

Figure 11. Time series of the cumulative number of visits to both feeders.

seems reasonable to expect colonies that forage to more collect more resources, and thus it may appear counter-intuitive to see that Control colonies (representative of small wild colonies) present relatively low foraging activity. However, foraging is a risky activity for workers, especially in extreme weather conditions (like the summer in Arizona, when the experiments were conducted). Thus, it might be adaptive for the group composition to yield moderate foraging activity, especially for small colonies that are less robust to loss of workers.

3.4.2 Effect of Group Composition on Collective Preference

Figure 12 shows the bifurcation diagram of the system's equilibirum with respect to the proportion of High attention individuals in the group (α). The diagram shows that only a very small proportion of High attention individuals with moderate individual preference for the Familiar source is required for producing collective preference. Nothing in the dynamics of Low attention individuals yields a distinction between the sources except recruitment by High attention bees, so the difference between visits to the Familiar and Novel feeders comes exclusively from the biased commitment of scouts to the Familiar

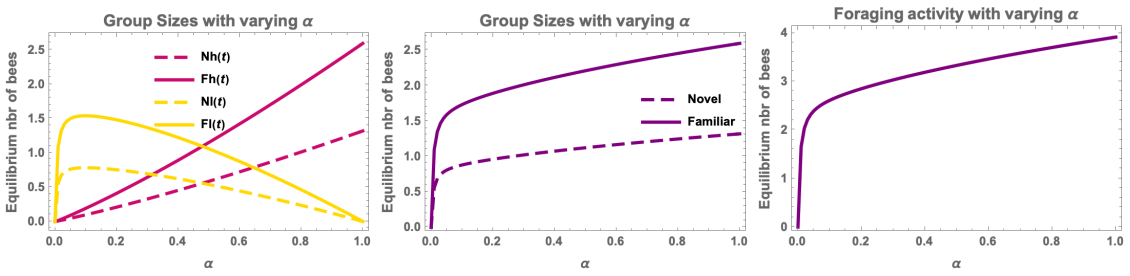

Figure 12. Bifurcation diagram of the model's equilibrium with respect to the proportion of High attention individuals in the colony (α).

source. Thus, Low attention individuals amplify the individual bias of High attention scouts to generate collective tendency to exploitation of Familiar sources. Note that the difference between the equilibrium number of workers at the Familiar and Novel feeders, regardless of their phenotype, also increases with α, and so does the total number of active foragers at equilibrium.

The bifurcation diagram allows us to infer the behavior of the system at equilibrium as α varies. However, in order to better compare these results to literature, I examine the behavior or the *cumulative* number of visits to each feeder after an average day of foraging. In fact, preference in Cook et al. (2020) is measured as the difference in the total visit count to each feeder at the end of the day. Experimental results show preference for High and Mix colonies, but not in Low or Control colonies. The model captures this trend of increasing collective preference with α, although it over-estimates preference in Low and Control colonies (see Figure 13). However, at the level of High and Low attention individuals within colonies, the model deviates from experimental observations. According to the experiments, preference among High attention individuals after 6 hours is extremely small and similar for Low and Control colonies, while it is large and virtually indistinguishable between High and Mix colonies (see left panel in Figure 14). In contrast, the model predicts a gradual increase in preference among High attention individuals as α increases (see Figure 15). Moreover,

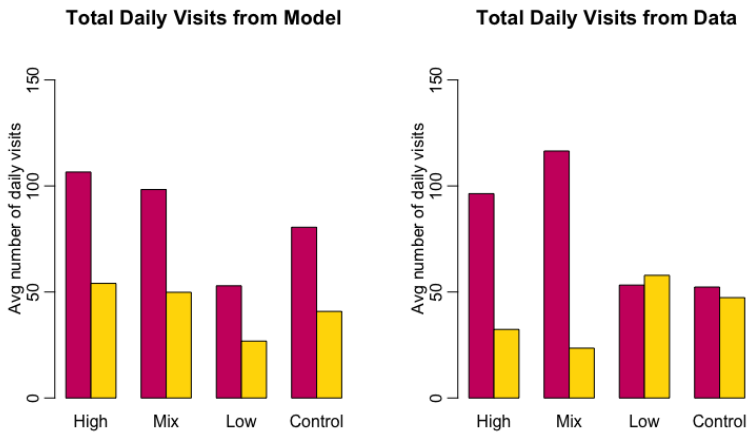

Figure 13. Average cumulative number of visits to the Novel (in yellow) and Familiar (in red) feeders after 6 hours of foraging for High, Mix, Low and Control colonies. The left panel shows the model results. The right panel shows experimental results using the dataset in Cook et al. (2020)

the data show no preference among Low attention individuals in Low colonies (see right panel in Figure 14), but a marked preference for Low attention bees in Mix colonies. Instead, the model shows the largest preference among Low attention individuals for low α values and a comparatively lower preference for Low attention bees in Mix colonies (see left panels in Figure 15)

However, notice that Low attention individuals in Control colonies exhibit an increased preference for the Familiar feeder around the middle of the foraging day (see Figure 14), which then decays to low values after 6 hours. This observation is relevant because, outside the experimental setting where feeders are fixed and available for the whole day, floral patches in the wild might only be available for a portion of the day. Thus, the initial portion of the foraging dynamics in the data is worth studying separately. I examine the model results for a shorter time interval (3h hours) and compare to experimental observations (see

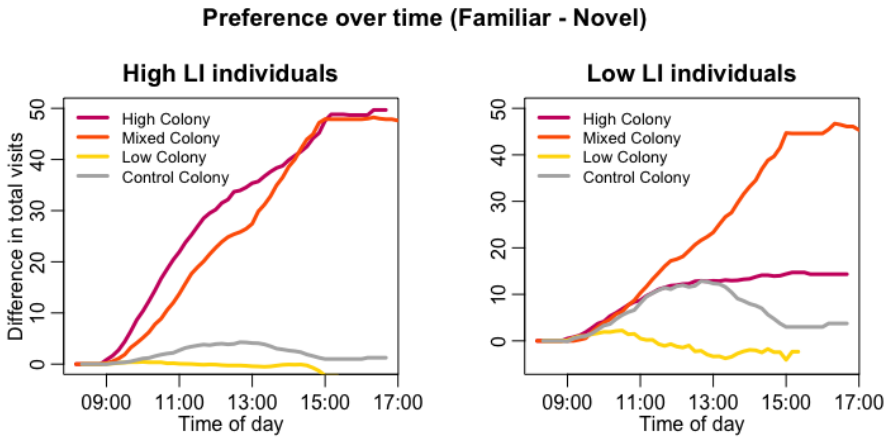

Figure 14. Time series of preference, defined as the difference in the cumulative average number of visits to the Familiar and Novel feeders, in the experimental setup from Cook et al. (2020). The left and right panels show preference over time for High and Low attention individuals, respectively, in each of the four colony types.

right panels of Figure 15). The preference patterns of High and Low attention individuals in different colonies are considerably better captured now. In both the data and the model, preference among High attention individuals increases with α (see left panel in Figure 14 and right panel in Figure 15). Contrastingly, preference among Low attention individuals is largest for Mix colonies in both experiments and the model (the maximum difference in the model occurs at α =36%, near the estimated 37% for Mix colonies). However, the model fails to predict the lack of preference in Low colonies and generally underestimates the magnitude of preference values.

3.4.3 Sensitivity Analysis

I now aim to identify the processes within the foraging dynamics that impact collective preference the most. In order to do this, I perform sensitivity analysis of preference, defined as difference between total number of visits to Familiar and Novel feeders after 6 hours of

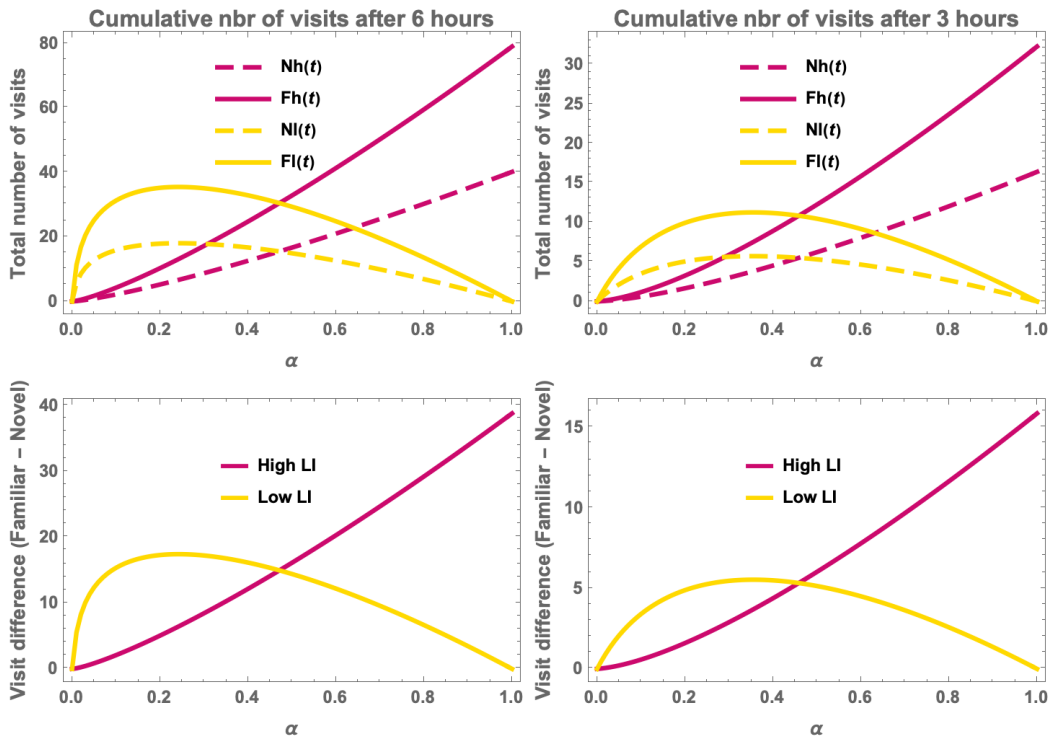

Figure 15. Effect of group composition on the cumulative number of visits to the Familiar and Novel feeders after 6 hours (left panels) or 3 hours (right panels). The horizontal axis shows α, the proportion of High attention individuals in the colony. The top and bottom panels show, respectively, the total number of visits to each feeder (*top*) and the difference between visits to the Familiar and Novel feeders, or preference (*bottom*). A fraction of 36% High attention yields the maximum preference among Low attention individuals after 3 hours.

foraging (following Cook et al. (2020)), to each of the model's parameters. I calculate the sensitivity indices by perturbing each parameter by 1% while keeping the others fixed and computing the percent change in preference with respect to the base value with unperturbed parameters (Cacuci, Ionescu-Bujor, and Navon 2005). The results are summarized in Figure 16.

The High attention parameters (indexed by h) have the most impact in High colonies, but this is reversed to Low attention parameters in all other colonies, where the majority of the population is Low attention type. Preference is most sensitive to recruitment (β) for lower

α (Low and Control colonies), but most sensitive to persistence (δ) for larger α (High and Mixed colonies). Thus, as the number of High attention individuals increases, the principal process driving preference switches from recruitment by Low attention bees to abandoning by High attention bees (inversely proportional to persistence). This is consistent with the fact that only High attention individuals have an individual bias or preference in the model, so collective preference depends largely on amplification through recruitment by Low attention individuals for Low and Control colonies. For High colonies, most of the population is inherently biased to committing to the Familiar feeder, so collective preference relies on maintenance of this commitment by the most abundant attention phenotype, represented by δ_{hf}.

In addition, the scouting bias q_h for High attention bees has a larger sensitivity index with respect to other parameters in Low colonies than all other colony types. Since there is only a small portion of High attention individuals, collective preference is mainly a product of amplification, and changes in q_h are consequently amplified more than in other colonies.

3.5 Conclusion

This paper presents the first mathematical model of self-organized foraging in honey bees that explicitly incorporates their learning phenotypes and relates them to foraging preferences. Results qualitatively reflect the observed increased foraging activity in colonies with higher proportions of High attention foragers (Figure 11), as well as the preference for familiar sources in such colonies (Figure 13). The model reproduced the preferences of High and Low attention individuals within colonies for short foraging times (3 hours) but deviated from the data for longer foraging times (6 hours) (Figure 15).

Towards answering my first question, about how colony-level differences in collective

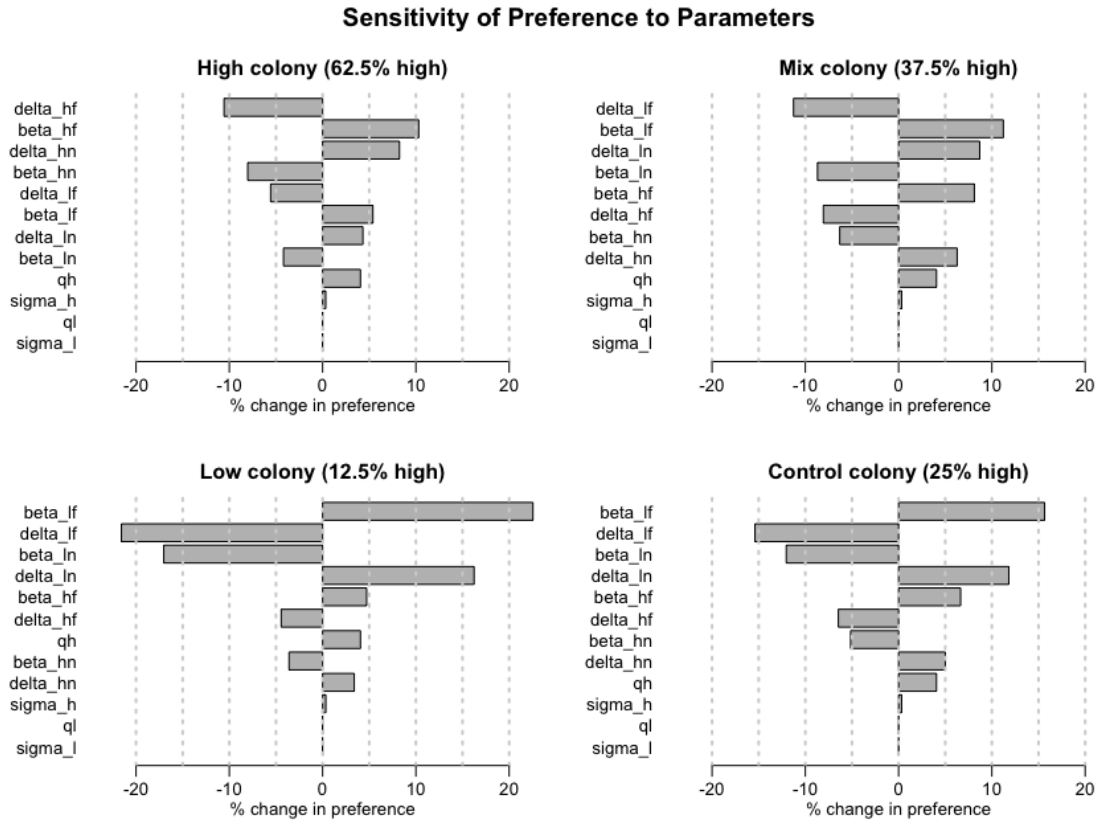

Figure 16. Local sensitivity analysis for preference with respect to the model parameters. The sensitivity indices are approximated as the percent change in preference in response to a 1% change in each of the model parameters, keeping all others fixed.

attention allocation emerge from different group compositions, this mechanistic model validates the empirical hypothesis that even low individual preference or bias, amplified by efficient communication, is enough to produce collective preference at the observed levels in different colonies (see Figure 12 and Figure 15). A better understanding of *how* collective differences emerge, however, is related to the second question: which individual processes are the main drivers colony preference for familiar resources over novel ones or viceversa? The sensitivity analysis in Section 3.4.3 revealed the processes to which collective preference is most sensitive, and examined how group composition affects the impact of different foraging parameters on preference. I found that recruitment is the main

parameter driving collective preference for low proportions of High attention individuals, but abandoning rates become more relevant for higher proportions (Figure 16). Thus, as the proportion of High attention bees increases, the collective tendency to exploit familiar resources becomes more sensitive to the individual decisions to stop exploiting a given source than to the social interactions of recruitment.

The framework introduced by this model can be used to study several aspects of individual variation and how it affects collective decisions. I showed here a scenario with variations in individual tendency to scout and likelihood of commitment to different sources. However, the same model could be used to to analyze differences in persistence across workers, like in Mosqueiro et al. (2017), (changing the abandonment rates), or recruitment. Variation exists across all of those processes, and that the observed colony-level variation is a product the interaction between all of them. Using the general framework presented here, different mechanisms could be studied in order to support or discard hypotheses about the origin of the collective variation in activity and preference. Modeling efforts in identifying the most relevant parameters in the collective decision–making process, in hand with experimental observations determining the scale at which they vary, are fundamental to understand how individual behaviors are integrated into collective cognition.

Chapter 4

A MATHEMATICAL FRAMEWORK FOR ADAPTIVE COLLECTIVE DEFENSE: CRISIS RESPONSE IN SOCIAL-INSECT COLONIES

4.1 Introduction

Efficiently allocating resources to tasks is an important function for any biological organism. At a fundamental level, resources necessary for biological function are both limited and have a bounded replenishment rate (Caetano-Anollés et al. 2022). Consequently, there are significant opportunity costs concomitant with any over-supply of resources to a task. Furthermore, resource deficits can spontaneously occur with previously balanced allocations if surrounding conditions suddenly change. These potential problems are amplified when allocated resources are inflexible or unable to be quickly reallocated from one task to another. Eusocial-insect colonies are valuable models to study these fundamental problems as their size (relative to other biological collectives) allows individuals to be directly observed and they can exhibit high degrees of diversity in worker specialization and must shape worker demographics in a completely decentralized manner (Camazine et al. 2003; Gordon 2002; Beshers and Fewell 2001). Intricate adaptive colony dynamics and sophisticated division of labor emerge exclusively from local interactions between individuals without global information and result in a highly complex, distributed organization that is in certain ways superior to hierarchical organizations with central control (Fewell 2003; Holbrook et al. 2009).

The efficient allocation of finite resources to the task of colony defense is an important problem to eusocial insects, which accumulate resources internally that can become targets

for kleptoparasitic robbing and raiding behavior by other insects (Baudier et al. 2019). Insect societies in general often exhibit some degree of specialization; for example, tasks are commonly determined by age, which is known as age-based polyethism and corresponds to specialization inside an age group (Baudier et al. 2019; Thomas D. Seeley 1982). As with any other task, increased use of specialized workers for defense is subject to a flexibility–specialization trade-off. On the one hand, specialization can increase group-level energetic efficiency in the long term (Jeanne 1986), but it also slows reactions to sudden changes (Dornhaus 2008), like unexpected threats (e.g., large raids from other colonies). For the case of social insects, extreme specialization takes the form of morphologically distinct individuals that perform a narrow range of tasks very efficiently but can be costly to produce. On the other hand, individuals that can flexibly switch between tasks according to demand allow a colony to quickly adapt to emergency needs, manifested in acute changes in task demand (Dornhaus 2008; Jongepier and Foitzik 2016), but these flexible generalists are individually less capable for some or all of the tasks in their repertoire. In this work, I examine how a hierarchy of mechanisms in eusocial-insect colonies can regulate task allocation to maintain colony growth and reproduction while dedicating sufficient workforce to group defense in response to emergent threats posed by their dynamic environment.

Tetragonisca angustula stingless bees, which employ a combination of defensive strategies found across other social insects and colonial animals: 1) morphological specialization (distinct soldiers (majors) are produced over weeks); 2) age-based polyethism (young majors transition to guarding tasks over days); and 3) task switching (small workers (minors) replace soldiers within minutes under crisis). To better understand how these timescales of reproduction, development, and behavior integrate to balance defensive demands with other colony needs,

The stingless bee *Tetragonisca angustula* is an ideal model organism to study the

flexibility–specialization trade-off in collective defense as colonies employ multiple task-allocation mechanisms ranging over different timescales and degrees of flexibility (Baudier et al. 2019). Although worker morphological specialization is very rare among bees, *T. angustula* colonies produce a minority of large-bodied workers (*majors*) that are more efficient at nest defense than their smaller nestmates (*minors*) but also require more resources to be produced (Grüter et al. 2012; Jones et al. 2012; Zweden et al. 2011). The size and future developmental trajectory of adult bees at eclosion (i.e., emerging in adult form from the pupal case) depends on their earlier feeding schedule while larval brood, which in turn is determined by their rearing location and the feeding behavior of nurse bees (Segers et al. 2015). Moreover, colonies exposed to a higher frequency of threats produce a larger proportion of majors (Segers, Zuben, and Grüter 2016), likely due to adaptive changes in how those brood are reared in response to the increased threat. In addition to morphological specialization, age-based polyethism is also present in the form of age-dependent task allocation. Young workers of all sizes perform mostly brood care and nest maintenance whereas older bees (about two weeks old) tend to work outside the nest, either foraging in the case of minors or guarding in the case of majors (Hammel et al. 2015). While age-based polyethism provides the colony some degree of flexibility, crisis situations that require a fast response are addressed through a third mechanism involving behavioral plasticity of minors. In response to guard loss, minor workers replace guards within minutes (Baudier et al. 2019), which provides a temporary defensive reinforcement to the colony during the relatively longer developmental period while new major guards are produced.

Several quantitative models of task allocation have been studied for eusocial insects (Beshers and Fewell 2001), but very little work has focused on the balance between colony growth and defense mechanisms. Kang and Theraulaz (2016) developed a multi-compartment differential-equation model for division of labor in social insect colonies that,

although not focusing on defense, included age-based polyethism and task switching as mechanisms regulating worker allocation. Their model does not account for morphological specialization and assumes that all tasks contribute equally to the eclosion of new adults. In a different study, Aoki and Kurosu (2003) explicitly modeled the production of morphologically distinct, non-reproductive soldiers based on their productivity for the colony. That model does focus on the balance between defense and reproduction, but the chosen organism has no allocation flexibility in terms of age-based polyethism or task switching. Recent work by Strickland et al. (2019) uses stingless bees as inspiration to develop an algorithm for allocation of guarding tasks in robots. Their study explores the value of a heterogeneous guarding force with different defense tasks for both robotic swarms and stingless bees in terms of performance, but it is not concerned with group growth or reproduction.

In order to better understand how social insects regulate colony growth and defense efficiently, I have designed a demographic model of task allocation in *T. angustula* colonies. The proposed model uses a system of differential equations that explicitly reflects processes occurring at three distinct timescales (i.e., morphological specialization, age-based polyethism, and behavioral plasticity) in relation to colony defense and growth. I use the model to study plausible conditions under which the studied defense mechanisms work in tandem to improve collective defense. Specifically, I address the following questions:

1. How do the parameters regulating morphological specialization, age-based polyethism, and behavioral plasticity impact the colony size and task allocation within the colony?
2. What degree of behavioral plasticity allows the colony to transiently compensate for loss of defenses without maintaining an unnecessary population of inefficient minor guards?

The remainder of the paper is organized as follows. In Section 4.2, I derive an ordinary-differential-equation model to describe the population dynamics and task allocation within

T. angustula stingless bee colonies. In Section 4.3, I provide a theoretical analysis of the model's dynamical properties. In Section 4.4, I study the interaction between morphological specialization, age-based polyethism, and behavioral plasticity for colony survival, growth and task allocation through bifurcation analysis and simulations in biologically realistic scenarios. Lastly, I include concluding remarks and future work in Section 4.5.

4.2 Model Derivation

In this section, I derive a dynamical model of task allocation in stingless bee colonies that includes: 1) morphological specialization, 2) age-based polyethism, and 3) task switching.

4.2.1 Worker Types and Task Types

I assume that all adult bees in a colony are either large-bodied majors (i.e., specialized for defense tasks) or smaller minors according to their body size at eclosion. This accounts for the morphological specialization observed by Grüter et al. (2012) and Segers et al. (2015). Because my focus is defense regulation, I consider only two types of tasks that majors and minors may perform: guarding or non-guarding. Both majors and minors begin their lives doing non-guarding tasks, but majors mature twice as fast as minors and spend the last half of their lives as defensive "soldiers" in guarding tasks (*guards* herein). However, minors only transition to guarding when there are sudden deficits in guarding and otherwise perform only non-guarding tasks. Thus, at any time, all adult individuals can be divided among four possible compartments:

- Major Non-guard (W): large-bodied bee performing non-guarding tasks
- Major Guard (G): large-bodied bee performing guarding tasks

- Minor Non-guard (w): smaller-bodied bee performing non-guarding tasks
- Minor Guard (g) smaller-bodied bee performing guarding tasks

Based on context, the variables (W, G, w, g) will refer to either the number of adult bees in each compartment or the name of the compartment itself. With this nomenclature, the population size P, subject to demographic changes, can be written as

$$P := W + G + w + g.$$

Next, I describe the dynamic fluxes into and out of these four compartments, which are summarized in Figure 17.

4.2.2 Production of New Major and Minor Workers

The queen lays eggs at an average rate Λ; however, I assume that the $G + g$ adult bees performing guarding tasks do not contribute to brood care. This assumption is based on the experimental observation that guards (G and g) mainly patrol, hover, or stand near the nest entrance (Hammel et al. 2015). So the fraction of eggs that successfully eclose to adults depends on the size of the working non-guard population, $W + w$. Consequently, a colony consisting entirely of guards (i.e., $P = G + g$) and no workers (i.e., $W = w = 0$) will not have a positive growth rate in this model, and so there is a trade-off between growth and defense that manifests through devoting resources to guards or workers. To describe the ecolsion rate of new adults, I follow Kang and Theraulaz (2016) and use a Hill function (Goutelle et al. 2008):

$$\Lambda \frac{(W+w)^2}{(W+w)^2 + b^2} = \frac{1}{1 + \left(\frac{b}{W+w}\right)^2}$$

where the half-saturation constant b represents the number of non-guarding workers ($W + w$) required for the eclosion rate to be half of the egg-laying rate Λ. The Hill exponent of 2

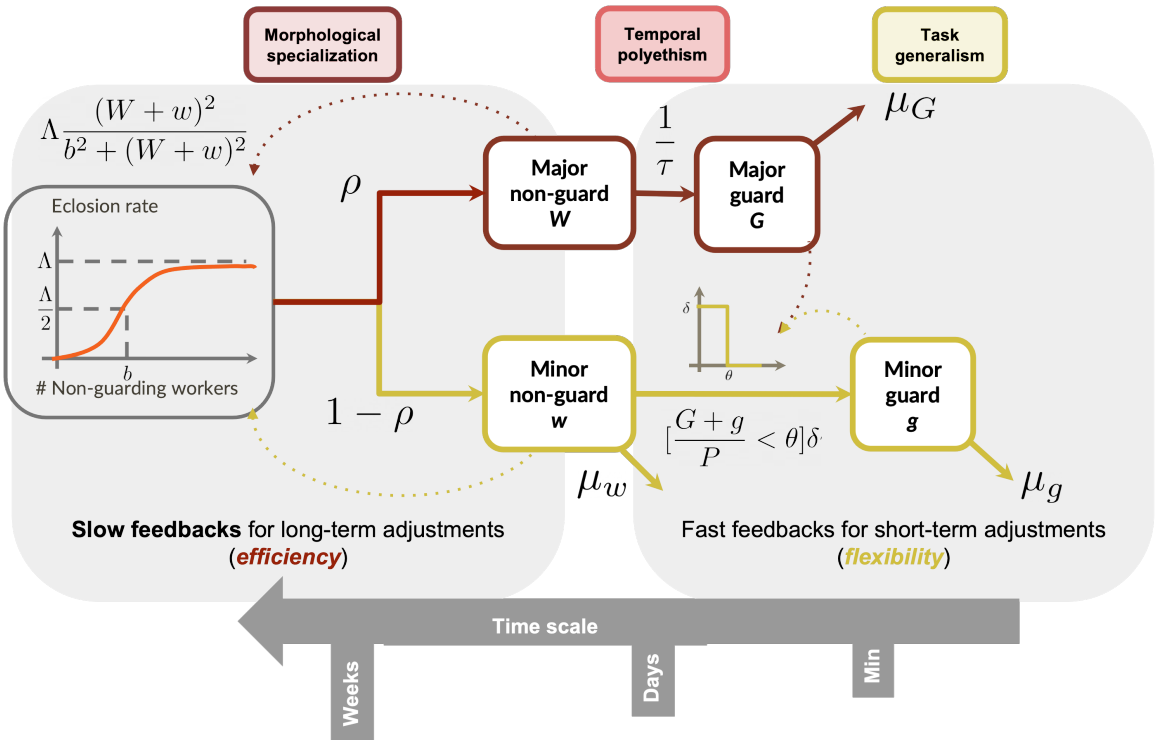

Figure 17. Model diagram. Eggs are laid at a constant rate Λ by the queen and a fraction of those, dependent on the non-guarding population, successfully eclose as adults (see text for more details). A percent ρ of the newborns are majors, the rest are minors. Young majors are workers inside the nest and transition to guarding tasks after a maturation time τ. Then they die at a rate μ_G. Minors usually perform non-guarding tasks and die at a rate μ_w, but if the proportion of guards in the colony drops below a threshold θ, they replace them as guards at a rate δ. Minor guards die at a rate μ_g. The Iverson (1962) bracket $[\cdot]$ is 1 when its predicate argument is true and 0 otherwise.

provides a type-III functional response where eclosion rate accelerates at low numbers of non-guard workers (i.e., when there is a high demand for nurses and foragers) but then has diminishing marginal returns at high numbers of workers (i.e., as brood-rearing demand is met).

Experimental studies have shown that the size of the adult bees is determined before eclosion by the feeding schedule that they experience as larvae (Segers et al. 2015) and that colonies exhibit two distinct body sizes corresponding to major and minor bees (Grüter et al. 2012). Guided by these facts, I assign a proportion $\rho \in (0, 1)$ of the newly emerged

adults to be majors (large-bodied bees, specialized for defense) and the remaining $1-\rho$ to be minors (smaller-bodied bees, primarily taking part in non-guarding tasks).

Evidence suggests that colonies can regulate the proportion of majors produced in the long term according to environmental threats (Segers, Zuben, and Grüter 2016). However, bees need approximately 5–6 weeks from egg to eclosion plus an additional 2 weeks of maturation to become guards, which means that rearing a new generation of guards requires 7–8 weeks (Segers, Zuben, and Grüter 2016). Thus, changes in the proportion of majors take approximately 2 bee lifespans to have an effect. In this model, I assume a constant proportion ρ and manipulate this parameter to observe its effect on system trajectories.

4.2.3 Developmental Dynamics of Majors

Majors perform in-nest tasks or foraging when they are young and transition to guarding when they reach middle age (Hammel et al. 2015). Once they start guarding, going back to non-guarding tasks is rare (Baudier et al. 2019). Recall that W and G represent the number of majors performing non-guarding and guarding tasks, respectively; I let τ be the average W-to-G maturation time for majors to start guarding after eclosion. Because majors transition into guarding at a relatively young age, I have omitted a mortality rate for major non-guards for simplicity. Mature major guards (G) die at a rate μ_G (see Figure 17). Thus, the life of majors is modeled by the system:

$$\begin{cases} \dfrac{dW}{dt} = \underbrace{\Lambda \dfrac{(W+w)^2}{b^2+(W+w)^2}\rho}_{\text{eclosion}} \underbrace{-\dfrac{1}{\tau}W}_{\text{maturation}} \\ \dfrac{dG}{dt} = \underbrace{\dfrac{1}{\tau}W}_{\text{maturation}} \underbrace{-\mu_G G}_{\text{death}} \end{cases} \tag{4.1}$$

The parameter τ implements age-based polyethism in the model, which is the correlation of age and task within insect colonies. It determines the time needed to raise a new generation

of guards, and thus it delays the effect of changing the proportion of majors produced, ρ, on colony defense. I will study how τ interacts with ρ in determining the availability of guards for the colony and how these two parameters relate to the process of guard replacement by minors in case of emergency.

4.2.4 Developmental Dynamics of Minors with Behavioral Switching

Under normal conditions, minor workers perform in-nest tasks during young and middle age and switch to foraging when they reach old age (Hammel et al. 2015). I denote by w the number of working minors in all of those tasks and μ_w their average mortality rate. The nominal life of a worker is therefore represented by:

$$\frac{dw}{dt} = \underbrace{\Lambda \frac{(W+w)^2}{b^2+(W+w)^2}(1-\rho)}_{\text{eclosion}} \underbrace{-\mu_w w}_{\text{death}}. \tag{4.2}$$

However, in the absence of guards G (e.g., due to a crisis where guards are lost after a raid by an invading colony), minors adopt guarding behavior. When guards were removed from a natural colony by Baudier et al. (2019), tracked minors were observed replacing guards just a few hours later. Thus, non-guarding minors w can transition to guarding minors g under the right conditions. To model this behavioral switch in minors, I assume that replacement occurs only when the total number of guards $G+g$ in the colony drops below a fraction θ of the total population P (i.e., when $(G+g)/P < \theta$). This characteristic models the scaling of guard demand with colony size. Furthermore, eusocial insects are known to exhibit density-dependent behaviors that are responsive to changes in local encounter rate . Consequently, the guard density $(G+g)/P$ may be able to be inferred by individual workers using only local encounter information. Thus, I assume that the rate of replacement is a function of the per-capita probability of finding a guard among all nestmates ($(G+g)/P$).

Based on the typical fraction of guards in wild colonies (Hammel et al. 2015), the nominal value of this ratio is between 1 and 6%; I assume that workers have the ability to detect drops in guard ratio to below this value.

For simplicity, and to emphasize the difference of timescales between the behavioral replacement and developmental maturation processes, I also assume that replacement is binary and instantaneous; it is non-existent while $\frac{G+g}{P} > \theta$, and it happens at a rate δ when $\frac{G+g}{P} \leq \theta$. So the behavioral w-to-g replacement rate is:

$$\delta \left[\frac{G+g}{P} \leq \theta \right] \tag{4.3}$$

where $[\cdot] : \{T, F\} \mapsto \{0, 1\}$ denotes the Iverson bracket (Iverson 1962). That is,

$$\left[\frac{G+g}{P} \leq \theta \right] = \begin{cases} 1, & \frac{G+g}{P} \leq \theta \\ 0, & \text{otherwise} \end{cases}.$$

Thus, combining ((4.2)) and ((4.3)), the general population dynamics of minor workers (guarding and non-guarding) facing potential crisis situations is the Variable Structure System (VSS) (Young and Özgüner 1999):

$$\begin{cases} \dfrac{dw}{dt} = \Lambda \dfrac{(W+w)^2}{b^2 + (W+w)^2}(1-\rho) - \mu_w w \underbrace{- \left[\dfrac{G+g}{P} \leq \theta \right] \delta w}_{\text{replacement}} \\ \dfrac{dg}{dt} = \underbrace{\left[\dfrac{G+g}{P} \leq \theta \right] \delta w}_{\text{replacement}} \underbrace{- \mu_g g}_{\text{death}} \end{cases}. \tag{4.4}$$

In this system, the switching behavior acts as a bang–bang control (Bellman, Glicksberg, and Gross 1956) on w-to-g replacement so as to regulate the guard ratio $(G+g)/P$ toward threshold parameter $\theta \in (0, 1)$. The magnitude of this threshold parameter represents how tolerant minors are to guard loss. In the ecologically relevant case where minor workers are responsible for most in-nest non-guarding work, the value of θ corresponds to an inherent

trade-off in task allocation. If minors are too tolerant to guard loss (low θ), their failure to replace lost guards may leave the colony vulnerable for a long time before the next generation of guards is mature. However, for high values of θ, minors switch to guarding tasks even when a relatively high proportion of the colony is already guarding, and so they will not contribute much to defense and will instead fail to fulfill other tasks needed by the colony. In the coming sections, I will study how the replacement threshold (θ) interacts with the slower processes of maturation and production of majors to keep colony defense and growth balanced.

4.2.5 Full Model

Combining ((4.1)) and ((4.4)) results in an autonomous ODE VSS that governs the general population dynamics of the colony:

$$\begin{cases} \dfrac{dW}{dt} = \Lambda \dfrac{(W+w)^2}{b^2+(W+w)^2}\rho - \dfrac{1}{\tau}W \\ \dfrac{dG}{dt} = \dfrac{1}{\tau}W - \mu_G G \\ \dfrac{dw}{dt} = \Lambda \dfrac{(W+w)^2}{b^2+(W+w)^2}(1-\rho) - \mu_w w - \left[\dfrac{G+g}{P} \leq \theta\right]\delta w \\ \dfrac{dg}{dt} = \left[\dfrac{G+g}{P} \leq \theta\right]\delta w - \mu_g g, \end{cases} \tag{4.5}$$

where a complete list of variables and parameters is summarized in Table 3. The reference parameter values that will be used throughout the analysis are in Table 4. Most values are taken from the literature from *T. angustula* stingless be colonies, but some are not found directly and must therefore be assumed. More details can be found in Section C.3.

The proposed model incorporates all three mechanisms involved in colony defense by *T. angustula* stingless bees: production of major guards, adjustable over generations

Name	Definition	Units
State variables		
W	number of non-guarding majors	nbr
G	number of guard majors	nbr
w	number of non-guarding minors	nbr
g	number of guard minors	nbr
P	total population size	nbr
Parameters		
Λ	egg-laying rate of queen	nbr/day
b	nbr. of non-guarding workers for $\Lambda/2$ eclosion rate	nbr
ρ	fraction of newborn majors	-
τ	maturation time of bees	days
μ_G	death rate of guarding majors	1/days
μ_g	death rate of guarding minors	1/days
μ_w	death rate of non-guarding minors	1/days
δ	guard replacement rate for minors	1/days
θ	replacement threshold for fraction of guards	nbr

Table 3. Variable and parameter definition

and mediated by the fraction ρ; maturation of such majors from non-guarding tasks to defensive guarding tasks (age-based polyethism), reflected in the maturation time τ; and quick replacement of guards by minor bees in case of emergency, where replacement rate δ is triggered when the guard ratio falls below threshold θ. This is the first mathematical model to include all three mechanisms in relation to colony defense in polymorphic eusocial insects, and specifically in bees, where morphological castes (Grüter et al. 2012) and replacement behavior (Baudier et al. 2019) have been described only recently.

4.3 Mathematical Analysis

I now analyze the model described in Section 4.2.5 to study how stingless bee colonies regulate colony growth and defense through mechanisms acting on three different timescales.

Name	Value/Range	Source
Λ	154 ind./day	(Koedam, Brone, and Van Tienen 1997)
b	700-1300	Assumed
ρ	1-6%	(Hammel et al. 2015)
τ	20 days	(Hammel et al. 2015)
μ_G	$[\frac{1}{6.9}, \frac{1}{2.9}]$ days^{-1}	(Grüter, Kärcher, and Ratnieks 2011)
μ_g	$[\frac{1}{6.9}, \frac{1}{2.9}]$ days^{-1}	(Grüter, Kärcher, and Ratnieks 2011)
μ_w	$[\frac{1}{35}, \frac{1}{20}]$ days^{-1}	(Grüter, Kärcher, and Ratnieks 2011; Hammel et al. 2015)
δ	≥ 4 days^{-1}	(Baudier et al. 2019)
θ	$0.2 - 1.2\%$	Assumed

Table 4. Parameter values for *T. angustula* stingless bees. For Λ, I use the average value of 6.41 eggs laid per hour reported by Koedam, Brone, and Van Tienen (1997) and multiply by 24 hours to get an approximate daily rate. For b, I know that newly founded colonies have about 500-1000 workers Van Veen and Sommeijer (2000) and I assume the Allee threshold E^b_- must be well below this range. I take an interval around b=1000, which, for $\Lambda = 154, \tau = 20, \mu_G = 1/5.4, \mu_g = 1/3, \mu_w = 1/28, \delta = 4, \rho = 0.06$, yields an Allee threshold of 250 individuals. For θ, I assume that it must be below γ_b for natural colonies, since they have no minor guards. With the same parameter values, I calculated the range for θ corresponding to ρ between 0.01 and 0.06.

Specifically, I will study how the maturation time of majors and replacement behavior of minors affects the impact of major production on guard availability and colony size.

4.3.1 Filippov System Description

The Full Model ((4.5)) is a Filippov system Filippov 1988; Meza et al. 2005; Silveira Costa and Meza 2006; Boukal and Kivan 1999 which can be converted to a generalized form. Let $H(Z) := (G + g) - \theta P$ with vector $Z = (W, G, w, g)^T$, and

$$F_{S_c}(Z) = \begin{pmatrix} \Lambda \dfrac{(W+w)^2}{b^2 + (W+w)^2}\rho - \dfrac{1}{\tau}W \\ \dfrac{1}{\tau}W - \mu_G G \\ \Lambda \dfrac{(W+w)^2}{b^2 + (W+w)^2}(1-\rho) - \mu_w w - \delta w \\ \delta w - \mu_g g, \end{pmatrix}, \tag{4.6}$$

$$F_{S_b}(Z) = \begin{pmatrix} \Lambda \dfrac{(W+w)^2}{b^2 + (W+w)^2}\rho - \dfrac{1}{\tau}W \\ \dfrac{1}{\tau}W - \mu_G G \\ \Lambda \dfrac{(W+w)^2}{b^2 + (W+w)^2}(1-\rho) - \mu_w w \\ -\mu_g g \end{pmatrix}, \tag{4.7}$$

Then System ((4.5)) can be rewritten as the following generalized Filippov system

$$\dot{Z} = \begin{cases} F_{S_c}(Z), & Z \in S_c, \\ F_{S_b}(Z), & Z \in S_b, \end{cases} \tag{4.8}$$

where $S_c = \left\{ Z \in \mathbb{R}_4^+ \mid H(Z) < 0 \right\}$, $S_b = \left\{ Z \in \mathbb{R}_4^+ \mid H(Z) > 0 \right\}$ are two regions divided by the discontinuity manifold

$$\Sigma = \left\{ Z \in \mathbb{R}_4^+ \mid H(Z) = 0 \right\}.$$

I denote System ((4.5)) defined in region S_c as *Crisis Mode with Replacement* and System ((4.5)) defined in region S_b as *Non-Crisis Mode without Replacement*. Definition 4.3.1 defines two types of equilibria relevant to this context Di Bernardo et al. 2008; Kuznetsov, Rinaldi, and Gragnani 2003.

Definition 4.3.1. A point Z^* is called a *regular* equilibrium of System ((4.5)) iff

$$F_{S_c}(Z^*) = 0, H(Z^*) < 0 \text{ or } F_{S_b}(Z^*) = 0, H(Z^*) > 0.$$

Alternativelty, a point Z^* is called a *virtual* equilibrium of System ((4.5)) iff

$$F_{S_c}(Z^*) = 0, H(Z^*) > 0 \text{ or } F_{S_b}(Z^*) = 0, H(Z^*) < 0.$$

In the following sections, I will prove that System ((4.5)) is positive invariant (Section 4.3.2) with a trivial Extinction Equilibrium (Section 4.3.3), and use the definitions above to analyze the model dynamics in each mode, with and without replacement (Section 4.3.4).

4.3.2 Positive Invariance

Toward validating the biological plausibility of ((4.5)), I first prove Theorem 4.3.1 (in Appendix C.2.1), which states that none of the population variables become negative over trajectories of the system.

Theorem 4.3.1. (Basic Dynamical Properties) *System* ((4.5)) *is positive invariant and bounded in* $\mathbb{R}^4_+$. *[Proof in Appendix C.2.1]*

4.3.3 Stability of the Extinction Equilibrium

The Full System ((4.5)) has a trivial extinction equilibrium at the origin; that is:

$$E^e := (W^*, G^*, w^*, g^*) = (0, 0, 0, 0).$$

By linearizing the system around the origin, I can study the stability of E^e (i.e., whether a small population would grow and persist or instead decline back to extinction). In Appendix C.2.2, I prove Theorem 4.3.2, which gives sufficient conditions for when E^e is globally stable.

Theorem 4.3.2. (Extinction equilibrium) *Model* ((4.5)) *always has the extinction equilibrium* $E^e := (W^*, G^*, w^*, g^*) = (0, 0, 0, 0)$. *which is always locally stable. Let* $\mu_u = \min\{1/\tau, \mu_w\}$ *and* $\Lambda < 2\mu_u b$. *Then* E^e *is globally stable. [Proof in Appendix C.2.2]*

The condition for global stability of E^e is not dependent upon the initial population size; it only depends on model parameters. In particular, the condition of an upper bound on egg-laying rate ($\Lambda < 2\mu_u b$) is equivalently a condition that the outflow of non-guarding workers must be greater than the inflow of non-guarding workers at the half-saturation population b; that is:

$$\frac{\Lambda}{2} < \mu_u b$$

In words, by definition of half-saturation population b, when there are b non-guarding workers, the eclosion rate that generates new non-guarding workers is $\Lambda/2$. However, each of those workers either dies (at rate μ_w) or transitions to guarding (at rate $1/\tau$) out of non-guarding work at a rate of at least μ_u. Consequently, if the inflow $\Lambda/2$ is dominated by the outflow $\mu_u b$, then the incipient population will decline over time.

However, even when the conditions for global stability of the extinction equilibrium E^e are not met, E^e is always locally stable by Theorem 4.3.2. Consequently, if an incipient population is not sufficiently large to escape the basin of attraction of E^e, the population will always go extinct. In fact, in the following sections, I will show that the system exhibits a strong Allee Effect (Stephens and Sutherland 1999); the system has both a upper, stable equilibrium as well as a lower, unstable equilibrium akin to a minimum-population threshold below which population growth is negative and ultimately evolves toward extinction.

4.3.4 Interior Equilibria

Now I analyze the system in search for positive attractors of F_{S_c} and F_{S_b}, that is, demographic equilibria towards which the population evolves when it does not go extinct. Note that F_{S_b} can be studied as a special case of F_{S_c} where the replacement rate is zero ($\delta = 0$). Thus, I start the analysis with the Crisis Mode with Replacement, governed by F_{S_c}, and then draw analogous conclusions for the Non-Crisis Mode without Replacement (F_{S_b}).

In the case when there is an insufficient number of guards (i.e., $H(Z) \leq 0$, or $(G + g)/P \leq \theta$), the minor-worker w-to-g replacement mechanism activates. In this state, the Full Model ((4.5)) behaves as the system $\dot{Z} = F_{S_c}$ defined in Equation ((4.6)). Any equilibrium $E^c = (W^*, G^*, w^*, g^*)$ of F_{S_c} must satisfy the following relations:

$$\begin{cases} \mu_G G^* = \dfrac{1}{\tau} W^* \\ \rho(\mu_w + \delta) w^* = \dfrac{1-\rho}{\tau} W^* \\ \mu_g g^* = \delta w^* \end{cases} \tag{4.9}$$

The relations in System ((4.9)) allow us to establish the condition for an equilibrium point to lay in the region of the state space where replacement occurs (S_c), that is, in order to be a *regular equilibrium* of the Full System ((4.5)). Define γ_c as the guard ratio $\dfrac{G^* + g^*}{P^*}$ at E^c,

that is

$$\gamma_c := \frac{\rho(\mu_w + \delta) + \mu_G \delta(1-\rho)/\mu_g}{\rho(\mu_w + \delta)(1 + \tau\mu_G) + (1-\rho)(1 + \delta/\mu_g)\mu_G}. \tag{4.10}$$

Then E^c is a regular equilibrium of Full System ((4.5)) if and only if $H(E^c) \leq 0$ or, equivalently, $\gamma_c \leq \theta$.

Furthermore, the equilibrium number of major workers W^* must satisfy:

$$\Lambda \frac{\left(W^* + \overbrace{\frac{(1-\rho)W^*}{\tau\rho(\mu_w+\delta)}}^{w^*}\right)^2}{b^2 + \left(W^* + \underbrace{\frac{(1-\rho)W^*}{\tau\rho(\mu_w+\delta)}}_{w^*}\right)^2}\rho = \frac{1}{\tau}W^*.$$

which simplifies to the quadratic equation

$$\Lambda W^* \left(1 + \frac{(1-\rho)}{\tau\rho(\mu_w+\delta)}\right)^2 \rho = \frac{1}{\tau}b^2 + \frac{1}{\tau}(W^*)^2 \left(1 + \frac{(1-\rho)}{\tau\rho(\mu_w+\delta)}\right)^2. \tag{4.11}$$

The roots of Equation ((4.11)) are the non-trivial, interior equilibria of F_{S_c} ((4.6)), whose stability follows from Theorem 4.3.3.

Theorem 4.3.3. (Existence and Stability of the Crisis Interior Equilibria)

Define condition

$$C_c : \frac{\Lambda}{2b}\left(\rho\tau + (1-\rho)\frac{1}{\mu_w + \delta}\right) \geq 1. \tag{4.12}$$

Then the Crisis System defined by F_{S_c} ((4.6)) has two interior equilibria, E^c_+ and E^c_-, if and only if C_c holds. Both have the form

$$(W^*, G^*, w^*, g^*) = (W^*, \frac{1}{\tau\mu_G}W^*, \frac{1-\rho}{\rho\tau(\mu_w+\delta)}W^*, \frac{\delta}{\mu_g}\frac{1-\rho}{\rho\tau(\mu_w+\delta)}W^*)$$

where

$$W^* = \frac{1}{2}\left(\Lambda\rho\tau \pm \sqrt{(\Lambda\rho\tau)^2 - \left(\frac{2b(\mu_w+\delta)\tau}{\frac{1-\rho}{\rho} + (\mu_w+\delta)\tau}\right)^2}\right) \tag{4.13}$$

Moreover,

1. *The interior equilibrium E_+^c is Locally Asymptotically Stable, and E_-^c is unstable.*
2. *Both E_+^c and E_-^c are* regular *equilibria of the Full System* ((4.5)) *if and only if*

$$\gamma_c < \theta$$

for γ_c defined in Equation ((4.10)).

[Proof in Appendix C.2.3]

In the special case when replacement rate $\delta = 0$, the vector field F_{S_c} ((4.6)) reduces to F_{S_b} ((4.7)). This allows us to analyze the Non-Crisis Mode without Replacement governed by F_{S_b} ((4.7)). Define $C_b := C_c|_{\delta=0}$ and

$$\gamma_b := \gamma_c|_{\delta=0} = \frac{\rho\mu_w}{\mu_G(1-\rho) + \rho\mu_w(1+\mu_G\tau)}, \tag{4.14}$$

which can also be written as

$$\gamma_b = \overbrace{\rho}^{\substack{\text{fraction} \\ \text{of majors}}} \frac{\overbrace{1/\mu_G}^{\substack{\text{guarding time} \\ \text{for majors}}}}{\underbrace{(1-\rho)/\mu_w + \rho(1/\mu_G + \tau)}_{\text{average bee lifespan}}}$$

Now I provide conditions for the existence and stability of interior equilibria in the Non-Crisis System F_{S_b} ((4.7)).

Theorem 4.3.4. (Existence and Stability of the Non-Crisis Interior Equilibria)

Define condition

$$C_b : \frac{\Lambda}{2b}\left(\rho\tau + (1-\rho)\frac{1}{\mu_w}\right) \geq 1. \tag{4.15}$$

Then the Non-Crisis System defined by F_{S_b} ((4.7)) has two interior equilibria $E_+^b = E_+^c|_{\delta=0}$ and $E_-^b = E_-^c|_{\delta=0}$ if and only if C_b holds.

Moreover,

1. *The interior equilibrium E^b_+ is Locally Asymptotically Stable, while E^b_- is unstable.*
2. *Both E^b_+ and E^b_- are* regular *equilibria of the Full System* ((4.5)) *if and only if*

$$\gamma_b > \theta$$

for γ_b defined in Equation ((4.14)).

[Proof in Appendix C.2.4]

As with Theorem 4.3.3 in the crisis mode, Theorem 4.3.4 (in the non-crisis mode) provides a sufficient condition for the existence of an interior regular attractor E^b_+ when the proportion of guards $(G + g)/P$ in the colony is above the replacement threshold θ (see Table 5 for a summary of the results from Theorems 4.3.3–4.3.4).

By Theorem 4.3.2, the extinction equilibrium E^e is always a local attractor of the full System ((4.5)). Theorem 4.3.4 provides a sufficient condition when the no-replacement Model ((4.7)) has a second attractor, E^b_+, separated from E^e by an unstable node E^b_-. Figure 18 illustrates such an example where the colony can survive if: (1) Condition C_b is satisfied, and (2) the initial population is above certain threshold related to E^b_- (see figure caption for parameter values).

From condition C_b of Theorem 4.3.4 for non-crisis System ((4.7)) without replacement, the non-trivial stable equilibrium E^b_+ can only exist when $\Lambda/2 \geq b/(\rho\tau + (1-\rho)/\mu_w)$; otherwise, the colony will collapse. That is, when there are b workers, the spontaneous regeneration rate due to eclosion ($\Lambda/2$) must be at least the average rate of attrition due to guard maturation or worker death ($b/(\rho\tau + (1-\rho)/\mu_w)$) in order to allow for the colony to grow to the non-trivial, stable equilibrium E^b_+ from a sufficiently large initial population size is sufficiently large. Furthermore, because of the ever-present local stability of the extinction equilibrium E^e, even when C_b is satisfied, if the population suddenly drops below a critical number (related to E^b_-), the colony can still go extinct.

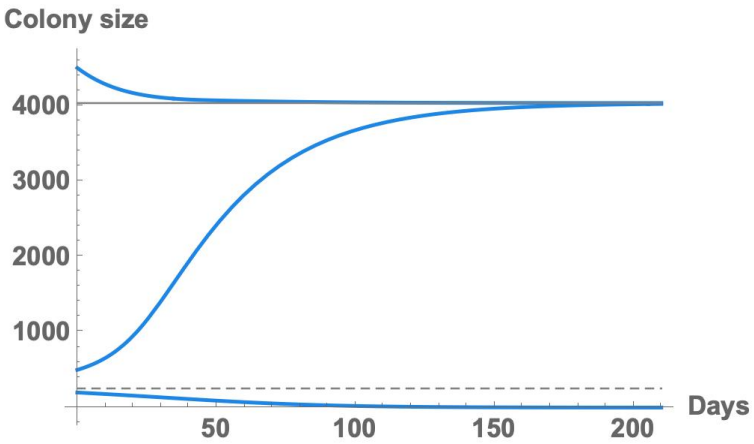

Figure 18. The system exhibits an Allee Effect. *Thick blue* lines represent trajectories with the same parameter values but different initial conditions. If the initial population is below the unstable equilibrium (*dashed horizontal line*) the population collapses. Otherwise, it establishes at the stable equilibrium (*solid horizontal line*). Parameter values: $\Lambda = 154, b = 1000, \rho = 0.06, \tau = 20, \mu_G = 1/5.4, \mu_g = 1/3, \mu_w = 1/28, \theta = 0.01, \delta = 4, W(0) = G(0) = g(0) = 0.w(0) = 200, 500, 4500$, respectively.

Assuming that C_b is satisfied and the initial population size is sufficiently large, the colony population will arrive at the stable equilibrium E^b_+, and the total population size will be:

$$W^* \left(1 + \frac{1-\rho}{\rho\mu_w\tau} + \frac{1}{\tau\mu_G}\right). \tag{4.16}$$

At E^c_+ and E^b_+ , the value of W^* given in ((4.13)) (with $\delta = 0$ for E^b_+) is increasing with Λ, the egg-laying rate, and decreasing with b, the non-guarding population for eclosion half-saturation. This means that the higher the queen's egg-laying rate and the smaller the number of non-guarding workers needed to ensure brood survival to eclosion, the larger a mature colony can become. However, if the population suddenly falls, the colony may move into the basin of attraction of extinction equilibrium E^e (discussed above); alternatively, the colony may move into crisis, guard-replacement mode if the guard ratio falls below threshold θ.

Remark 4.3.1. Note that, when $\delta > 0$, condition C_c automatically satisfies condition C_b

because

$$\underbrace{\rho\tau + (1-\rho)\frac{1}{\mu_w + \delta}}_{*} \leq \underbrace{\rho\tau + (1-\rho)\frac{1}{\mu_w}}_{\dagger}.$$

That is, the average time for a non-guarding worker to transition to guarding in the crisis mode ($*$ above) is less than in the non-crisis mode ($\dagger$ above). Consequently, by Theorem 4.3.3, persistence of the colony in crisis mode requires a faster egg-laying rate Λ or a reduction in the number of non-guarding workers necessary to ensure a high probability of development of eggs to eclosion.

4.3.4.1 Virtual and Regular Equilibria

As noted in Theorem 4.3.3 and Theorem 4.3.4, the fraction $\frac{G+g}{P}$ of guards in the colony determines whether the equilibria are virtual or regular. Because only regular equilibria can be approached by the system's trajectories, a complete analysis of the system's dynamics requires further characterizing the guard ratios γ_c and γ_b.

Theorem 4.3.5. (Characterization of the Equilibrium Guard Ratios)

1. *The ratio*

$$\gamma_b = \frac{\rho\mu_w}{\mu_G(1-\rho) + \rho\mu_w(1+\mu_G\tau)}$$

is monotonically increasing with respect to ρ, while the ratio

$$\gamma_c = \frac{\rho\left(\mu_w + \delta\right) + \mu_G(1-\rho)\frac{\delta}{\mu_g}}{\mu_G(1-\rho)\left(\frac{\delta}{\mu_g} + 1\right) + \rho\left(\mu_w + \delta\right)\left(1 + \tau\mu_G\right)}$$

is monotonically decreasing with respect to ρ if $\mu_g \leq \delta\tau\mu_G$ and monotonically increasing otherwise

2. *Moreover, I always have*

$$\gamma_b \leq \gamma_c.$$

Therefore, two regular attractors cannot coexist in the Full System ((4.5)).

[Proof in Appendix C.2.6]

The fact that the base ratio of guards γ_b is increasing with respect to ρ is natural given that, without replacement, all guards are majors and therefore increasing ρ directly increases the proportion of guards in the colony. However, in the crisis system, the effect of increasing ρ on the guard proportion depends on the parameter values since the guard population is a mix of both minors and majors. The condition $\mu_g \leq \delta\tau\mu_G$ or, equivalently,

$$\frac{1/\tau}{\mu_G} \leq \frac{\delta}{\mu_g}$$

can be interpreted as follows: majors mature at a rate $1/\tau$ into the guard group G and perform defense tasks for an average time $1/\mu_G$. Analogously, minors are recruited into the guard group g at a rate δ and perform the task for $1/\mu_g$ time units. If $\frac{1/\tau}{\mu_G} \leq \frac{\delta}{\mu_g}$, this means that there are more recruitment events in a guard's lifespan for minors than for majors, and therefore increasing the proportion of majors ρ ultimately decreases the total proportion of guards in the colony (γ_c is decreasing with respect to ρ). Conversely, if $\frac{1/\tau}{\mu_G} > \frac{\delta}{\mu_g}$ then the majors have more recruitment events per guard lifespan, and thus increasing major production (ρ) increases the fraction of guards in the colony γ_c.

4.3.5 Dynamics on the Switching Boundary Σ

I have studied the dynamics of the crisis mode F_{S_c} ((4.6)), where minors adopt guarding tasks in response to a lack of soldiers, and the non-crisis mode F_{S_b} ((4.7)) (without replacement by minors). Each of these systems has two interior equilibrium points, one stable and one unstable, which may both be virtual or regular according to the value of the replacement threshold $theta$. It remains to analyze the system behavior on the switching boundary Σ.

Trajectories of the Full System ((4.5)) may remain in one of the regions S_c and S_b, cross the switching surface Σ or slide along it. In order to investigate the crossing and sliding dynamics, I first determine the existence of a *crossing set* and a *sliding set* on Σ Filippov 1988; Silveira Costa and Meza 2006; Boukal and Kivan 1999; Tang, Liang, et al. 2012; Xiao, Zhao, and Tang 2013; Tang, Xiao, et al. 2012.

Let

$$\sigma(Z) := \langle H_z(Z), F_{S_c}(Z)\rangle\langle H_z(Z), F_{S_b}(Z)\rangle, \tag{4.17}$$

where $\langle\cdot\rangle$ denotes the standard scalar product and $H_Z(Z)$ is the non-vanishing gradient of smooth function H on Σ. Define the *crossing set* $\Sigma_C \subset \Sigma$ as

$$\Sigma_C = \{Z \in \Sigma \mid \sigma(Z) > 0\},$$

and the *sliding set* $\Sigma_S \subset \Sigma$ as

$$\Sigma_S = \{Z \in \Sigma \mid \sigma(Z) \leq 0\},$$

where $\Sigma_S = \Sigma \setminus \Sigma_C$. For System ((4.5)), I can obtain that

$$\begin{aligned}\sigma(Z) &= \theta^2\left(\tfrac{\Lambda(W+w)^2\rho}{(b^2+(W+w)^2)} - W/\tau\right)^2 + (1-\theta)^2(W/\tau - \mu_G G)^2 \\ &+ \theta^2\left(\tfrac{\Lambda(W+w)^2(1-\rho)}{(b^2+(W+w)^2)} - \mu_w w\right)^2 + (1-\theta)^2(g\mu_g)^2 \\ &+ \delta w\left(-\theta^2\left(\tfrac{\Lambda(W+w)^2(1-\rho)}{(b^2+(W+w)^2)} - \mu_w w\right) - (1-\theta)^2 g\mu_g\right)\end{aligned}$$

for all

$$Z \in \Sigma = \left\{Z \in \mathbb{R}^+_4 \mid H(Z) = 0\right\} = \left\{Z \in \mathbb{R}^+_4 \mid (G+g) - \theta(G+g+W+w) = 0\right\}.$$

The boundary Σ may also contain particular points, called "pseudoequilibria" (Di Bernardo et al. 2008), that act as equilibria within the sliding set Σ_S. In order to characterize them, I assign a vector field $g(Z)$, which is a linear combination of the vector fields $F_{S_c}(Z)$, and $F_{S_b}(Z)$, to each point $Z \in \Sigma_S$:

$$g(Z) = \lambda F_{S_c}(Z) + (1-\lambda)F_{S_b}(Z) \tag{4.18}$$

where $\lambda : \Sigma \to [0, 1]$.

Definition 4.3.2. A point $Z \in \Sigma_S$ is a *pseudoequilibrium* if $g(Z) = 0$.

The system $g(Z)$ can be expressed as below:

$$\begin{cases} \dfrac{dW}{dt} = \Lambda \dfrac{(W+w)^2}{b^2+(W+w)^2}\rho - \dfrac{1}{\tau}W \\ \dfrac{dG}{dt} = \dfrac{1}{\tau}W - \mu_G G \\ \dfrac{dw}{dt} = \Lambda \dfrac{(W+w)^2}{b^2+(W+w)^2}(1-\rho) - \mu_w w - (1-\lambda)\delta w \\ \dfrac{dg}{dt} = (1-\lambda)\delta w - \mu_g g. \end{cases} \tag{4.19}$$

It follows that a pseudoequilibrium $E^p = (W^*, G^*, g^*, w^*)$ must satisfy the relations

$$\begin{cases} G^* = \dfrac{1}{\tau\mu_G}W^*, \\ g^* = \dfrac{1-\rho}{\rho\tau(\mu_w + \delta(1-\lambda^*))}W^*, \text{and} \\ w^* = \dfrac{\delta(1-\lambda^*)}{\mu_g}\dfrac{1-\rho}{\rho\tau(\mu_w+\delta(1-\lambda^*))}W^*, \end{cases} \tag{4.20}$$

where $\lambda^* = \lambda(E^p)$. From this relations, I can find the ratio of guards at pseudoequilibria. Define γ_p as the ratio $\frac{G^*+g^*}{P^*}$ for G^*, g^* and $P^* = W^* + w^* + G^* + g^*$ as in Equation ((4.20)) above, that is,

$$\gamma_p := \frac{\rho(\mu_w + \delta(1-\lambda^*)) + \mu_G\delta(1-\lambda^*)(1-\rho)/\mu_g}{\rho(\mu_w+\delta(1-\lambda^*))(1+\tau\mu_G) + (1-\rho)(1+\delta(1-\lambda^*)/\mu_g)\mu_G}. \tag{4.21}$$

Note that, to be contained in Σ, the pseudoequilibrium must satisfy the condition

$$\gamma_p = \theta.$$

From this equality I can find the value of $\lambda^* = \lambda(E^p)$ as

$$\lambda^* = \frac{\mu_G\mu_g\theta(\delta\tau\rho + 1 - \rho + \mu_w\rho\tau) - (1-\theta)(\delta(\mu_G(1-\rho)+\mu_g\rho) + \mu_g\mu_w\rho)}{\delta(\mu_G\mu_g\rho\tau\theta - (1-\theta)(\mu_G(1-\rho)+\mu_g\rho))} \tag{4.22}$$

These relations yield the following Theorem 4.3.6, which establishes the existence of two pseudoequilibria on Σ when the Full System ((4.5)) has no regular equilibria.

Theorem 4.3.6. *Define condition*

$$C_p : \frac{\Lambda}{2b}\frac{(1-\theta)(\mu_g\rho + \mu_G(1-\rho) + \mu_G\mu_w\tau\rho)}{\mu_G(\theta\mu_g + \mu_w(1-\theta))} \geq 1. \tag{4.23}$$

Then System ((4.5)) *has two pseudoequilibria E^p_+ and E^p_- on the switching surface Σ if and only if C_p holds and $\gamma_b \leq \theta < \gamma_c$. The pseudoequilibria have the form*

$$(W^*, G^*, g^*, w^*) = \left(W^*, \frac{1}{\tau\mu_G}W^*, \frac{(1-\theta)(\mu_G(1-\rho) - \mu_g\rho) + \theta\mu_G\mu_g\rho\tau)}{\mu_G\rho\tau(\theta\mu_g + \mu_w(1-\theta))}W^*, \right.$$
$$\left. \frac{-\mu_w\rho + \theta(\mu_G(1-\rho) + \mu_w\rho(1+\mu_G\tau))}{\mu_G\rho\tau(\theta\mu_g + \mu_w(1-\theta))}W^*\right)$$

with

$$W^*|_{E^p_\pm} = \frac{1}{2}\rho\tau\left(\Lambda \pm \sqrt{\Lambda^2 - \left(\frac{2b\mu_G(\theta\mu_g + (1-\theta)\mu_w)}{(1-\theta)(\mu_G(1-\rho) + \mu_g\rho + \mu_G\mu_w\rho\tau)}\right)^2}\right)$$

[Proof in Appendix C.2.5]

The pseudoequilibrium existence condition C_p can be derived from the crisis existence condition C_c (4.3.4) by substituting the value of δ for $\delta(1-\lambda^*)$. Indeed, C_p can be written as

$$\frac{\Lambda}{2b}(\rho\tau + (1-\rho)\frac{1}{\mu_w + \delta(1-\lambda^*)}) \geq 1$$

which, like C_c and C_b, sets a minimum egg-laying rate Λ to ensure that there are enough individuals contributing to egg eclosion (W and w compartments) despite major maturation and worker death (see discussion of Theorems 4.3.3-4.3.4). For $\gamma_b \leq \theta \leq \gamma_c$, condition C_p is met automatically when

$$C_c : \frac{\Lambda}{2b}(\rho\tau + (1-\rho)\frac{1}{\mu_w + \delta}) \geq 1$$

holds, since λ^* takes values between 0 and 1 and thus

$$\frac{\Lambda}{2b}(\rho\tau + (1-\rho)\frac{1}{\mu_w + \delta(1-\lambda^*)}) \geq \frac{\Lambda}{2b}(\rho\tau + (1-\rho)\frac{1}{\mu_w + \delta}).$$

Similarly, condition C_p implies condition C_b from Theorem 4.3.4 since

$$\frac{\Lambda}{2b}(\rho\tau + (1-\rho)\frac{1}{\mu_w}) \geq \frac{\Lambda}{2b}(\rho\tau + (1-\rho)\frac{1}{\mu_w + \delta(1-\lambda^*)}).$$

Therefore, I have

$$C_c \implies C_p \implies C_b.$$

4.4 Interacting Defense Mechanisms

Now I study the interaction between the three mechanisms determining guard allocation, namely the major production regulated by ρ, the age-based polyethism regulated by the maturation time τ, and the replacement by minors that occurs when the guard proportion drops below θ. In particular, I am interested in determining

1. The effect of these three parameters on colony size and task allocation
2. The parameter combinations keep the system out of crisis, that is, governed by the Non-Crisis System ((4.7)).

4.4.1 Behavioral Plasticity

The parameter θ is the threshold fraction of guards in the colony below which minors will adopt guarding tasks. It can be interpreted as the colony demand for guards (the higher θ, the higher the demand), or as the degree of plasticity of minors (the higher θ, the more likely minors are to switch to guarding tasks). Because, as noted in Theorem 4.3.5, the

equilibrium ratio of guards γ_c in the crisis regime (with replacement) is always greater than the corresponding ratio γ_b in the non-crisis regime (without replacement), there are only three possible alternatives for the threshold ratio θ and they determine the system's behavior, as illustrated in Figure 19.

1. $\gamma_b \leq \gamma_c \leq \theta$

   By Theorem 4.3.6, there are no pseudoequilibria. Then I have the following cases based on condition C_c:

   a) C_c holds: **Crisis (E^c_+)**

      - Condition C_c implies the existence of the Crisis Attractor E^c_+, which is a regular equilibrium of the Full System ((4.5)) because $\gamma_c \leq \theta$ (Theorem 4.3.3);
      - Condition $C_c \implies C_b$, so the Non-Crisis Attractor E^b_+ exists, but as a virtual equilibrium of the Full System ((4.5)) because $\gamma_b \leq \theta$ (Theorem 4.3.4);

      Thus, because of the Allee Effect, trajectories either converge to E^c_+ or collapse to E^e if the population drops below a critical size.

   b) C_c does not hold ($\neg C_c$): **Extinction (E^e)**

      - There is no Crisis Attractor E^c_+;
      - The Non-Crisis Attractor E^b_+ exists as a virtual equilibrium of the Full System ((4.5)) if C_b holds and does not exist otherwise;

      It follows that the only attractor is the extinction equilibrium E^e.

   The ratio of guards at equilibrium, even with replacement, is less than θ. Then the model converges to the Crisis Attractor E^c_+ (like the orange "Crisis" trajectories in Figure 20) or extinction E^e. Biologically, this would represent a situation where

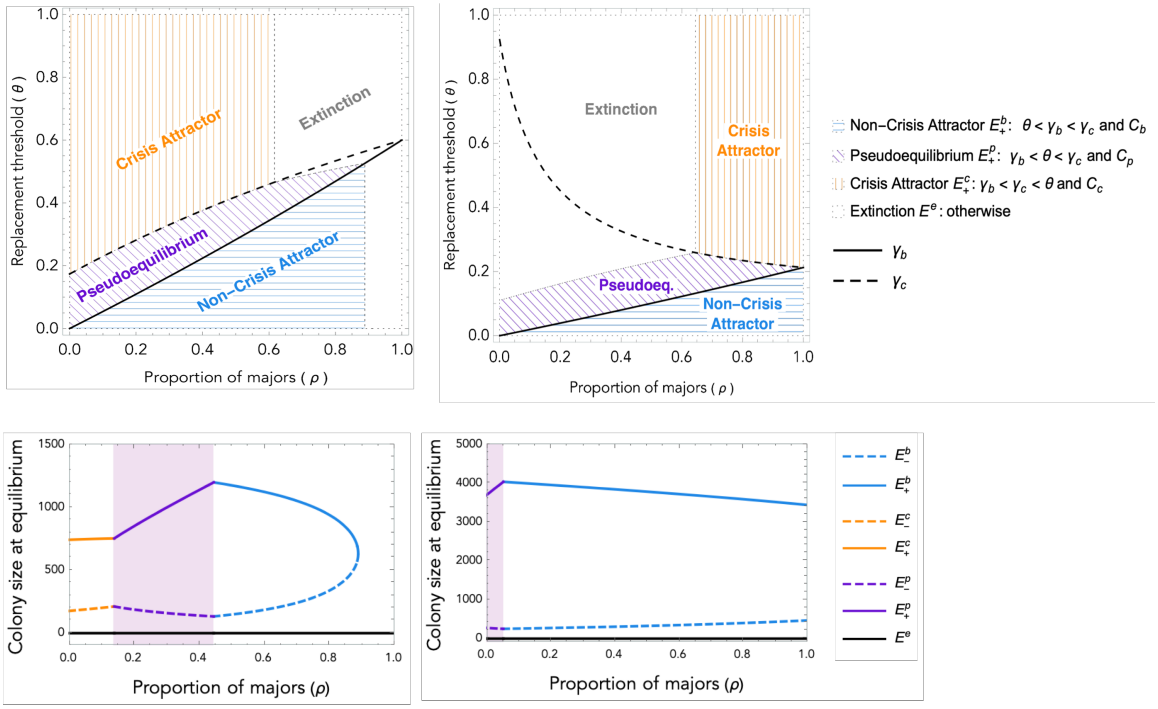

Figure 19. Model behavior with respect to ρ and θ. *Top panels*: In different regions of the ρ vs θ space, the system may have a crisis attractor, a pseudoequilibrium, a non-crisis attractor (with no minor guards), or only an extinction equilibrium. The crisis and non-crisis guard ratios, γ_c and γ_b, separate the regions. By Theorem 4.3.5, γ_c might be increasing (*top left panel*) or decreasing (top right panel). *Bottom panels*: Below each of the *top panels*, the corresponding bifurcation diagram for colony size with respect to ρ is shown for a fixed value of θ. In the *bottom left* panel, $\theta = 0.25$ and as ρ increases, the system transitions from crisis to pseudoequilibrium, to non-crisis, where the population decreases until it suddenly drops to extinction. In the *bottom right* panel, $\theta = 0.01$ and the system transitions from pseudoequilibrium, with an increasing population, to non-crisis, where the colony size decreases but does not reach an extinction state. Parameter values: (*left panels*) $\Lambda = 50, b = 300, \tau = 10, \mu_G = 1/15, \mu_g = 1/7, \mu_w = 1/28, \delta = 0.03$; (*right panels*) $\Lambda = 154, b = 1000, \tau = 20, \mu_G = 1/5.4, \mu_g = 1/3, \mu_w = 1/28, \delta = 4$. The parameters in the *right panels* are approximated values for real *T. angustula* colonies (see Table 4 and Section C.3).

minors keep transitioning to guarding even when all the major and replacement guards that the colony can produce are defending the nest. This is typically not observed in real colonies, where the guarding population consists mainly of major bees.

2. $\theta < \gamma_b \leq \gamma_c$

   By Theorem 4.3.6, there are no pseudoequilibria. Then I have the following cases based on condition C_b:

   a) C_b holds: **Non-crisis (E^b_+)**

      - Condition C_b implies the existence of the Non-Crisis Attractor E^b_+, which is a regular equilibrium of the Full System ((4.5)) because $\theta \leq \gamma_b$ (Theorem 4.3.4);
      - The Crisis Attractor E^c_+ exists as a virtual equilibrium of the Full System ((4.5)) if C_c holds and does not exist otherwise;

      Thus, trajectories either converge to E^b_+ or collapse to E^e if the population drops below the Allee threshold.

   b) C_b does not hold ($\neg C_b$): **Extinction (E^e)**

      - The Non-Crisis Attractor E^b_+ does not exist;
      - Since $\neg C_b \implies \neg C_c$, there is no Crisis Attractor E^c_+;

      It follows that the only attractor is the extinction equilibrium E^e and the population collapses.

   The ratio of guards at equilibrium is greater than θ, even without replacement. Then the model converges to the Non-Crisis Attractor E^b_+ (like the blue "Non-crisis" trajectories in Figure 20) or extinction E^e. This is the typical situation for colonies in the field: enough guards are produced such that minor replacement is not required. Replacement would be activated upon guard removal, and would accelerate the recovery of the base

guard proportion in the colony, γ_b. However, even without replacement, the original proportion of guards would be eventually reached.

3. $\gamma_b \leq \theta < \gamma_c$

   The Crisis and Non-crisis Attractors E^c_+ and E^b_+ exist as virtual equilibria of the Full System ((4.5)) if their respective existence conditions C_c and C_b are met, and do not exist otherwise. Then I have the following cases based on condition C_p:

   a) C_p: **Regulating (E^p_+)**

      - Condition C_p implies the existence of pseudoequilibrium $E^p_+ \in \Sigma_s$ because $\gamma_b \leq \theta < \gamma_c$ (Theorem 4.3.6);

      Thus, trajectories either converge to the pseudoequilibrium E^p_+ or collapse to E^e if the population drops below a critical size.

   b) C_p does not hold ($\neg C_p$): **Extinction (E^e)**

      - No pseudoequilibria exist.

      It follows that the only attractor is the extinction equilibrium E^e and the population collapses.

   This would represent a colony where the natural production of major guards is too low, which triggers replacement by minors, but the mixed guarding population resulting from replacement is large enough to prevent further replacements. If the existence condition is not satisfied, the population collapses to extinction, like in the previous cases (see gray "Extinction" trajectories in Figure 20). However, convergence to a pseudoequilibrium in this case implies a persistent population of minor guards (see purple "Pseudoequilibrium" trajectories in Figure 20), which is not typically observed in real colonies.

The simulations in Figure 20 illustrate system trajectories converging to the "Crisis",

"Pseudoequilibrium", "Non-crisis", and "Extinction" attractors. The parameter values are typical values for *Tetragonisca angustula* stingless bee colonies (see Table 4), the same values used in the top right panel of Figure 19. Note how there are no minor guards at equilibrium in the "Non-crisis" attractor, but there is a persistent population of them for the "Crisis" and "Pseudoequilibrium" attractors. This is not efficient, since minor guards have a lower performance at defense tasks and thus are meant to be a back-up for exceptional situations where major guards are missing. In fact, although real colonies in the field present a mixed guard population after guard removal (Baudier et al. 2019), they usually have major bees defending the nest.

The value of θ must be less than γ_b in order for the system to operate in non-crisis mode. The maximum value of γ_b, the fraction of guards without replacement, is at $\rho = 1$, with an all-major colony. Thus, θ must be less than $\gamma_b|_{\rho=1} = \frac{1}{1+\mu_G\tau} = \frac{1\mu_G}{\tau+1/\mu_G}$, which is the fraction of their lives that majors spend as guards. If θ is greater than this proportion, then the colony is guaranteed to either go extinct or maintain a persistent population of minor inefficiently allocated to guarding tasks. Moreover, if the colony is in a crisis state (orange regions in Figure 19), decreasing θ will always lead the system to a non-crisis mode (blue regions in Figure 19) but increasing θ will not force the colony into extinction. However, increasing θ from a non-crisis state may lead to either crisis mode, with a persistent population of minor guards, or directly to extinction, without ever transitioning to a crisis mode. That is, a colony that can sustain itself in the crisis attractor, with a stable population of minors dedicated to guarding, will not collapse because of demographic factors if the demand for guards increases or minors become exceedingly plastic (meaning that they would adopt guarding tasks even if the whole population was already guarding). This is because, in crisis, the colony is simply unable to meet its demand for guards ($\gamma_c < \theta$), so increasing this demand makes no difference for task allocating or colony size (the colony is already

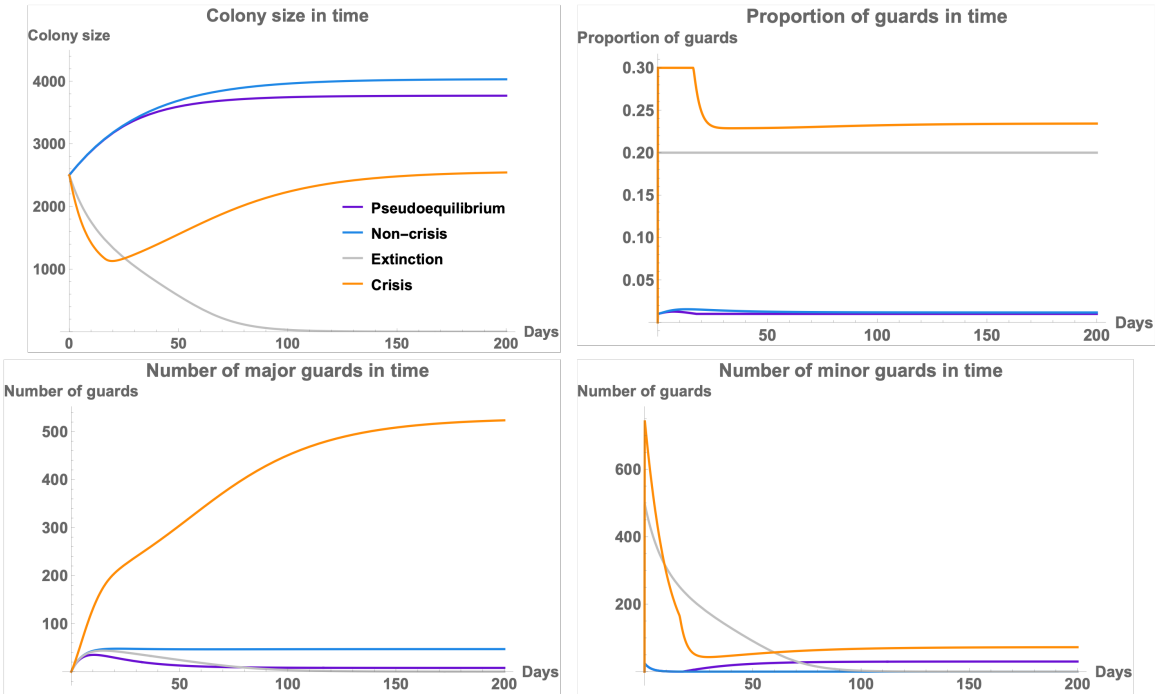

Figure 20. System trajectories illustrating the "Non-crisis"($\rho = 0.06, \theta = 0.01$), "Pseudoequilibrium" ($\rho = 0.01, \theta = 0.01$) and "Crisis" ($\rho = 0.8, \theta = 0.3$) and "Extinction"($\rho = 0.06, \theta = 0.2$) attractors. Each trajectory has a different combination of ρ and θ corresponding to one of the four regions in the 2-parameter bifurcation in the *top right panel* of Figure 19. Note the persistent population of minor (replacement) guards in the "Crisis" and "Regulating" cases.
($\Lambda = 154, b = 1000, \tau = 20, \mu_G = 1/5.4, \mu_g = 1/3, \mu_w = 1/28, \delta = 4$)

producing all the major and replacement guards it can). However, it may become exposed to higher environmental risks, like robbery and attacks.

4.4.2 Morphological Specialization

The fraction ρ represents the proportion of eggs that eclose into majors, which mature into soldiers. As seen in Figure 19, for sufficiently small values of θ, increasing ρ can keep the system in non-crisis mode, without replacement guards. However, as shown in the bottom panels of Figure 19, increasing ρ may also reduce colony size and even lead to

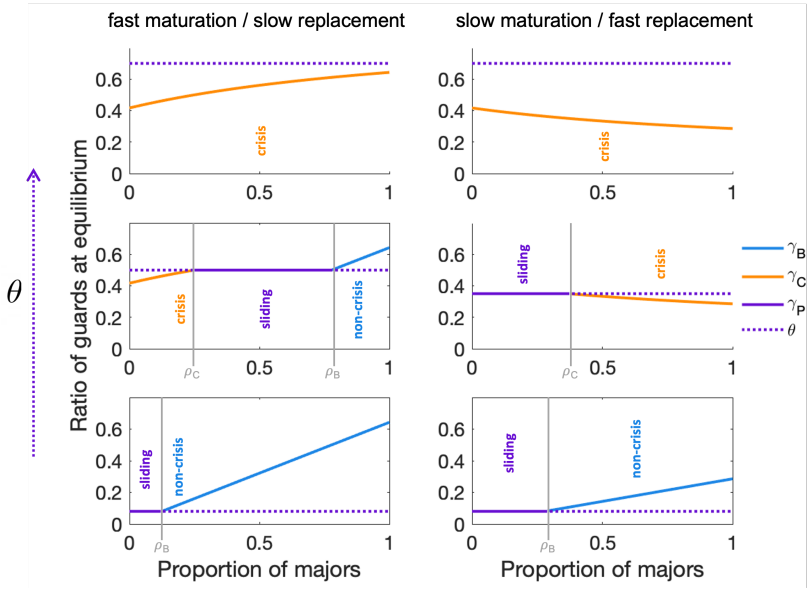

Figure 21. Proportion of guards at equilibrium for different combinations of ρ and θ. The system converges to the "Crisis" mode ((4.6)), "Sliding" mode ((4.19)) or "Non-Crisis" mode ((4.7)) as the proportion of majors ρ changes. ρ_C and ρ_B are the values of ρ, if any, such that $\gamma_c|_{\rho=\rho_C} = \theta$ and $\gamma_b|_{\rho=\rho_B} = \theta$, respectively. In all panels, $b = 100, \mu_g = 1/10$, $\mu_w = 1/28, \Lambda = 100, \delta = 1/14$. In the *left* column γ_c is increasing, with $\tau = 10$ and $\mu_G = 1/(28 - \tau)$ so that majors and minors have an average lifespan of 28 days, and the θ values are 0.7 in the first row, 0.5 in the second and 0.08 in the third. The *right* column shows decreasing γ_c, with $\tau = 20, \mu_G = 1/(28 - \tau)$. The θ values are 0.7 in the first row, 0.35 in the second and 0.08 in the third

colony extinction. The effect of modifying the production of majors ρ depends on the value of θ and whether γ_c is increasing or decreasing. There are six possible cases illustrated in Figure 21.

Define ρ_C as the value of ρ, if any, such that $\gamma_c|_{\rho=\rho_C} = \theta$. Correspondingly, define ρ_B as the value of ρ, if any, such that $\gamma_b|_{\rho=\rho_B} = \theta$.

1. Increasing γ_c ($\gamma_b|_{\rho=0} < \gamma_c|_{\rho=0} < \gamma_c|_{\rho=1} = \gamma_b|_{\rho=1}$)

    a) High value of θ:

$$\theta \geq \gamma_c|_{\rho=1} = 1/(1 + \mu_G \tau)$$

The system is in the "Crisis" state for all values of ρ, but increasing ρ increases the proportion of guards at equilibrium.

b) Intermediate value of θ:

$$\delta/(\delta + \mu_g) = \gamma_c|_{\rho=0} < \theta < \gamma_b|_{\rho=1} = 1/(1 + \mu_G\tau)$$

As ρ increases, the system transitions from the "Crisis" state ($0 < \rho < \rho_C$) to the "Regulating" state ($\rho_C < \rho < \rho_B$) and the "Base" state ($\rho > \rho_B$). In this case, increasing the production of majors is a long-term solution for keeping the system out of crisis.

c) Low value of θ:

$$0 < \theta < \gamma_c|_{\rho=0}$$

As ρ increases, the system transitions from the "Regulating" state ($0 < \rho < \rho_B$) to the "Base" state ($\rho_B < \rho < 1$). In this case, increasing the production of majors is a long-term solution for **increasing** the guard proportion.

2. Decreasing γ_c ($\gamma_b|_{\rho=0} < \gamma_c|_{\rho=1} = \gamma_b|_{\rho=1} < \gamma_c|_{\rho=0}$)

a) High value of θ:

$$\theta \geq \gamma_c|_{\rho=1}$$

The system is in the "Crisis" state for all values of ρ, but increasing the proportion of majors ρ **decreases** the proportion of guards in the long term.

b) Intermediate value of θ:

$$\gamma_c|_{\rho=1} < \theta < \gamma_c|_{\rho=0}$$

As ρ increases, the system transitions from the "Regulating" state ($0 \leq \rho \leq \rho_C$) to the "Crisis" state ($\rho_C < \rho \leq 1$). In this case, increasing the production of majors **decreases** the guard proportion in the long term.

c) Low value of θ:

$$0 < \theta < \gamma_c|_{\rho=1}$$

As ρ increases, the system transitions from the "Regulating" state ($0 \leq \rho < \rho_B$) to the "Base" state ($\rho_B \leq \rho \leq 1$). In this case, increasing the production of majors is a long-term solution for **increasing** the guard proportion.

These cases reveal the situations where the colony can function normally, in the "Non-Crisis" regime, and where an increment in the major production is actually beneficial for colony defense. For example, if major and minor guards live equally long on average and replacement happens at a faster rate than maturation (decreasing γ_c), then increasing the production of majors enhances colony defense only if the proportion of guards can drop very low without triggering replacement (case 2c). In fact, cases 2a-2c show that the minimum proportion of guards required to defend the colony without replacement (θ) must be less than $\gamma_b|_{\rho=1}$, that is the equilibrium proportion of guards if all bees are majors. If θ is greater than this value, then increasing the production of majors ρ actually decreases the fraction the population dedicated to guarding.

The colony size bifurcation diagrams in the *left and right bottom panels* of Figure 19 are examples of cases 1b and 2c, respectively. They have the same parameters as the *top panels* directly above them, and shows colony size with respect to ρ for a fixed θ value of 0.25 (left) and 0.01 (right). While the parameters on the *right panels* are biologically realistic for *T. angustula* stingless be colonies, the parameters on the *left panels* were chosen to produce a representative diagram with the four possible dynamical outcomes and are not based on these reference values. They would represent an analogous system (like a different species or an artificial system) where γ_c is increasing, so $\mu_g > \delta\tau\mu_G$ by Theorem 4.3.5. Thus, the ratio between the death rates of minor and major guards must be greater than the ratio between replacement and maturation rates. In this *bottom left panel* of Figure 19, corresponding to

case 1b, ρ_C and ρ_B are well defined. For ρ values below ρ_C, the colony size is dictated by the crisis model ((4.6)) because the parameters satisfy condition ((4.10)) but not ((4.14)). Similarly, for ρ values above ρ_B the system follows the non-crisis model ((4.7)) because only condition ((4.14)) holds. However, higher ρ values violate the Existence Condition (4.3.4) for the Base Model, so the only stable equilibrium is extinction. However, the fraction of guards in the colony increases with ρ in case 1b. Thus, increasing the production of majors in this scenario may reinforce colony defense by increasing the fraction of the population allocated to guarding, but may also reduce the colony size or even cause extinction.

On the other hand, the *bottom right panel* of Figure 19, which falls under case 2c, represents a realistic situation for stingless bee colonies. Since the death rates for major and minor guards are similar and replacement happens much faster than maturation, I have $\mu_g \leq \delta\tau\mu_G$ and γ_c is increasing by Theorem 4.3.5. Thus, the system cannot transition between crisis and non-crisis states by changing the production of majors. As seen in the *top right panel* of Figure 19, for high values of θ, the colony will go extinct for low ρ values and persist in a crisis state for high enough ρ values. However, for the small θ values that presumably exist in real colonies, the system transitions from a pseudoequilibrium to the non-crisis attractor as ρ increases, with the population size peaking at ρ_B, where the transition happens. This might suggest why such a small proportion of majors exists in real colonies: the production is enough to supply the demand indicated by θ, but not much greater, since this would decrease colony size.

4.4.3 Maturation Time τ

I have mentioned the role of the maturation rate in determining whether the fraction of guards at the crisis attractor, γ_c, is increasing or decreasing with respect to ρ. In real

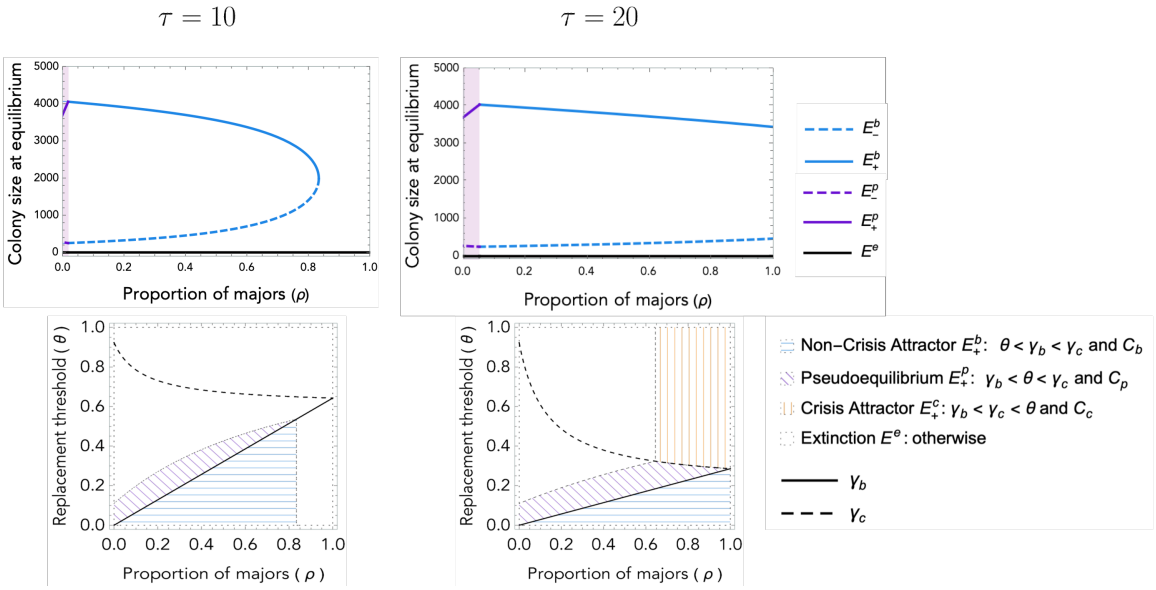

Figure 22. Effect of τ on colony size bifurcation with respect to ρ (*top*) and system sybamics with respect to ρ and θ (*bottom*). Parameter values: $\Lambda = 154, b = 1000, \tau = 20, \mu_G = 1/5.4, \mu_g = 1/3, \mu_w = 1/28, \delta = 4$. In *top panels*, $\theta = 0.01$

stingless-bee colonies, the maturation rate that is considerably slower than the replacement rate, δ, and so γ_c is increasing like in the right panels of Figure 19 and Figure 21. However, the maturation rate also has an important role in defining the existence conditions C_b, C_p and C_c. As seen in Figure 22, decreasing the maturation time τ also reduces the region in the θ-ρ space where the colony can survive. Thus, a colony where majors mature faster will be able to sustain less majors, since high values of ρ lead to extinction. Also note that the colony size peaks at a smaller value of ρ for faster maturation times. If colonies regulate their major production to be near this peak, then this result suggests that colonies where the transition of majors to guarding happens faster are expected to produce a lower number of majors.

Figure 23 shows the equilibrium task allocation as ρ varies for the same values of τ (10 days and 20 days). For $\tau = 20$, which is a biologically realistic value, increasing ρ

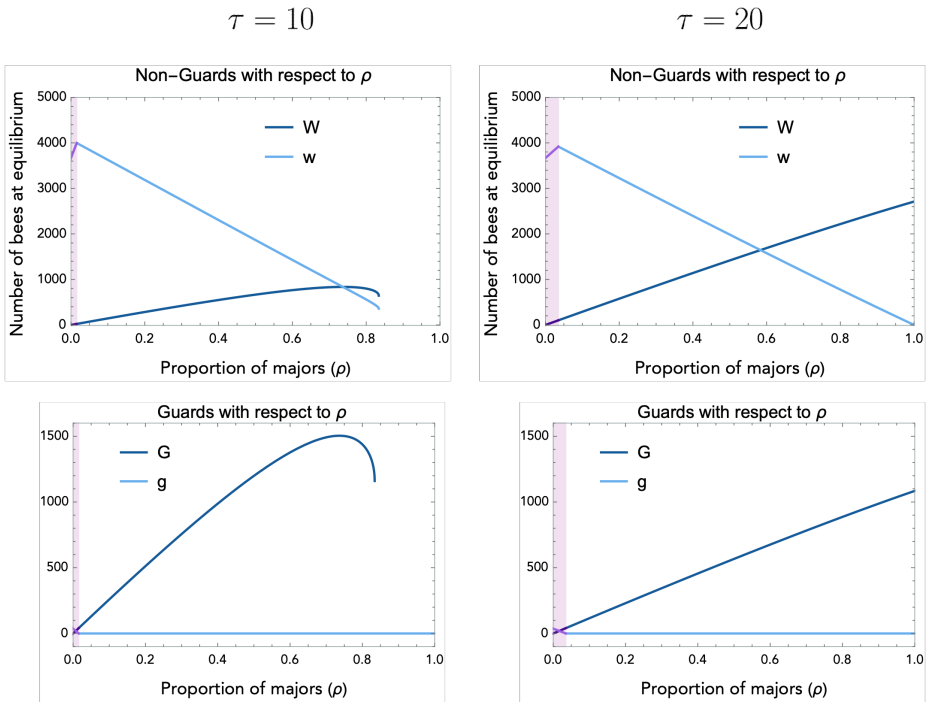

Figure 23. Bifurcation diagram for all population groups with respect to ρ for $\tau = 10$ and $\tau = 20$. Only stable interior attractors are shown, although extinction is always a stable equilibrium. .

produces an increment in the non-guarding and guarding major populations (W and G, respectively, represented by darker lines). There are no minor guards g in the non-crisis case, which constitutes most ρ values (except for the shaded areas, corresponding to a pseudoequilibrium). While there are still no minor guards for $\tau = 10$, the major population does not simply increase with ρ. In fact, both guarding and non-guarding populations peak at a high value of ρ and then decrease before collapsing drastically to extinction. Thus, for very fast maturation rates, increasing the production of majors may, perhaps counterintuitively, decrease the number of guards in the colony.

4.5 Conclusion

In this work, I developed a framework for modeling task allocation for collective defense motivated by the stingless bee *T. angustula*. I studied morphological specialization, age-based polyethism and behavioral plasticity as mechanisms regulating group defense at different timescales and interacting to maintain colony growth while responding efficiently to crisis situations.

Our analysis provides basic conditions for colony survival: a non-guarding worker must spend enough time rearing brood to ensure that at least one new adult is recruited before she dies or switches to a guarding task (see Theorem 4.3.2). Even if this condition is satisfied, the colony may still inevitably collapse if it reaches low numbers, which is known as strong Allee Effect (see Theorem 4.3.2, Theorem 4.3.4).

The model provides the conditions under which the studied mechanisms work in tandem to improve collective defense, and the scenarios where their simultaneous implementation can be detrimental. I asked how the parameters regulating morphological specialization, age-based polyethism, and behavioral plasticity impact the colony size and task allocation within the colony. The theoretical results illustrated in Figure 21 show that increasing the production of majors, who later specialize in defense, can actually have a negative impact on the fraction of the colony dedicated to guarding (see Theorem 4.3.5). This is the case if the colony relies on replacement minor guards to satisfy a minimum required guard proportion (due to either large major death rates or slow maturation of majors), and reduces the available pool of minors by increasing the production of majors. I also showed in Figure 22 that, for the parameter values corresponding to stingless bees, the colony size peaks at low proportions of majors ($\rho \approx 5\%$) and then decreases (but not to extinction) when more majors are produced. However, if majors mature into guards at a faster rate,

then the colony size peaks at a lower proportion of majors, and high major proportions do cause extinction. Moreover, as shown in Figure 23, if the maturation time is short then a high production of majors may also decrease the number of guards in the colony.

I also asked how plastic minors should be to allow for a transient recovery from guard loss without maintaining an inefficient body of minor guards. As shown in Figure 19, for the reference parameter values, if minors were more plastic or the colony demand for guards were to increase, the colony could even go extinct. In fact, a colony producing 6% majors will have at most around 1% of the population as guards. If the demand for guards were between 1% and 12% and minors switched to guarding with these proportions, then the colony would have a persistent population of minor guards. If the demand increased above 12%, then the colony would go extinct (see "Extinction" trajectory in Figure 20), since all minors would adopt guarding tasks at a fast rate and there would not be enough workers taking care of the brood. If the colony produced a majority of majors, above circa 65%, then even if all minors always adopted guarding tasks, the colony could survive (with a persistent population of minor guards, like the orange "Crisis" trajectory in Figure 20). This is because there would be enough young majors taking care of the brood even if all minors switch to guarding.

This work provided a theoretical exploration regarding how morphological specialization, age-based polyethism and behavioral plasticity interact at different timescales to regulate group defense and colony growth. However, a more precise comparison to experimental results will require further research on biologically accurate parameter values. For example, while the maturation and mortality rates are available in the literature and were used for simulations, the half-saturation parameter b of the functional response requires fitting to eclosion data that was not available for this work. Future work also includes exploring continuous alternatives for the replacement function used, since the step function used

here was chosen for simplicity and not based on a biological sharp switch. Lastly, a richer analysis of the balance between reproduction and defense could be obtained by conducting a study of the risks that the colony engages in for being unprotected, that is, quantifying the cost of reducing the guard population in terms of potential attacks or robbing.

I have presented a mathematical framework for understanding the demographic factors constraining collective defense regulation at different timescales and specialization degrees in social insect colonies. The scenarios shown here shed light on the regulation of specialization and crisis response in colonies, but can also be adapted to understand variation at different timescales in the defensive dynamics of other biological systems that are harder to observe. Moreover, this work can guide the design of potential eusocial-insect inspired solutions the human domain, like team defense strategies, manufacturing systems and just-in-time supply chains.

Chapter 5

CONCLUSION

This Dissertation analyzes how collective differences emerge from variation at the individual level through mathematical models, using eusocial insects as model organisms. In Chapter 2, I introduce a Markov-chain decision model to study how rock ant colonies choose the best among candidate nests when they must emigrate. In particular, it captures the individual quorum-based recruitment decisions of workers and how they determine the collective balance between speed of the migration and accuracy of nest choice. The model presents a framework for understanding the cognitive processes balancing speed and accuracy under different conditions in ants and reproduces core features of the latency and outcome characteristics from empirical observations in real ants. Furthermore, because the model predicts bounded decision latencies even for ambiguous evidence, it provides a novel logical connection between critical encounter rate and worst-case decision latency. Although there is no explicit colony diversity in form of distinct worker types, there is explicit randomness in individual decisions with average parameters shared by the group. Thus, variation in colony performance can sometimes be a natural effect of stochasticity at the individual level, but also colonies with different distribution parameters will have consistent differences in collective performance. In this low within-group heterogeneity case, noisy behavior may be important to prevent drastic switches where the whole colony cascades into fast transport to a poor nest alternative (for a similar discussion about the potential collective benefit of individual noise in harvester-ant foraging regulation see (Davidson et al. 2016)). This chapter contributes to understanding the colony-level implications of individual-level cognitive parameters of decision making. More generally, the excitable

encounter-driven finite-state approach in the model suggests a novel path for incorporating neuron-like behavior into multi-scale models of collective cognition in biological systems.

While Chapter 2 focuses on individual-level modeling of stochastic decisions, Chapter 3 scales up to mean-field colony-level modeling in order to capture group composition in honey-bee colonies. The polyandry of honey-bee queens produces intra-colony genetic variation that manifests in cognitive diversity between foragers (Smith and Cook 2020), and group compositions with certain degrees of heterogeneity may be favoured by environment. Thus, I develop an ODE model to study how honey-bee colonies allocate foragers to explore the landscape and exploit available food sources and, particularly, how cognitive diversity among workers influences the collective attention allocation between novel and familiar resources. Moreover, I establish which are the main individual interactions and processes driving collective attention allocation. The model reproduces the observed increased foraging activity in colonies with higher proportions of high-attention foragers, as well as the preference for familiar sources in such colonies. It also provides mechanistic support for the empirical hypothesis that individual preference, amplified by efficient communication, is sufficient to produce collective preference at the observed levels in different colonies. Moreover, sensitivity analysis reveals that collective preference is most sensitive to changes in recruitment when the fraction of high attention individuals in the colony is small, but to persistence instead for larger proportions of high attention foragers. The model suggests future empirical research avenues focusing on these individual processes that heavily impact collective behavior in a heterogeneous population, and thus contributes to understanding the role of individual cognitive variation in regulating the collective trade-off between exploring new resources and exploiting known ones.

In the absence of genetic diversity, heterogeneity may be induced by a colony in other ways. In stingless bees, the brood-feeding behavior of nurse bees causes permanent mor-

phological differences in the body sizes of workers. This morphological variation between majors (large workers with better defensive abilities) and minors (smaller workers) is complemented by behavioral plasticity in the form of age-based polyethism and fast task switching. Thus, there are multiple dimensions in which diversity may be tuned. The model in Chapter 4 shows that, along each of these dimensions, heterogeneity is beneficial only in a certain range that depends on the others. Outside of this range, certain group compositions may compromise colony adaptation and survival. Indeed, while colony size peaks at low proportions of majors, colonies die if minors are too plastic, defensive demands are too high, or if there is a high proportion of quickly developing majors. For fast maturation, increasing major production may actually decrease defenses. This model elucidates the demographic factors constraining collective defense regulation in social insects while also suggesting new explanations for variation in defensive allocation in biological systems at smaller scales, where the mechanisms underlying defensive processes are not easily observable. In fact, results from eusocial insects have been used to understand some aspects of immune-system responses (Moses et al. 2019), and further research may elucidate the drivers of collective variation in these systems. Moreover, our work helps to establish social insects as model organisms for understanding other systems where the transaction costs for component turnover are nontrivial, as in manufacturing systems and just-in-time supply chains.

5.1 Limitations and Future Work

This Dissertation considers group heterogeneity in the form of distinct types of individuals interacting in a group. However, it still assumes that sub-populations of each type are homogeneous. In natural systems, variation is found as a distribution across the

population, as opposed to discrete types of individuals. Thus, the models presented here could be expanded to include continuous distributions of attention phenotypes in Chapter 3 or replacement thresholds, ages and sizes in Chapter 4.

5.2 Broader Impacts

Environmental challenges for colonies require group decision making, efficient resource collection and effective defense against threats, which are problems relevant to human societies as well. Understanding how other social systems with such ecological success address these challenges has the potential to inspire solutions in the human domain. For example, studying the role of heterogeneity of workers within colonies may shed light on the importance of diversity in teams for group problem solving in humans.

Furthermore, the collective cognitive-like properties of eusocial-insect colonies make them tractable model systems to elucidate general problems in other cognitive architectures. For example, humans exhibit irrational choices based on relative (not absolute) item valuation. Similarly, acellular slime molds exhibit irrational biases between food items (Latty and Beekman 2011). In contrast, eusocial-insect colonies of some species choose rationally whereas single insects or humans do not, apparently because colonies evaluate alternatives simultaneously (Sasaki, Stott, and Pratt 2019; Sasaki and Pratt 2012). Thus, highly tractable alternative model systems could help tackle problems in cognitive science, like the emergence of irrationality in the human brain, and suggest ways to organize humans in groups to restore rationality.

Moreover, models of collective behavior in social insects have the potential of inspiring algorithms that capitalize on heterogeneity in artificial intelligence and swarm robotics, where simple components with no central control must solve complex tasks through in-

dividual interactions. Component-level variation arises in engineered systems during the manufacturing processes (Escalante 1999). Similarly, in distributed computing systems, performance varies between nodes added at different times due to technological advancements. Currently, engineering seeks robustness to variation: quality control systems attempt to suppress manufacturing variation (Escalante 1999; Lee et al. 2020) and computing techniques are designed to perform well despite node heterogeneity (Tuncer et al. 2017). However, novel ways to capitalize on unavoidable variation in future artificially intelligent collectives may arise from advancing the study of natural systems where function emerges from intrinsic component-level variation.

REFERENCES

Abbott, L. F., and Thomas B. Kepler. 2008. "Model neurons: From Hodgkin-Huxley to hopfield." In *Statistical Mechanics of Neural Networks,* 5–18. Springer Berlin Heidelberg, April. Accessed July 8, 2020. https://doi.org/10.1007/3540532676_37.

Aoki, Shigeyuki, and Utako Kurosu. 2003. "Logistic model for soldier production in aphids." *Insectes Sociaux* 50 (3): 256–261. https://doi.org/10.1007/s00040-003-0675-3.

Ayalon, Oran, Yigal Sternklar, Ehud Fonio, Amos Korman, Nir S. Gov, and Ofer Feinerman. 2021. "Sequential Decision-Making in Ants and Implications to the Evidence Accumulation Decision Model." *Frontiers in Applied Mathematics and Statistics* 7 (June): 672773. Accessed September 27, 2022. https://doi.org/10.3389/fams.2021.672773.

Batra, Suzanne. 1966. "Nests and Social Behavior of Halictine bees of India (Hymenoptera: Halictidae)." *The Indian Journal of Entomology* 28 (September). Accessed September 1, 2021. https://digitalcommons.usu.edu/bee_lab_ba/105.

Baudier, Kaitlin M, Madeleine M Ostwald, Christoph Grüter, Francisca H I D Segers, David W Roubik, Theodore P Pavlic, Stephen C Pratt, and Jennifer H Fewell. 2019. "Changing of the guard: Mixed specialization and flexibility in nest defense (Tetragonisca angustula)." *Behavioral Ecology* 30 (4): 1041–1049. https://doi.org/10.1093/beheco/arz047.

Bazhenov, Maxim, Ramon Huerta, and Brian H Smith. 2013. "A computational framework for understanding decision making through integration of basic learning rules." Publisher: Soc Neuroscience, *Journal of Neuroscience* 33 (13): 5686–5697. https://doi.org/10.1523/JNEUROSCI.4145-12.2013.

Behmer, Spencer T. 2009. "Animal Behaviour: Feeding the Superorganism." Publisher: Elsevier Ltd, *Current Biology* 19 (9): R366–R368. https://doi.org/10.1016/j.cub.2009.03.033.

Bellman, Richard, Irving Glicksberg, and Oliver Gross. 1956. "On the "bang-bang" control problem." *Quarterly of Applied Mathematics* 14 (1): 11–18.

Beshers, Samuel N, and Jennifer H Fewell. 2001. "Models of Division of Labor in Social Insects." *Annual Review of Entomology* 46 (1): 413–440. https://doi.org/10.1146/annurev.ento.46.1.413.

Bhagavan, Seetha, Shirly Shirley Benatar, Susan Cobey, and Brian H. Smith. 1994. "Effect of genotype but not age or cast on olfactory learning performance in the honey bee, Apis mellifera." Publisher: Elsevier, *Animal Behaviour* 48 (6): 1357–1369.

Borofsky, Talia, Victor J. Barranca, Rebecca Zhou, Dora von Trentini, Robert L. Broadrup, and Christopher Mayack. 2020. "Hive minded: like neurons, honey bees collectively integrate negative feedback to regulate decisions." Publisher: Academic Press, *Animal Behaviour* 168 (October): 33–44. https://doi.org/10.1016/j.anbehav.2020.07.023.

Boukal, David S, and Vlastimil Kivan. 1999. "Lyapunov functions for Lotka–Volterra predator–prey models with optimal foraging behavior." Publisher: Springer, *Journal of Mathematical Biology* 39 (6): 493–517.

Brandes, C. 1991. "Genetic differences in learning behavior in honeybees (Apis mellifera capensis)." Publisher: Springer, *Behavior Genetics 1991 21:3* 21, no. 3 (May): 271–294. Accessed July 14, 2021. https://doi.org/10.1007/BF01065820.

Britton, Nicholas F, Nigel R Franks, Stephen C Pratt, and Thomas D Seeley. 2002. "Deciding on a new home: How do honeybees agree?" Publisher: The Royal Society, *Proceedings of the Royal Society B: Biological Sciences* 269 (1498): 1383–1388. https://doi.org/10.1098/rspb.2002.2001.

Cacuci, Dan G, Mihaela Ionescu-Bujor, and Ionel Michael Navon. 2005. *Sensitivity and uncertainty analysis: Applications to large-scale systems.* Vol. 2. Publication Title: Sensitivity and Uncertainty Analysis: Applications to Large-Scale Systems. CRC Press.

Caetano-Anollés, Kelsey, Brent Ewers, Shilpa Iyer, Jeffrey R Lucas, Theodore P Pavlic, Andre P Seale, and Yu Zeng. 2022. "A Minimal Framework for Describing Living Systems: A Multi-Dimensional View of Life Across Scales" [in en]. *Integrative and Comparative Biology* 61, no. 6 (February): 2053–2065. Accessed October 3, 2022. https://doi.org/10.1093/icb/icab172.

Camazine, Scott, Jean-Louis Deneubourg, Nigel R. Franks, James Sneyd, Eric Bonabeau, and Guy Theraulaz. 2003. *Self-organization in biological systems.* Vol. 7. Princeton university press.

Camazine, Scott, and James Sneyd. 1991. "A model of collective nectar source selection by honey bees: Self-organization through simple rules." Publisher: Elsevier, *Journal of Theoretical Biology* 149 (4): 547–571. https://doi.org/10.1016/S0022-5193(05)80098-0.

Chandra, Sathees B C, Geraldine A Wright, and Brian H Smith. 2010. "Latent inhibition in the honey bee, Apis mellifera: Is it a unitary phenomenon?" Publisher: Springer, *Animal cognition* 13 (6): 805–815.

Chandra, Sathees B.C. C, Jay S. Hosler, and Brian H. Smith. 2000. "Heritable variation for latent inhibition and its correlation with reversal learning in honeybees (Apis

mellifera).” *Journal of Comparative Psychology* 114 (1): 86–97. https://doi.org/10.1037/0735-7036.114.1.86.

Chandra, Sathees B.C. C, Gregory J. Hunt, Susan Cobey, and Brian H Smith. 2001. “Quantitative trait loci associated with reversal learning and latent inhibition in honeybees (Apis mellifera).” Publisher: Springer, *Behavior genetics* 31 (3): 275–285. https://doi.org/10.1023/A:1012227308783.

Chopard, Bastien, Jean-Luc Falcone, Pierre Kunzli, Lourens Veen, and Alfons Hoekstra. 2018. “Multiscale modeling: recent progress and open questions.” Publisher: Springer, *Multiscale and Multidisciplinary Modeling, Experiments and Design* 1 (1): 57–68.

Clemens, Jan, Stefanie Krämer, and Bernhard Ronacher. 2014. “Asymmetrical integration of sensory information during mating decisions in grasshoppers.” Publisher: National Academy of Sciences, *Proceedings of the National Academy of Sciences of the United States of America* 111, no. 46 (November): 16562–16567. Accessed October 14, 2020. https://doi.org/10.1073/pnas.1412741111.

Cook, Chelsea N., Natalie J. Lemanski, Thiago Mosqueiro, Cahit Ozturk, Jürgen Gadau, Noa Pinter-Wollman, and Brian H. Smith. 2020. “Individual learning phenotypes drive collective behavior.” Publisher: Figshare, *Proceedings of the National Academy of Sciences of the United States of America* 117 (30): 17949–17956. Accessed July 14, 2021. https://doi.org/10.1073/pnas.1920554117.

Cook, Chelsea N., Thiago Mosqueiro, Colin S. Brent, Cahit Ozturk, Jürgen Gadau, Noa Pinter-Wollman, and Brian H. Smith. 2019. “Individual differences in learning and biogenic amine levels influence the behavioural division between foraging honeybee scouts and recruits.” Publisher: Wiley Online Library, *Journal of Animal Ecology* 88 (2): 236–246. https://doi.org/10.1111/1365-2656.12911.

Couzin, Iain D. 2007. “Collective minds.” Publisher: Nature Publishing Group, *Nature* 445, no. 7129 (February): 715. Accessed July 1, 2020. https://doi.org/10.1038/445715a.

———. 2009. “Collective cognition in animal groups.” Publisher: Elsevier Current Trends, *Trends in Cognitive Sciences* 13, no. 1 (January): 36–43. Accessed February 10, 2020. https://doi.org/10.1016/j.tics.2008.10.002.

Couzin, Iain D, Jens Krause, Richard James, Graeme D Ruxton, and Nigel R Franks. 2002. “Collective Memory and Spatial Sorting in Animal Groups.” Publisher: Academic Press, *Journal of Theoretical Biology* 218, no. 1 (September): 1–11. Accessed October 14, 2021. https://doi.org/10.1006/JTBI.2002.3065.

Dacke, Marie, and Mandyam V. Srinivasan. 2008. “Evidence for counting in insects” [in en]. *Animal Cognition* 11, no. 4 (October): 683–689. Accessed September 27, 2022. https://doi.org/10.1007/s10071-008-0159-y.

Dada, Joseph O., and Pedro Mendes. 2011. “Multi-scale modelling and simulation in systems biology.” Publisher: Oxford University Press, *Integrative Biology* 3 (2): 86–96. https://doi.org/10.1039/c0ib00075b.

DasGupta, Shamik, Clara Howcroft Ferreira, and Gero Miesenböck. 2014. “FoxP influences the speed and accuracy of a perceptual decision in Drosophila.” Publisher: American Association for the Advancement of Science, *Science* 344, no. 6186 (May): 901–904. Accessed October 14, 2020. https://doi.org/10.1126/science.1252114.

Davidson, Jacob D, Roxana P Arauco-Aliaga, Sam Crow, Deborah M Gordon, and Mark S Goldman. 2016. “Effect of interactions between harvester ants on forager decisions.” Publisher: Frontiers, *Frontiers in ecology and evolution* 4 (OCT): 115. https://doi.org/10.3389/fevo.2016.00115.

Delgado, Maria del Mar, Maria Miranda, Silvia J. Alvarez, Eliezer Gurarie, William F. Fagan, Vincenzo Penteriani, Agustina di Virgilio, and Juan Manuel Morales. 2018. “The importance of individual variation in the dynamics of animal collective movements.” Publisher: The Royal Society, *Philosophical Transactions of the Royal Society B: Biological Sciences* 373, no. 1746 (May). Accessed October 13, 2021. https://doi.org/10.1098/RSTB.2017.0008.

Detrain, Claire, and Jean Louis Deneubourg. 2008. “Collective Decision-Making and Foraging Patterns in Ants and Honeybees.” ISBN: 9780123743299, *Advances in Insect Physiology,* https://doi.org/10.1016/S0065-2806(08)00002-7.

Di Bernardo, Mario, Chris J Budd, Alan R Champneys, Piotr Kowalczyk, Arne B Nordmark, Gerard Olivar Tost, and Petri T Piiroinen. 2008. “Bifurcations in nonsmooth dynamical systems.” Publisher: SIAM, *SIAM Review* 50 (4): 629–701.

Dinet, Céline, Alphée Michelot, Julien Herrou, and Tâm Mignot. 2021. “Linking single-cell decisions to collective behaviours in social bacteria.” Publisher: The Royal Society, *Philosophical Transactions of the Royal Society B: Biological Sciences* 376, no. 1820 (March). Accessed September 1, 2021. https://doi.org/10.1098/rstb.2019.0755.

Dornhaus, Anna. 2008. “Specialization does not predict individual efficiency in an ant.” *PLoS Biology,* https://doi.org/10.1371/journal.pbio.0060285.

Dussutour, A., M. Beekman, S. C. Nicolis, and B. Meyer. 2009. “Noise improves collective decision-making by ants in dynamic environments.” *Proceedings of the Royal Society B: Biological Sciences* 276 (1677): 4353–4361. https://doi.org/10.1098/rspb.2009.1235.

Escalante, Edgardo J. 1999. “Quality and Productivity Improvement: a Study of Variation and Defects in Manufacturing.” *Quality Engineering* 11 (3): 427–442. https://doi.org/10.1080/08982119908919259.

Feinerman, Ofer, and Amos Korman. 2017. “Individual versus collective cognition in social insects.” *Journal of Experimental Biology* 220 (1): 73–82. Accessed February 8, 2022. https://doi.org/10.1242/jeb.143891.

Feller, William. 1968. *An Introduction to Probability Theory and Its Applications: Volume I.* Vol. 1. John Wiley \& Sons.

Fewell, Jennifer H. 2003. “Social insect networks.” *Science,* https://doi.org/10.1126/science.1088945.

Filippov, A. F. 1988. “Equations with the right-hand side continuous in x and discontinuous in t.” In *Differential Equations with Discontinuous Righthand Sides,* 3–47. Springer.

Franks, Nigel R., Anna Dornhaus, Jon P. Fitzsimmons, and Martin Stevens. 2003. “Speed versus accuracy in collective decision making.” *Proceedings of the Royal Society B: Biological Sciences,* https://doi.org/10.1098/rspb.2003.2527.

Gordon, Deborah M, Brian C Goodwin, and L E H Trainor. 1992. “A parallel distributed model of the behaviour of ant colonies.” Publisher: Academic Press, *Journal of Theoretical Biology* 156, no. 3 (June): 293–307. Accessed June 28, 2021. https://doi.org/10.1016/S0022-5193(05)80677-0.

Gordon, Deborah M. 2002. “The organization of work in social insect colonies.” *Complexity,* https://doi.org/10.1002/cplx.10048.

Goutelle, Sylvain, Michel Maurin, Florent Rougier, Xavier Barbaut, Laurent Bourguignon, Michel Ducher, and Pascal Maire. 2008. “The Hill equation: a review of its capabilities in pharmacological modelling.” *Fundamental \& clinical pharmacology* 22:633–648.

Grüter, C, MH Kärcher, and FLW Ratnieks. 2011. “The natural history of nest defence in a stingless bee, Tetragonisca angustula (Latreille)(Hymenoptera: Apidae), with two distinct types of entrance guards.” Publisher: SciELO Brasil, *Neotropical entomology* 40:55–61.

Grüter, Christoph, Cristiano Menezes, Vera L. Imperatriz-Fonseca, and Francis L.W. Ratnieks. 2012. "A morphologically specialized soldier caste improves colony defense in a neotropical eusocial bee." *Proceedings of the National Academy of Sciences of the United States of America* 109 (4): 1182–1186. https://doi.org/10.1073/pnas.1113398109.

Guo, Xiaohui, Jun Chen, Asma Azizi, Jennifer Fewell, and Yun Kang. 2020. "Dynamics of social interactions, in the flow of information and disease spreading in social insects colonies: Effects of environmental events and spatial heterogeneity." Publisher: Elsevier Ltd, *Journal of Theoretical Biology* 492:1–10. https://doi.org/10.1016/j.jtbi.2020.110191.

Hammel, Benedikt, Ayrton Vollet-Neto, Cristiano Menezes, Fabio S Nascimento, Wolf Engels, and Christoph Grüter. 2015. "Soldiers in a stingless bee: Work rate and task repertoire suggest they are an elite force." Publisher: University of Chicago Press Chicago, IL, *American Naturalist* 187 (1): 120–129. https://doi.org/10.1086/684192.

Hills, Thomas T, Peter M Todd, David Lazer, A David Redish, Iain D Couzin, Melissa Bateson, Roshan Cools, et al. 2015. "Exploration versus exploitation in space, mind, and society." Publisher: Elsevier, *Trends in Cognitive Sciences* 19 (1): 46–54. https://doi.org/10.1016/j.tics.2014.10.004.

Holbrook, C. Tate, Rebecca M. Clark, Raphaël Jeanson, Susan M. Bertram, Penelope F. Kukuk, and Jennifer H. Fewell. 2009. "Emergence and consequences of division of labor in associations of normally solitary sweat bees." *Ethology,* https://doi.org/10.1111/j.1439-0310.2009.01617.x.

Holland, John H. 2014. *Complexity: a very short introduction.* Oxford University Press (OUP).

Iverson, Kenneth E. 1962. *A Programming Language.* New York: Wiley.

Jandt, J. M., and D. M. Gordon. 2016. "The behavioral ecology of variation in social insects." Publisher: Elsevier Inc. *Current Opinion in Insect Science* 15 (June): 40–44. Accessed October 20, 2020. https://doi.org/10.1016/j.cois.2016.02.012.

Jeanne, R L. 1986. "The evolution of the organization of work in social insects." *Monit. Zool. Ital.*

Jones, Sam M., Jelle S. van Zweden, Christoph Grüter, Cristiano Menezes, Denise A. Alves, Patrícia Nunes-Silva, Tomer Czaczkes, Vera L. Imperatriz-Fonseca, and Francis L.W. Ratnieks. 2012. "The role of wax and resin in the nestmate recognition system of a

stingless bee, Tetragonisca angustula." ISBN: 0026501112, *Behavioral Ecology and Sociobiology* 66 (1): 1–12. https://doi.org/10.1007/s00265-011-1246-7.

Jongepier, Evelien, and Susanne Foitzik. 2016. "Fitness costs of worker specialization for ant societies." *Proceedings of the Royal Society B: Biological Sciences* 283 (1822). https://doi.org/10.1098/rspb.2015.2572.

Kacelnik, Alex, Marco Vasconcelos, Tiago Monteiro, and Justine Aw. 2011. "Darwin's "tug-of-war" vs. starlings' "horse-racing": How adaptations for sequential encounters drive simultaneous choice." *Behavioral Ecology and Sociobiology* 65 (3): 547–558. https://doi.org/10.1007/s00265-010-1101-2.

Kang, Yun, and Guy Theraulaz. 2016. "Dynamical Models of Task Organization in Social Insect Colonies" [in en]. *Bulletin of Mathematical Biology* 78, no. 5 (May): 879–915. Accessed October 3, 2022. https://doi.org/10.1007/s11538-016-0165-1.

Kao, Albert B, and Iain D Couzin. 2019. "Modular structure within groups causes information loss but can improve decision accuracy." *Philosophical Transactions of the Royal Society B: Biological Sciences* 374 (1774). https://doi.org/10.1098/rstb.2018.0378.

Koedam, D, M Brone, and PGM Van Tienen. 1997. "The regulation of worker-oviposition in the stingless bee Trigona (Tetragonisca) angustula Illiger (Apidae, Meliponinae)." Publisher: Springer, *Insectes sociaux* 44 (3): 229–244.

Kuznetsov, Yu A, Sergio Rinaldi, and Alessandra Gragnani. 2003. "One-parameter bifurcations in planar Filippov systems." Publisher: World Scientific, *International Journal of Bifurcation and Chaos* 13 (08): 2157–2188.

Lamport, Leslie. 2012. "Buridan's Principle." Publisher: Springer, *Foundations of Physics* 42, no. 8 (August): 1056–1066. Accessed July 8, 2020. https://doi.org/10.1007/s10701-012-9647-7.

Latty, Tanya, and Madeleine Beekman. 2011. "Irrational decision-making in an amoeboid organism: Transitivity and context-dependent preferences." *Proceedings of the Royal Society B: Biological Sciences* 278 (1703): 307–312. Accessed August 25, 2021. https://doi.org/10.1098/rspb.2010.1045.

Lee, J., J. Son, S. Zhou, and Y. Chen. 2020. "Variation Source Identification in Manufacturing Processes Using Bayesian Approach with Sparse Variance Components Prior" [in English]. *IEEE Transactions on Automation Science and Engineering* 17 (3): 1469–1485. https://doi.org/10.1109/TASE.2019.2959605.

Lemanski, Natalie J., Chelsea N. Cook, Brian H. Smith, and Noa Pinter-Wollman. 2019. "A multiscale review of behavioral variation in collective foraging behavior in honey bees." *Insects* 10 (11): 18–20. https://doi.org/10.3390/insects10110370.

Mancinelli, Sara, and Simona Lodato. 2018. "Decoding neuronal diversity in the developing cerebral cortex: from single cells to functional networks." Publisher: Elsevier Current Trends, *Current Opinion in Neurobiology* 53 (December): 146–155. Accessed July 19, 2021. https://doi.org/10.1016/J.CONB.2018.08.001.

Marshall, James A R, Rafal Bogacz, Anna Dornhaus, Robert Planqué, Tim Kovacs, and Nigel R Franks. 2009. "On optimal decision-making in brains and social insect colonies." Publisher: The Royal Society, *Journal of the Royal Society Interface* 6 (40): 1065–1074.

Mazza, Valeria, Jana A. Eccard, Marco Zaccaroni, Jens Jacob, and Melanie Dammhahn. 2018. "The fast and the flexible: cognitive style drives individual variation in cognition in a small mammal." *Animal Behaviour* 137:119–132. Accessed January 18, 2022. https://doi.org/10.1016/j.anbehav.2018.01.011.

McEntire, Kira D, Matthew Gage, Richard Gawne, Michael G Hadfield, Catherine Hulshof, Michele A Johnson, Danielle L Levesque, Joan Segura, and Noa Pinter-Wollman. 2022. "Understanding Drivers of Variation and Predicting Variability Across Levels of Biological Organization" [in en]. *Integrative and Comparative Biology* 61, no. 6 (February): 2119–2131. Accessed September 23, 2022. https://doi.org/10.1093/icb/icab160.

Meza, Magno Enrique Mendoza, Amit Bhaya, Eugenius Kaszkurewicz, and Michel Iskin da Silveira Costa. 2005. "Threshold policies control for predator-prey systems using a control Liapunov function approach." Publisher: Elsevier, *Theoretical Population Biology* 67 (4): 273–284.

Miramontes, Octavio, Ricard V. Sole, and B. C. Goodwin. 2001. "Neural networks as sources of chaotic motor activity in ants and how complexity develops at the social scale." Publisher: World Scientific Publishing Company, *International Journal of Bifurcation and Chaos in Applied Sciences and Engineering* 11, no. 6 (November): 1655–1664. Accessed July 22, 2021. https://doi.org/10.1142/S0218127401002912.

Mitchell, Melanie. 2009. *Complexity: a guided tour*. ISSN: 10121587. Oxford University Press (OUP). https://doi.org/10.22201/ceiich.24485705e.2015.6.49482.

Moses, Melanie E., Judy L. Cannon, Deborah M. Gordon, and Stephanie Forrest. 2019. "Distributed Adaptive Search in T Cells: Lessons From Ants." *Frontiers in Immunology* 10 (June): 1357. Accessed October 6, 2022. https://doi.org/10.3389/fimmu.2019.01357.

Mosqueiro, Thiago, Chelsea N Cook, Ramon Huerta, Jürgen Gadau, Brian H Smith, and Noa Pinter-Wollman. 2017. "Task allocation and site fidelity jointly influence foraging regulation in honeybee colonies." Publisher: The Royal Society Publishing, *Royal Society Open Science* 4 (8): 170344.

Musco, Cameron, Hsin-Hao Su, and Nancy A. Lynch. 2017. "Ant-inspired density estimation via random walks" [in en]. *Proceedings of the National Academy of Sciences* 114, no. 40 (October): 10534–10541. Accessed September 27, 2022. https://doi.org/10.1073/pnas.1706439114.

Navas-Zuloaga, M. Gabriela, Theodore P. Pavlic, and Brian H. Smith. 2022. "Alternative model systems for cognitive variation: eusocial-insect colonies" [in en]. *Trends in Cognitive Sciences* 26, no. 10 (October): 836–848. Accessed October 6, 2022. https://doi.org/10.1016/j.tics.2022.06.011.

O'shea-Wheller, Thomas A., Naoki Masuda, Ana B. Sendova-Franks, and Nigel R. Franks. 2017. "Variability in individual assessment behaviour and its implications for collective decision-making." Publisher: Royal Society, *Proceedings of the Royal Society B: Biological Sciences* 284, no. 1848 (February). Accessed April 8, 2021. https://doi.org/10.1098/rspb.2016.2237.

Papoulis, Athanasios, and S Unnikrishna Pillai. 2002. *Probability, random variables, and stochastic processes.* Tata McGraw-Hill Education.

Pavlic, Theodore P., Jake Hanson, Gabriele Valentini, Sara Imari Walker, and Stephen C. Pratt. 2021. "Quorum sensing without deliberation: biological inspiration for externalizing computation to physical spaces in multi-robot systems." Publisher: Springer US ISBN: 0123456789, *Swarm Intelligence* 15 (1): 171–203. https://doi.org/10.1007/s11721-021-00196-4.

Pavlic, Theodore P., and Kevin M. Passino. 2010. "When rate maximization is impulsive" [in en]. *Behavioral Ecology and Sociobiology* 64, no. 8 (August): 1255–1265. Accessed September 27, 2022. https://doi.org/10.1007/s00265-010-0940-1.

Piñero, Jordi, Ricard Solé, Jordi Pinero, and Ricard Solé. 2019. "Statistical physics of liquid brains." Publisher: The Royal Society, *Philosophical Transactions of the Royal Society B: Biological Sciences* 374 (1774): 20180376. https://doi.org/10.1098/rstb.2018.0376.

Pinter-Wollman, Noa. 2012. "Personality in social insects: How does worker personality determine colony personality?" *Current Zoology* 58 (4): 580–588. https://doi.org/10.1093/czoolo/58.4.580.

Pinter-Wollman, Noa, Ashwin Bala, Andrew Merrell, Jovel Queirolo, Martin C Stumpe, Susan Holmes, and Deborah M Gordon. 2013. "Harvester ants use interactions to regulate forager activation and availability." Publisher: Elsevier, *Animal behaviour* 86 (1): 197–207.

Pratt, Stephen C. 2005a. "Behavioral mechanisms of collective nest-site choice by the ant Temnothorax curvispinosus." Publisher: Springer, *Insectes Sociaux* 52 (4): 383–392.

———. 2005b. "Quorum sensing by encounter rates in the ant Temnothorax albipennis." Publisher: Oxford University Press, *Behavioral Ecology* 16 (2): 488–496.

———. 2019. "Nest site choice in social insects." In *Encyclopedia of Animal Behavior,* 766–774. Elsevier, January. Accessed November 16, 2020. https://doi.org/10.1016/B978-0-12-809633-8.01262-0.

Pratt, Stephen C., David J .T. T Sumpter, Eamonn B. Mallon, and Nigel R. Franks. 2005. "An agent-based model of collective nest choice by the ant Temnothorax albipennis." Publisher: Elsevier, *Animal Behaviour* 70 (5): 1023–1036.

Pratt, Stephen C., and David J.T. Sumpter. 2006. "A tunable algorithm for collective decision-making." *Proceedings of the National Academy of Sciences of the United States of America* 103, no. 43 (October): 15906–15910. Accessed October 20, 2020. https://doi.org/10.1073/pnas.0604801103.

Ratcliff, Roger. 1978. "A theory of memory retrieval." Publisher: American Psychological Association, *Psychological review* 85 (2): 59.

Ratcliff, Roger, Philip L Smith, Scott D Brown, and Gail McKoon. 2016. "Diffusion decision model: Current issues and history." Publisher: Elsevier, *Trends in cognitive sciences* 20 (4): 260–281.

Richardson, Thomas O., Charles Mullon, James A.R. Marshall, Nigel R. Franks, and Thomas Schlegel. 2018. "The influence of the few: A stable 'oligarchy' controls information flow in house-hunting ants." Publisher: Royal Society Publishing, *Proceedings of the Royal Society B: Biological Sciences* 285, no. 1872 (February). Accessed April 8, 2021. https://doi.org/10.1098/rspb.2017.2726.

Robinson, Elva J.H., Nigel R. Franks, Samuel Ellis, Saki Okuda, and James A.R. Marshall. 2011. "A simple threshold rule is sufficient to explain sophisticated collective decision-making." *PLoS ONE,* https://doi.org/10.1371/journal.pone.0019981.

Roitman, Jamie D, and Michael N Shadlen. 2002. "Response of neurons in the lateral intraparietal area during a combined visual discrimination reaction time task." Publisher: Soc Neuroscience, *Journal of neuroscience* 22 (21): 9475–9489.

Sasaki, Takao, and Stephen C Pratt. 2012. "Groups have a larger cognitive capacity than individuals." Publisher: Cell Press, *Current Biology* 22, no. 19 (October): R827–R829. Accessed February 10, 2020. https://doi.org/10.1016/j.cub.2012.07.058.

———. 2018. "The psychology of superorganisms: Collective decision making by insect societies." Publisher: Annual Reviews, *Annual review of entomology* 63:259–275.

Sasaki, Takao, Stephen C Pratt, and Alex Kacelnik. 2018. "Parallel vs. comparative evaluation of alternative options by colonies and individuals of the ant Temnothorax rugatulus." *Scientific Reports* 8 (1): 1–8. https://doi.org/10.1038/s41598-018-30656-7.

Sasaki, Takao, Benjamin Stott, and Stephen C. Pratt. 2019. "Rational time investment during collective decision making in Temnothorax ants." *Biology Letters* 15 (10). Accessed January 25, 2022. https://doi.org/10.1098/rsbl.2019.0542.

Scheiner, Samuel M, and Robert D Holt. 2012. "The genetics of phenotypic plasticity. X. Variation versus uncertainty." *Ecology and Evolution* 2 (4): 751–767. Accessed October 5, 2022. https://doi.org/10.1002/ece3.217.

Seeley, T. D. 1989. "The honey bee colony as a superorganism." *American Scientist* 77 (6): 546–553.

Seeley, Thomas D. 1995. *The Wisdom of the Hive*. Publication Title: The Wisdom of the Hive. Harvard University Press. https://doi.org/10.2307/j.ctv1kz4h15.

———. 1982. "Adaptive significance of the age polyethism schedule in honeybee colonies." *Behavioral Ecology and Sociobiology,* https://doi.org/10.1007/BF00299306.

———. 1997. "Honey bee colonies are group-level adaptive units." *American Naturalist* 150 (SUPPL.). Accessed October 27, 2021. https://doi.org/10.1086/286048.

Seeley, Thomas D., and Susannah C. Buhrman. 1999. "Group decision making in swarms of honey bees." Publisher: Springer, *Behavioral Ecology and Sociobiology 1999 45:1* 45 (1): 19–31. Accessed October 14, 2021. https://doi.org/10.1007/S002650050536.

Seeley, Thomas D., Scott Camazine, and James Sneyd. 1991. "Collective decision-making in honey bees: how colonies choose among nectar sources." Publisher: Springer, *Behavioral Ecology and Sociobiology* 28 (4): 277–290. https://doi.org/10.1007/BF00175101.

Segers, Francisca H.I.D., Cristiano Menezes, Ayrton Vollet-Neto, Dorothee Lambert, and Christoph Grüter. 2015. "Soldier production in a stingless bee depends on rearing location and nurse behaviour." *Behavioral Ecology and Sociobiology* 69 (4): 613–623. https://doi.org/10.1007/s00265-015-1872-6.

Segers, Francisca H.I.D., Lucas Von Zuben, and Christoph Grüter. 2016. "Local differences in parasitism and competition shape defensive investment in a polymorphic eusocial bee." *Ecology* 97 (2): 417–426. https://doi.org/10.1890/15-0793.1.

Shettleworth, Sara J. 2009. *Cognition, evolution, and behavior.* Oxford University Press.

Silveira Costa, Michel Iskin da, and Magno Enrique Mendoza Meza. 2006. "Application of a threshold policy in the management of multispecies fisheries and predator culling." Publisher: OUP, *Mathematical Medicine and Biology: A Journal of the IMA* 23 (1): 63–75.

Smith, Brian H, and Chelsea N Cook. 2020. "Experimental psychology meets behavioral ecology: what laboratory studies of learning polymorphisms mean for learning under natural conditions, and vice versa." Publisher: Taylor & Francis, *Journal of Neurogenetics,* 1–6.

Solé, Ricard, Melanie Moses, and Stephanie Forrest. 2019. "Liquid brains, solid brains." Publisher: The Royal Society, *Philosophical Transactions of the Royal Society B: Biological Sciences* 374 (1774): 20190040. https://doi.org/10.1098/rstb.2019.0040.

Stephens, Philip A., and William J. Sutherland. 1999. "Consequences of the Allee effect for behaviour, ecology and conservation." Publisher: Elsevier Ltd, *Trends in Ecology and Evolution* 14, no. 10 (October): 401–405. Accessed May 20, 2021. https://doi.org/10.1016/S0169-5347(99)01684-5.

Strickland, Laura, Kaitlin Baudier, Kenneth Bowers, Theodore P. Pavlic, and Charles Pippin. 2019. "Bio-inspired Role Allocation of Heterogeneous Teams in a Site Defense Task" [in en]. In *Distributed Autonomous Robotic Systems,* edited by Nikolaus Correll, Mac Schwager, and Michael Otte, 9:139–151. Series Title: Springer Proceedings in Advanced Robotics ISBN2: 978-3-030-05816-6. Cham: Springer International Publishing. Accessed October 3, 2022. https://doi.org/10.1007/978-3-030-05816-6_10.

Sumpter, David J T, and Stephen C Pratt. 2003. "A modelling framework for understanding social insect foraging." Publisher: Springer, *Behavioral Ecology and Sociobiology* 53 (3): 131–144.

Tang, Sanyi, Juhua Liang, Yanni Xiao, and Robert A Cheke. 2012. "Sliding bifurcations of Filippov two stage pest control models with economic thresholds." Publisher: SIAM, *SIAM Journal on Applied Mathematics* 72 (4): 1061–1080.

Tang, Sanyi, Yanni Xiao, Ning Wang, and Hulin Wu. 2012. "Piecewise HIV virus dynamic model with CD4+ T cell count-guided therapy: I." Publisher: Elsevier, *Journal of Theoretical Biology* 308:123–134.

Thieme, Horst R. 2018. *Mathematics in population biology*. Princeton University Press.

Tuncer, Ozan, Emre Ates, Yijia Zhang, Ata Turk, Jim Brandt, Vitus J. Leung, Manuel Egele, and Ayse K. Coskun. 2017. "Diagnosing performance variations in HPC applications using machine learning." In *Lecture Notes in Computer Science (including subseries Lecture Notes in Artificial Intelligence and Lecture Notes in Bioinformatics),* vol. 10266 LNCS, 355–373. ISSN: 16113349. Springer, Cham, June. Accessed March 3, 2022. https://doi.org/10.1007/978-3-319-58667-0_19.

Usher, Marius, and James L. McClelland. 2001. "The time course of perceptual choice: The leaky, competing accumulator model." Publisher: American Psychological Association Inc. *Psychological Review* 108 (3): 550–592. Accessed July 8, 2020. https://doi.org/10.1037/0033-295X.108.3.550.

Valentini, Gabriele, Naoki Masuda, Zachary Shaffer, Jake R. Hanson, Takao Sasaki, Sara Imari Walker, Theodore P. Pavlic, and Stephen C. Pratt. 2020. "Division of labour promotes the spread of information in colony emigrations by the ant Temnothorax rugatulus." Publisher: Royal Society Publishing, *Proceedings of the Royal Society B: Biological Sciences* 287, no. 1924 (April). Accessed April 8, 2021. https://doi.org/10.1098/rspb.2019.2950.

Vallverdú, Jordi, Oscar Castro, Richard Mayne, Max Talanov, Michael Levin, Frantisek Baluška, Yukio Gunji, Audrey Dussutour, Hector Zenil, and Andrew Adamatzky. 2018. "Slime mould: The fundamental mechanisms of biological cognition." Publisher: Elsevier, *BioSystems* 165 (March): 57–70. Accessed September 1, 2021. https://doi.org/10.1016/j.biosystems.2017.12.011.

Van Veen, JW, and Marinus J Sommeijer. 2000. "Colony reproduction in Tetragonisca angustula (Apidae, Meliponini)." Publisher: Springer, *Insectes sociaux* 47 (1): 70–75.

Varela, Francisco J., Antonio Coutinho, Bruno Dupire, and Nelson N. Vaz. 1988. "Cognitive Networks: Immune, Neural, and Otherwise." In *Theoretical Immunology*. Num Pages: 17. CRC Press.

Weinstein, Steven, and Theodore P. Pavlic. 2017. “Noise and function.” ArXiv: 1608.04824 ISBN: 9781316584200, *From Matter to Life: Information and Causality,* 174–198. https://doi.org/10.1017/9781316584200.009.

Wilson, Edward O. 1971. *The Insect Societies.* Cambridge, Massachusetts, USA: Harvard University Press [Distributed by Oxford University Press]. Accessed September 1, 2021. https://www.cabdirect.org/cabdirect/abstract/19720503745.

Xiao, Yanni, Tingting Zhao, and Sanyi Tang. 2013. “Dynamics of an infectious diseases with media/psychology induced non-smooth incidence.” Publisher: American Institute of Mathematical Sciences, *Mathematical Biosciences and Engineering* 10 (2): 445.

Young, K David, and Ümit Özgüner. 1999. *Variable Structure Systems, Sliding Mode and Nonlinear Control.* Vol. 247. Springer.

Zweden, Jelle S. van, Christoph Grüter, Sam M. Jones, and Francis L.W. Ratnieks. 2011. “Hovering guards of the stingless bee Tetragonisca angustula increase colony defensive perimeter as shown by intra- and inter-specific comparisons.” *Behavioral Ecology and Sociobiology* 65 (6): 1277–1282. https://doi.org/10.1007/s00265-011-1141-2.

APPENDIX A

SUPPLEMENTARY MATERIAL FOR CHAPTER 2

A.1 Convergence

First, we show that the decision process ends with probability 1, that is, one of the absorbing states is reached in a finite number of steps and the expected time between steps is finite. The latter, also called average holding time, can be computed from the transition rates as $\frac{\tau}{1+\lambda\tau}$, which is a finite quantity. Now we verify that the probability of the process involving an infinite number of steps is 0.

Consider the embedded (jump) discrete chain $\mathbf{v}^{k+1} = P^\top \mathbf{v}^k$ defined by matrix

$$P \triangleq \begin{bmatrix} 1 & 0 & 0 & 0 & ... & 0 \\ \frac{1/\tau}{1/\tau+\lambda} & 0 & \frac{\lambda}{1/\tau+\lambda} & 0 & 0 & 0 \\ 0 & \frac{1/\tau}{1/\tau+\lambda} & 0 & \frac{\lambda}{1/\tau+\lambda} & \ddots & 0 \\ 0 & 0 & \ddots & \ddots & \ddots & 0 \\ 0 & \ddots & 0 & \frac{1/\tau}{1/\tau+\lambda} & 0 & \frac{\lambda}{1/\tau+\lambda} \\ 0 & ... & 0 & 0 & 0 & 1 \end{bmatrix},$$

as described in the main text. The jump chain process is equivalent to a one-dimensional discrete-time random walk, where in each step there is a $p \triangleq \frac{\lambda}{1/\tau+\lambda}$ probability of going up and a $q \triangleq 1 - p = \frac{1/\tau}{1/\tau+\lambda}$ probability of going down, akin to the classical gambler's ruin problem. In the original continuous-time process, these steps occur at random, exponentially distributed time intervals, but the sequence of states is the same between the discrete-time and continuous-time processes. As in the gambler's ruin problem, the probability of an infinite trace can be shown to be zero.

If $p = 0$ or $p = 1$, the process is guaranteed to end in exactly n steps. Therefore we consider $0 < p < 1$ and define Q_i as the conditional probability of an infinite process given an initial state of $X_0 = i$. That is,

$$Q_i \triangleq P(S = \infty | X_0 = i)$$

where S is the number of steps until absorption. Note that the first transition can take the state to either $i - 1$ or $i + 1$ and therefore

$$Q_i = \begin{cases} 0 & \text{if } i = -n, \\ pQ_{i+1} + (1-p)Q_{i-1} & \text{if } -n < i < n, \\ 0 & \text{if } i = n. \end{cases} \tag{A.1}$$

Thus, a recursive argument can be used to find Q_i.

First, consider the case where $p \neq 1/2$. Solving the characteristic equation $pr^2 - r + (1-p) = 0$ of the recurrence relation in Equation (A.1) yields the roots $r = ((1-p)/p)$ and $r = 1$. It follows that the general solution has the form

$$Q_i = \left(\frac{(1-p)}{p}\right)^i A + (1)^i B$$

for constants $A, B \in \mathbb{R}$. However, by the boundary conditions in Equation (A.1), it must be the case that:

$$0 = \left(\frac{(1-p)}{p}\right)^{-n} A + B = \left(\frac{(1-p)}{p}\right)^{n} A + B$$

so that $\left(\frac{(1-p)}{p}\right)^{-n} A = \left(\frac{(1-p)}{p}\right)^{n} A$, which is true if and only if $A = 0$ or $\left(\frac{(1-p)}{p}\right)^{n} = \left(\frac{(1-p)}{p}\right)^{-n}$. Because the latter requires $p = 1/2$ and we are focusing on the case where $p \neq 1/2$, we conclude that $A = 0$, and so $B = 0$ as well. Consequently, the conditional probability $Q_i = 0$ for $p \neq 1/2$.

Next, consider the case of $p = 1/2$. The general solution takes the form $Q_i = Ai + B$. Then, by the boundary conditions in Equation (A.1), $-An + B = An + B = 0$, and so $A = B = 0$. Thus the conditional probability Q_i of taking an infinite number of steps to make a choice starting from state $X_0 = i$ is $Q_i = 0$, which is in agreement with the case of $p \neq 1/2$ above.

A.2 Decision Probabilities (limit distribution)

Let P_∞ denote the limiting probability distribution for the process, defined by

$$P_\infty(i) \triangleq P(X_\infty = i)$$

where i is a state in $\mathcal{R}_X$ and $X_\infty \triangleq \lim_{t\to\infty} X_t$. Let P_i^T and P_i^R denote the conditional probability that the decision outcome is to recruit by transporting or tandem running, respectively, given that the ant is in an initial state of $X_0 = i$. For the absorbing states, $P_n^T = 1$ and $P_{-n}^T = 0$. Thus, assume that the ant starts in a transient state $X_0 = i$ where $|i| < n$. After the first transition, it moves to either state $i - 1$ or $i + 1$. Therefore, because the process is Markovian,

$$P_i^T = qP_{i-1}^T + pP_{i+1}^T, \tag{A.2}$$

which is a recurrence relation that has an analytical solution that follows from the characteristic equation $pr^2 - r + q = 0$. There are two special cases:

- When $p = q$, the characteristic equation has a double root ($r = 1$). For this case, Equation (A.2) has a solution of the form $P_i^T = iA + B$ for some constants $A, B \in \mathbb{R}$ that, to be consistent with the absorbing states, must be such that:

$$\begin{cases} nA + B = P_n^T = 1 \\ -nA + B = P_{-n}^T = 0 \end{cases},$$

  and so $A = 1/(2n)$, $B = 1/2$, and $P_i^T = (i + n)/(2n)$. When the process starts at state $i = X_0 = 0$, the conditional probability of recruiting by transport is $P_0^T = 1/2$, which reflects the symmetry of no initial bias in this special $p = q$ case.

- In the more general case where $p \neq q$ (but $q \triangleq 1-p$), the characteristic equation yields the particular solutions $P_i^T = 1$ and $P_i^T = (q/p)^i$. The general solution then has the form

$$P_i^T = \left(\frac{q}{p}\right)^i A + (1)^i B$$

for constants $A, B \in \mathbb{R}$. To fix these constants, the conditional probabilities for the case of the absorbing states can be used as boundary conditions. Thus, it must be the case that:

$$\begin{cases} A\left(\frac{q}{p}\right)^{-n} + B = P_{-n}^T = 0 \\ A\left(\frac{q}{p}\right)^{n} + B = P_{n}^T = 1 \end{cases},$$

and so

$$A = \frac{(q/p)^n}{(q/p)^{2n}-1} \quad \text{and} \quad B = -\frac{1}{(q/p)^{2n}-1}.$$

Therefore, for $i \in \mathcal{R}_X$,

$$P_i^T = \frac{(q/p)^{n+1}-1}{(q/p)^{2n}-1}.$$

So the conditional probability of recruiting by transporting when starting in the neutral initial state $i = X_0 = 0$ is:

$$\begin{aligned} P_0^T &= \frac{(q/p)^n - 1}{(q/p)^{2n}-1} = \frac{(q/p)^n - 1}{\left((q/p)^n - 1\right)\left((q/p)^n + 1\right)} \\ &= \frac{1}{(q/p)^n + 1} = \frac{(p/q)^n}{(p/q)^n + 1} = \frac{(\lambda\tau)^n}{(\lambda\tau)^n + 1}. \end{aligned} \tag{A.3}$$

Conveniently, when $p = q$ (or, equivalently, $\lambda\tau = 1$), $P_0^T = 0.5$ as in the special $p = q$ case above.

A.3 Decision Latency (hitting time)

We will begin by using a recursive approach to find the expected number of steps of the process before absorption. Knowing the average duration of the exponentially distributed time intervals between transitions, we will compute the expected decision time.

Let S_i be the number of steps until absorption when starting form state i. Clearly, S_{-n} and S_n are both 0 since $\pm n$ are absorbing states. After the first transition occurs, the conditional expectation of the number of steps is just $S_{i+1} + 1$ if the state increased by one and $S_{i-1} + 1$ if it decreased. We derive the following recursion:

$$S_i = pS_{i+1} + qS_{i-1} + 1.$$

This is an inhomogeneous difference equation with boundary conditions

$$S_n = 0 \ , \ S_{-n} = 0.$$

The homogeneous solution is

$$A\left(\frac{q}{p}\right)^i + B \qquad \text{for } p \neq q$$

as before, and a particular solution can be found by assuming a linear form $S_i = ia + b$ and substituting in the recursion to get $S_i = i/(q-p)$. Thus,

$$S_i = A\left(\frac{q}{p}\right)^i + B + \frac{i}{q-p}.$$

Using the boundary conditions, we get

$$A = \frac{2n\left(\frac{q}{p}\right)^n}{(p-q)\left(\left(\frac{q}{p}\right)^{2n} - 1\right)} \, B = -\frac{n\left(\left(\frac{q}{p}\right)^{2n} + 1\right)}{(p-q)\left(\left(\frac{q}{p}\right)^{2n} - 1\right)}.$$

Substituting and setting $i = 0$ (to focus on the case of $X_0 = i = 0$),

$$S_0 = -\frac{n\left(\left(\frac{q}{p}\right)^n - 1\right)}{(p-q)\left(\left(\frac{q}{p}\right)^n + 1\right)}$$

When $p = q$, the particular solution $S_i = -i^2$ can be found by assuming a quadratic form $S_i = ai^2 + bi + c$, which yields $a = -1, b = c = 0$. Thus,

$$S_i = Ai + B - i^2$$

with boundary conditions $0 = \pm An + B - n^2$, so $A = 0, B = n^2$ so

$$S_i = n^2 - i^2.$$

For the initial state $X_0 = i = 0$, we obtain

$$S_0 = \begin{cases} -\dfrac{n\left(\left(\frac{q}{p}\right)^n - 1\right)}{(p-q)\left(\left(\frac{q}{p}\right)^n + 1\right)} & \text{if } p \neq q, \\ n^2 & \text{if } p = q. \end{cases}$$

Substituting the values for p and q and multiplying by the average holding time, $\frac{\tau}{1+\lambda\tau}$, we obtain the decision latency for the initial neutral state 0,

$$L_o \triangleq \begin{cases} \dfrac{n\tau\left(1-(\lambda\tau)^n\right)}{(1-\lambda\tau)\left(1+(\lambda\tau)^n\right)} & \text{if } \lambda\tau \neq 1, \\ \dfrac{\tau n^2}{2} & \text{if } \lambda\tau = 1. \end{cases}$$

APPENDIX B

SUPPLEMENTARY MATERIAL FOR CHAPTER 3

B.1 Parameter values

B.1.1 Abandoning rate δ

Familiar feeder is 4m away from colony. Novel feeder changes every day, average distance is 4.3m. According to behavioral experiments by Mosqueiro et al Mosqueiro et al. 2017 there is a linear relationship between distance and inter-visit interval t, dictated by

$$t = \alpha d + \beta$$

where $\alpha = 0.28 \pm 0.05$ and $\beta = 2.3 \pm 0.3$

$$\delta_f = \frac{1}{2.86 * 3.462}$$

B.1.2 High LI proportion: α values

All colonies are composed by 650 workers from selected lines and 650 control workers (not selected for LI phenotype). Control colonies are made up entirely by control workers. The proportion of High LI individuals among controls was estimated to be 25% by expert elicitation (Dr. Chelsea Cook). The selected population of the colonies is either 100% High LI (High colonies), 50% High LI and 50% Low LI (Mix colonies) or 100% Low LI (Low colonies). Thus, we estimate alpha to be 62.5%, 37.5%, 12.5% and 12.5% in High, Mix, Low and Control colonies, respectively.

B.2 Model fitting

Figure 24 shows model fit parabolas

Best-fit estimate of q_h : 0.663463 1 SD confidence interval [0.6427357 , 0.6852647] Best-fit estimate of β : 0.005755989 1 SD confidence interval [0.005669123 , 0.005834892] Best-fit estimate of σ_h : 0.002053488 1 SD confidence interval [0.001712935 , 0.002462578]

B.3 Sensitivity

Figure 25 shows sensitivity lines

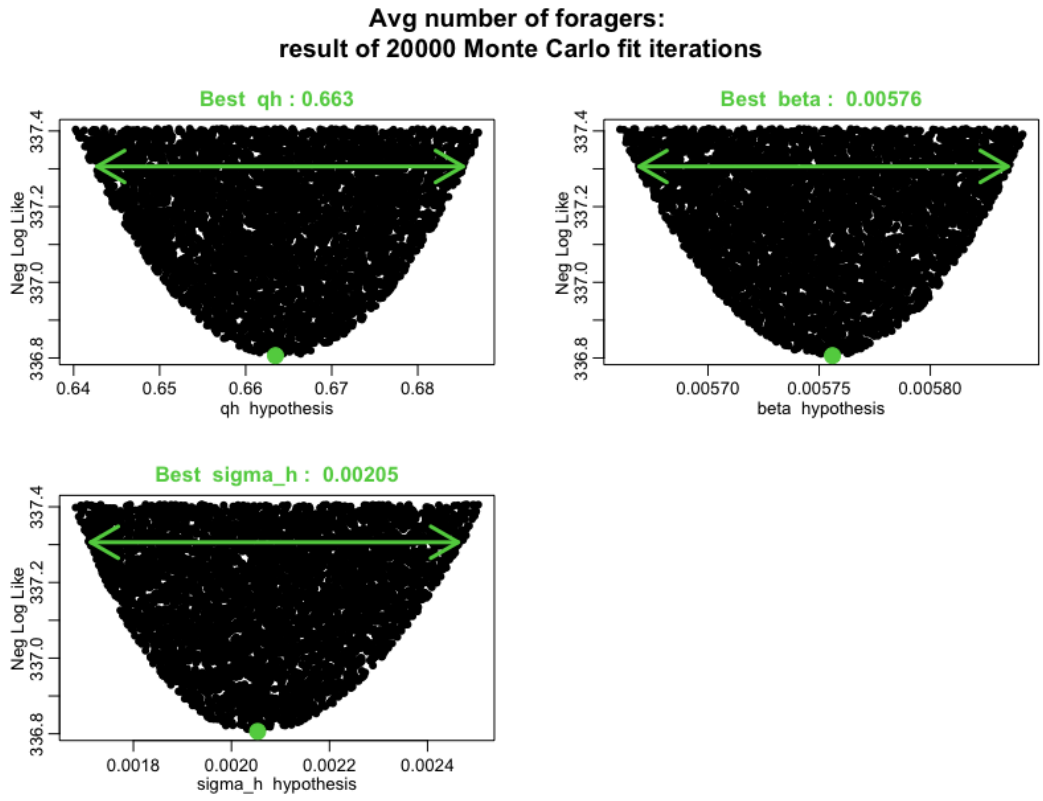

Figure 24. Results from the Graphical Monte-Carlo method for fitting the model to the time-series data.

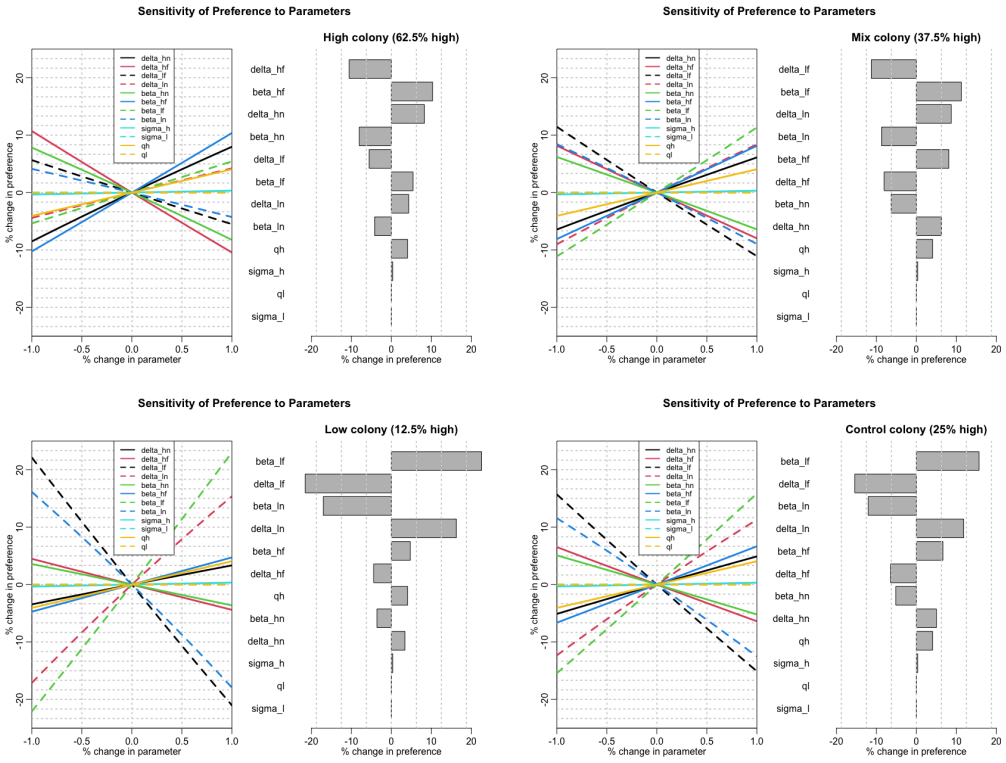

Figure 25. Sensitivity analysis for the four High LI proportions studied. All parameters were perturbed by 1% and the percent change in preference (measured as the difference between the total number of visits to the familiar and novel feeders after 6 hours of simulation). Left panels show the linearity of the preference with respect to the parameters in the range of the perturbation.

APPENDIX C

SUPPLEMENTARY MATERIAL FOR CHAPTER 4

C.1 Summary of System Dynamics

Table 5 summarizes the dynamics of Full System ((4.5)).

C.2 Mathematical Proofs

C.2.1 Proof of Theorem 4.3.1 (Basic Dynamical Properties)

Theorem. (Basic Dynamical Properties) *Model* ((4.5)) *is positive invariant and bounded in* $\mathbb{R}^4_+$

Proof. If $(W, G, w, g) \in \mathbb{R}^4_+$, then

$$\begin{aligned}
\frac{dW}{dt}\Big|_{W=0} &= \Lambda \frac{w^2}{b^2 + w^2}\rho \geq 0 \\
\frac{dG}{dt}\Big|_{G=0} &= \frac{1}{\tau}W \geq 0 \\
\frac{dw}{dt}\Big|_{w=0} &= \Lambda \frac{W^2}{b^2 + W^2}(1-\rho) \geq 0 \\
\frac{dg}{dt}\Big|_{g=0} &= \left[\frac{G}{P} \leq \theta\right]\delta w = \begin{cases} 0\ , \ \frac{G}{P} > \theta, \\ \delta w\ , \ \frac{G}{P} \leq \theta \end{cases} \geq 0,
\end{aligned}$$

because all parameter values are nonnegative and $0 \leq \rho \leq 1$. It follows that Model ((4.5)) is positive invariant in $\mathbb{R}^4_+$ by Theorem A.4 from Thieme (2018).

To show boundedness, we first prove that W is bounded:

$$\frac{dW}{dt} = \Lambda \frac{(W+w)^2}{b^2 + (W+w)^2}\rho - \frac{1}{\tau}W \leq \Lambda\rho - \frac{1}{\tau}W.$$

This yields

$$\limsup_{t\to\infty} W \leq \Lambda\rho\tau.$$

Now let $V = W + G + w + g$ and $\mu = \min\{\mu_G, \mu_w, \mu_g\}$. Then we have

$$\begin{aligned}
\frac{dV}{dt} &= \Lambda \frac{(W+w)^2}{b^2 + (W+w)^2} - (\mu_G G + \mu_w w + \mu_g g) \\
&\leq \Lambda - \mu V + \mu W \leq \Lambda + \mu\Lambda\rho\tau - \mu V,
\end{aligned}$$

which gives $\limsup_{t\to\infty} V \leq \Lambda/\mu + \Lambda\rho\tau$.

□

Non-Crisis Mode without Replacement $\theta < \frac{G^*+g^*}{P^*} = \frac{\rho\mu_w}{\mu_G(1-\rho)+\rho\mu_w(1+\mu_G\tau)}$			
	Extinction	Interior	
	E^e	E_+	E_-
W^*	0	$\frac{1}{2}\left(\Lambda\rho\tau+\sqrt{(\Lambda\rho\tau)^2-\left(\frac{2b\tau\mu_w}{\frac{1-\rho}{\rho}+\tau\mu_w}\right)^2}\right)$	$\frac{1}{2}\left(\Lambda\rho\tau-\sqrt{(\Lambda\rho\tau)^2-\left(\frac{2b\tau\mu_w}{\frac{1-\rho}{\rho}+\tau\mu_w}\right)^2}\right)$
G^*	0	$\frac{1}{\tau\mu_G}W^*$	$\frac{1}{\tau\mu_G}W^*$
w^*	0	$\frac{(1-\rho)}{\rho\tau\mu_w}W^*$	$\frac{(1-\rho)}{\rho\tau\mu_w}W^*$
g^*	0	0	0
E.C.	None	$\frac{\Lambda}{2b}(\rho\tau+(1-\rho)\frac{1}{\mu_w})\geq 1$	
L.S.	Stable	Stable	Unstable
Crisis Mode with Replacement $\theta \geq \frac{G^*+g^*}{P^*} = \frac{\rho\left(\mu_w+\delta\right)+\mu_G(1-\rho)\frac{\delta}{\mu_g}}{\mu_G(1-\rho)\left(\frac{\delta}{\mu_g}+1\right)+\rho\left(\mu_w+\delta\right)\left(1+\tau\mu_G\right)}$			
	Extinction	Interior	
	E^e	E_+	E_-
W^*	0	$\frac{1}{2}\left(\Lambda\rho\tau+\sqrt{(\Lambda\rho\tau)^2-\left(\frac{2b\tau(\mu_w+\delta)}{\frac{1-\rho}{\rho}+\tau(\mu_w+\delta)}\right)^2}\right)$	$\frac{1}{2}\left(\Lambda\rho\tau-\sqrt{(\Lambda\rho\tau)^2-\left(\frac{2b\tau(\mu_w+\delta)}{\frac{1-\rho}{\rho}+\tau(\mu_w+\delta)}\right)^2}\right)$
G^*	0	$\frac{1}{\tau\mu_G}W^*$	$\frac{1}{\tau\mu_G}W^*$
w^*	0	$\frac{(1-\rho)}{\rho\tau(\mu_w+\delta)}W^*$	$\frac{(1-\rho)}{\rho\tau(\mu_w+\delta)}W^*$
g^*	0	$\frac{\delta(1-\rho)}{\mu_g\rho\tau(\mu_w+\delta)}W^*$	$\frac{\delta(1-\rho)}{2\mu_g\rho\tau(\mu_w+\delta)}W^*$
E.C.	None	$\frac{\Lambda}{2b}(\rho\tau+(1-\rho)\frac{1}{\mu_w+\delta})\geq 1$	
L.S.	Stable	Stable	Unstable
Sliding Mode $\gamma_b < \theta < \gamma_c$			
		E_+^p	E_-^p
W^*		$\frac{1}{2}\rho\tau\left(\Lambda+\sqrt{\Lambda^2-\left(\frac{2b\mu_G(\theta\mu_g+(1-\theta)\mu_w)}{(1-\theta)(\mu_G(1-\rho)+\mu_g\rho+\mu_G\mu_w\rho\tau)}\right)^2}\right)$	$\frac{1}{2}\rho\tau\left(\Lambda-\sqrt{\Lambda^2-\left(\frac{2b\mu_G(\theta\mu_g+(1-\theta)\mu_w)}{(1-\theta)(\mu_G(1-\rho)+\mu_g\rho+\mu_G\mu_w\rho\tau)}\right)^2}\right)$
G^*		$\frac{1}{\tau\mu_G}W^*$	$\frac{1}{\tau\mu_G}W^*$
w^*		$\frac{(1-\theta)(\mu_G(1-\rho)-\mu_g\rho)+\theta\mu_G\mu_g\rho\tau)}{\mu_G\rho\tau(\theta\mu_g+\mu_w(1-\theta))}W^*$	$\frac{(1-\theta)(\mu_G(1-\rho)-\mu_g\rho)+\theta\mu_G\mu_g\rho\tau)}{\mu_G\rho\tau(\theta\mu_g+\mu_w(1-\theta))}W^*$
g^*		$\frac{-\mu_w\rho+\theta(\mu_G(1-\rho)+\mu_w\rho(1+\mu_G\tau))}{\mu_G\rho\tau(\theta\mu_g+\mu_w(1-\theta))}W^*$	$\frac{-\mu_w\rho+\theta(\mu_G(1-\rho)+\mu_w\rho(1+\mu_G\tau))}{\mu_G\rho\tau(\theta\mu_g+\mu_w(1-\theta))}W^*$
E.C.		$\frac{\Lambda}{2b}\frac{(1-\theta)(\mu_g\rho+\mu_G(1-\rho)+\mu_G\mu_w\tau\rho)}{\mu_G(\theta\mu_g+\mu_w(1-\theta))}\geq 1$	
L.S.		Stable*	Unstable*

Table 5. Summary of the model's dynamics: Equilibrium points for the non-crisis and crisis modes (i.e., without and with guard replacement by minors), including existence conditions (E.C) and local stability (L.S.). *The local stability of the pseudoequilibria $E_\pm^p$ was shown only numerically, not analytically.

C.2.2 Proof of Theorem 4.3.2 (Extinction equilibrium)

Theorem. *Model* ((4.5)) *always has the extinction equilibrium*

$$E^e := (W^*, G^*, w^*, g^*) = (0, 0, 0, 0),$$

which is locally stable. If $\mu_u = \min\{1/\tau, \mu_w\}$ *and* $\Lambda < 2\mu_u b$*, then* E^e *is globally stable.*

Proof. When the population is zero, $W = w = G = g = 0$ and

$$\frac{dW}{dt} = \frac{dw}{dt} = \frac{dG}{dt} = \frac{dg}{dt} = 0.$$

This means that the system has an extinction equilibrium

$$E^e := (W^*, G^*, w^*, g^*) = (0, 0, 0, 0).$$

We can analyze the stability of this point by studying the linearized system near the origin. It is necessary to evaluate two cases of the Jacobian matrix, one for each case of $[\frac{G+g}{P} \leq \theta]$. The Jacobian matrix of the system can be reduced to

$$\begin{pmatrix} \frac{2b^2W^*}{\tau} - \frac{1}{\tau} & 0 & \frac{2b^2W^*}{\tau} & 0 \\ \frac{1}{\tau} & -\mu_G & 0 & 0 \\ \frac{2b^2(1-\rho)W^*}{\rho\tau} & 0 & \frac{2b^2(1-\rho)W^*}{\rho\tau} - \mu_w & 0 \\ 0 & 0 & 0 & -\mu_g \end{pmatrix}$$

when $\frac{G+g}{P} \leq \theta$, and

$$\begin{pmatrix} \frac{2b^2W^*}{\tau} - \frac{1}{\tau} & 0 & \frac{2b^2W^*}{\tau} & 0 \\ \frac{1}{\tau} & -\mu_G & 0 & 0 \\ \frac{2b^2(1-\rho)W^*}{\rho\tau} & 0 & \frac{2b^2(1-\rho)W^*}{\rho\tau} - \mu_w - \delta & 0 \\ 0 & 0 & \delta & -\mu_g \end{pmatrix}$$

when $\frac{G+g}{P} > \theta$. Evaluating at E^e, we get

$$\begin{pmatrix} -\frac{1}{\tau} & 0 & 0 & 0 \\ \frac{1}{\tau} & -\mu_G & 0 & 0 \\ 0 & 0 & -\mu_w & 0 \\ 0 & 0 & 0 & -\mu_g \end{pmatrix} \text{ and } \begin{pmatrix} -\frac{1}{\tau} & 0 & 0 & 0 \\ \frac{1}{\tau} & -\mu_G & 0 & 0 \\ 0 & 0 & -\mu_w - \delta & 0 \\ 0 & 0 & \delta & -\mu_g \end{pmatrix}$$

respectively. The eigenvalues of these matrices are

$$\left\{-\frac{1}{\tau}, -\mu_g, -\mu_G, -\mu_w\right\} \text{ and } \left\{-\frac{1}{\tau}, -\mu_g, -\mu_G, -\mu_w - \delta\right\}$$

which are all negative values. This means that the zero equilibrium is locally stable, regardless of the value of $\frac{G+g}{P}$ in its vicinity.

Now assume that $\Lambda < 2\mu_u b$ for $\mu_u = \min\{1/\tau, \mu_w\}$. We will show that E^e is globally asymptotically stable.

Let

$$u = W + w.$$

Then

$$\begin{aligned}\frac{du}{dt} &= \Lambda\frac{(W+w)^2}{b^2+(W+w)^2} - W/\tau - \mu_w w \\ &< \Lambda\frac{u^2}{b^2+u^2} - \mu_u u = u\frac{\Lambda u - \mu_u(b^2+u^2)}{b^2+u^2} \\ &= \mu_u u\frac{\phi}{b^2+u^2}\end{aligned}$$

for

$$\phi = -\left(u - \frac{\Lambda}{2\mu_u}\right)^2 + \frac{\left(\frac{\Lambda}{\mu_u}\right)^2 - 4b^2}{4}.$$

Because $\Lambda/\mu_u < 2b$, ϕ is negative. Therefore, both W and w collapse to zero if $\Lambda/\mu_u < 2b$. In this case,

$$\frac{dG}{dt} = -\mu_G G \text{ and } \frac{dg}{dt} = -\mu_g g.$$

Therefore, G and g also collapse to extinction. This completes the proof. □

C.2.3 Proof of Theorem 4.3.3 (Existence and Stability of the Crisis Interior Equilibria)

Theorem. *Define condition*

$$C_c : \frac{\Lambda}{2b}\left(\rho\tau + (1-\rho)\frac{1}{\mu_w+\delta}\right) \geq 1.$$

Then the Crisis System defined by F_{S_c} ((4.6)) has two interior equilibria, E^c_+ and E^c_-, if and only if C_c holds. Both have the form

$$(W^*, G^*, w^*, g^*) = (W^*, \frac{1}{\tau\mu_G}W^*, \frac{1-\rho}{\rho\tau(\mu_w+\delta)}W^*, \frac{\delta}{\mu_g}\frac{1-\rho}{\rho\tau(\mu_w+\delta)}W^*)$$

where

$$W^* = \frac{1}{2}\left(\Lambda\rho\tau \pm \sqrt{(\Lambda\rho\tau)^2 - \left(\frac{2b(\mu_w+\delta)\tau}{\frac{1-\rho}{\rho}+(\mu_w+\delta)\tau}\right)^2}\right) \tag{C.1}$$

Moreover,

1. *The interior equilibrium E_+^c is Locally Asymptotically Stable, and E_-^c is unstable.*
2. *Both E_+^c and E_-^c are* regular *equilibria of the Full System* ((4.5)) *if and only if*

$$\gamma_c < \theta$$

for γ_c defined in Equation ((4.10)).

Proof. From relations ((4.9)), each equilibrium of System ((4.6)) takes the form:

$$(W^*, G^*, w^*, g^*) = (W^*, \frac{1}{\tau\mu_G}W^*, \frac{1-\rho}{\rho\tau(\mu_w+\delta)}W^*, \frac{\delta}{\mu_g}\frac{1-\rho}{\rho\tau(\mu_w+\delta)}W^*).$$

Furthermore, the value of W^* in an interior equilibrium of the System ((4.6)) must be a root of Equation ((4.11)), which can be rearranged as:

$$f(W^*) = W^{*2} - \Lambda\tau\rho W^* + (\frac{b(\mu_w+\delta)\tau}{\frac{1-\rho}{\rho}+(\mu_w+\delta)\tau})^2.$$

with all parameters being positive and finite, and that root must be positive by Theorem 4.3.1. It follows that there are at most two interior equilibria, E_+^c and E_-^c, and those equilibria are such that:

$$W^* = \frac{1}{2}\left(\Lambda\rho\tau \pm \sqrt{\underbrace{(\Lambda\rho\tau)^2 - (\frac{2b(\mu_w+\delta)\tau}{\frac{1-\rho}{\rho}+(\mu_w+\delta)\tau})^2}_{*}}\right),$$

Thus condition C_c of this theorem, equivalent to the discriminant ($*$ above) being positive, holds if and only if the two positive, real roots described by ((C.3)) exist.

1. We study the local stability of the equilibrium points using the Jacobian matrix J of the linearized system in their vicinity. From System ((4.6)), we get

$$J = \begin{pmatrix} \frac{2b^2\Lambda\rho(w+W)}{\left(b^2+(w+W)^2\right)^2} - \frac{1}{\tau} & 0 & \frac{2b^2\Lambda\rho(w+W)}{\left(b^2+(w+W^*)^2\right)^2} & 0 \\ \frac{1}{\tau} & -\mu_G & 0 & 0 \\ -\frac{2b^2\Lambda(\rho-1)(w^*+W^*)}{\left(b^2+(w^*+W^*)^2\right)^2} & 0 & -\frac{2b^2\Lambda(\rho-1)(w\ +W\ )}{\left(b^2+(w\ +W\ )^2\right)^2} - \mu_w - \delta & 0 \\ 0 & 0 & \delta & -\mu_g \end{pmatrix}.$$

From the characteristic polynomial, and using Equations ((4.6)) to obtain an equation in terms of W, it follows that the eigenvalues of J satisfy the equation

$$(\mu_g+\lambda)(\mu_G+\lambda)\left(\lambda^2+\lambda B+C\right)$$

where

$$\begin{aligned} B :=& \frac{1}{\tau}+\mu_w+\delta-h, \\ =& \frac{W}{(W+w)\left(b^2+(W+w)^2\right)\tau\rho}\left(\rho\frac{w}{W}\left(b^2+(W+w)^2\right)\right. \\ & \left. +(1-\rho)\frac{W}{w}\left(b^2+(W+w)^2\right)+(W+w+b)(W+w-b)\right), \\ C :=& \frac{1}{\tau}(\mu_w+\delta)-\rho h(\mu_w+\delta)-\frac{1}{\tau}(1-\rho)h, \\ =& \frac{\frac{(\mu_w+\delta)}{\tau}W}{b^2+(W+w)^2}f'(W), \end{aligned}$$

where $h = \frac{2b^2\Lambda(W+w)}{\left(b^2+(W+w)^2\right)^2}$. This yields the two negative eigenvalues $-\mu_g$ and $-\mu_G$, and two additional ones, λ_+ and λ_-, that satisfy a quadratic equation. Define the sum and product of λ_+ and λ_- as

$$\Pi := \lambda_+\lambda_- = C$$
$$\Sigma := \lambda_+ + \lambda_- = -B.$$

With this terminology, we analyze the sign of λ_+ and λ_- for each of the interior equilibria E_+^c and E_-^c.
From the existence condition of equilibrium we have that

$$W + w - b = \frac{1}{2}\left(1 + \frac{1-\rho}{\tau\rho(\mu_w+\delta)}\right)\sqrt{(\Lambda\rho\tau)^2 - \left(\frac{2b(\mu_w+\delta)\tau}{\frac{1-\rho}{\rho} + (\mu_w+\delta)\tau}\right)^2}$$
$$+ \frac{1}{2}\left(1 + \frac{1-\rho}{\tau\rho(\mu_w+\delta)}\right)\tau\rho\Lambda - b > 0.$$

Thus, we have $B > 0$. Because $g'(W) < 0$ at equilibrium E^c_- and $g'(W) > 0$ at equilibrium E^c_+, then we have $C|_{E^c_-} < 0$ and $C|_{E^c_+} > 0$. According to the Routh–Hurwitz condition, we can get that E^c_- is always unstable and E^c_+ is locally asymptotically stable.

2. By Definition 4.3.1, Z^* is a regular equilibrium of System ((4.5)) iff $F_{S_c}(Z^*) = 0$, $H(Z^*) < 0$ or $F_{S_b}(Z^*) = 0$, $H(Z^*) > 0$, with F_{S_c} and F_{S_b} defined in Equations ((4.6)) and ((4.7)), and $H(Z) = (G + g) - \theta P$. By construction,

$$F_{S_c}(E^c_+) = F_{S_c}(E^c_-) = 0.$$

Moreover, note that both E^c_- and E^c_+ have the same guard ratio $\dfrac{G^* + g^*}{P^*}$, defined as γ_c in Equation ((4.10)). It follows that

$$H(E^c_-) < 0 \iff H(E^c_+) < 0 \iff \gamma_c < 0.$$

Thus, both E^c_- and E^c_+ are regular equilibria of System ((4.5)) iff $\gamma_c < \theta$.

□

C.2.4 Proof of Theorem 4.3.4 (Existence and Stability of the Non-Crisis Interior Equilibria)

Theorem. *Define condition*

$$C_b : \frac{\Lambda}{2b}\left(\rho\tau + (1-\rho)\frac{1}{\mu_w}\right) \geq 1. \tag{C.2}$$

Then the Non-Crisis System defined by F_{S_b} ((4.7)) has two interior equilibria $E^b_+ = E^c_+|_{\delta=0}$ and $E^b_- = E^c_-|_{\delta=0}$ if and only if C_b holds.

Moreover,

1. *The interior equilibrium E^b_+ is Locally Asymptotically Stable, while E^b_- is unstable.*

2. *Both* E_+^b *and* E_-^b *are* regular *equilibria of the Full System* ((4.5)) *if and only if*

$$\gamma_b > \theta$$

for γ_b *defined in Equation* ((4.14)).

Proof. The Non-Crisis System F_{S_b} ((4.7)) is identical to the Crisis System F_{S_c} ((4.6)) when $\delta = 0$. Thus, following the same analysis as the previous proof in Section C.2.3 in the special case $\delta = 0$, we get that F_{S_b} ((4.7)) has two positive, real equilibria E_+^b and E_-^b, of the form

$$(W^*, G^*, w^*, g^*) = (W^*, \frac{1}{\tau\mu_G}W^*, \frac{1-\rho}{\rho\tau\mu_w}W^*, 0)$$

with

$$W^* = \frac{1}{2}\left(\Lambda\rho\tau \pm \sqrt{\underbrace{(\Lambda\rho\tau)^2 - \left(\frac{2b\mu_w\tau}{\frac{1-\rho}{\rho} + \mu_w\tau}\right)^2}_{*}}\right). \tag{C.3}$$

if and only if the discriminant ($*$ above) is guaranteed to be positive or, equivalently, condition C_b of this theorem holds.

1. We study the local stability of the equilibrium points using the Jacobian matrix J of the linearized system in their vicinity. From System ((4.7)), we get

$$J = \begin{pmatrix} \frac{2b^2\Lambda\rho(w+W)}{(b^2+(w+W)^2)^2} - \frac{1}{\tau} & 0 & \frac{2b^2\Lambda\rho(w+W)}{(b^2+(w+W^*)^2)^2} & 0 \\ \frac{1}{\tau} & -\mu_G & 0 & 0 \\ -\frac{2b^2\Lambda(\rho-1)(w^*+W^*)}{(b^2+(w^*+W^*)^2)^2} & 0 & -\frac{2b^2\Lambda(\rho-1)(w\ +W\ )}{(b^2+(w\ +W\ )^2)^2} - \mu_w & 0 \\ 0 & 0 & 0 & -\mu_g \end{pmatrix}.$$

From the characteristic polynomial, it follows that the eigenvalues of J are roots of

$$(\mu_g + \lambda)(\mu_G + \lambda)\left(\lambda^2 + \lambda B + C\right) = 0$$

where

$$\begin{aligned}
B :=& \frac{1}{\tau} + \mu_w - h, \\
=& \frac{W}{(W+w)\left(b^2+(W+w)^2\right)\tau\rho} \left(\rho \frac{w}{W} \left(b^2+(W+w)^2\right) \right. \\
& \left. + (1-\rho)\frac{W}{w}\left(b^2+(W+w)^2\right) + (W+w+b)(W+w-b) \right), \\
C :=& \frac{\mu_w}{\tau} - \mu_w \rho h - \frac{1}{\tau}(1-\rho)h, \\
=& \frac{\frac{\mu_w}{\tau} W}{b^2+(W+w)^2} f'(W),
\end{aligned}$$

and $h = (2b^2\Lambda(W+w))/(b^2+(W+w)^2)^2$. Consequently, there are two negative eigenvalues $-\mu_g$ and $-\mu_G$, and two additional ones, λ_+ and λ_-, that satisfy a quadratic equation. Define the sum and product of λ_+ and λ_- as

$$\Pi := \lambda_+ \lambda_- = C$$

$$\Sigma := \lambda_+ + \lambda_- = -B.$$

With this terminology, we analyze the sign of λ_+ and λ_- for each of the interior equilibria E_+^b and E_-^b.
From the existence condition C_b, we have that

$$W + w - b = \frac{1}{2}\left(1 + \frac{1-\rho}{\tau\rho\mu_w}\right) \sqrt{(\Lambda\rho\tau)^2 - \left(\frac{2b\mu_w\tau}{\frac{1-\rho}{\rho} + \mu_w\tau}\right)^2} + \frac{1}{2}\left(1 + \frac{1-\rho}{\tau\rho\mu_w}\right)\tau\rho\Lambda - b > 0.$$

Thus, we have $B > 0$. Because $f'(W) < 0$ at equilibrium E_-^b and $f'(W) > 0$ at equilibrium E_+^b, then we have $C|_{E_-^b} < 0$ and $C|_{E_+^b} > 0$. According to Routh–Hurwitz condition, we get that E_-^b is always unstable and E_+^b is locally asymptotically stable. This completes this proof.

2. By Definition 4.3.1, Z^* is a regular equilibrium of System ((4.5)) iff $F_{S_c}(Z^*) = 0$, $H(Z^*) < 0$ or $F_{S_b}(Z^*) = 0$, $H(Z^*) > 0$, with F_{S_c} and F_{S_b} defined in Equations ((4.6)) and ((4.7)), and $H(Z) = (G+g) - \theta P$. By construction,

$$F_{S_b}(E_+^b) = F_{S_b}(E_-^b) = 0.$$

Moreover, note that both E_-^b and E_+^b have the same guard ratio $\dfrac{G^*+g^*}{P^*}$, defined as γ_b in Equation ((4.14)). It follows that

$$H(E_-^b) < 0 \iff H(E_+^b) < 0 \iff \gamma_b < 0.$$

Thus, both E_-^b and E_+^b are regular equilibria of System ((4.5)) iff $\gamma_b > \theta$.

□

C.2.5 Proof of Theorem 4.3.6 (Existence of Pseudoequilibria)

Theorem. *Define condition*

$$C_p : \frac{\Lambda}{2b}\frac{(1-\theta)(\mu_g\rho + \mu_G(1-\rho) + \mu_G\mu_w\tau\rho)}{\mu_G(\theta\mu_g + \mu_w(1-\theta))} \geq 1.$$

Then System ((4.5)) *has two pseudoequilibria E_+^p and E_-^p on the switching surface Σ if and only if C_p holds and $\gamma_b \leq \theta < \gamma_c$. The pseudoequilibria have the form*

$$(W^*, G^*, g^*, w^*) = \left(W^*, \frac{1}{\tau\mu_G}W^*, \frac{(1-\theta)(\mu_G(1-\rho) - \mu_g\rho) + \theta\mu_G\mu_g\rho\tau)}{\mu_G\rho\tau(\theta\mu_g + \mu_w(1-\theta))}W^*, \right.$$
$$\left. \frac{-\mu_w\rho + \theta(\mu_G(1-\rho) + \mu_w\rho(1+\mu_G\tau))}{\mu_G\rho\tau(\theta\mu_g + \mu_w(1-\theta))}W^*\right)$$

with

$$W^*|_{E_\pm^p} = \frac{1}{2}\rho\tau\left(\Lambda \pm \sqrt{\Lambda^2 - \left(\frac{2b\mu_G(\theta\mu_g + (1-\theta)\mu_w)}{(1-\theta)(\mu_G(1-\rho) + \mu_g\rho + \mu_G\mu_w\rho\tau)}\right)^2}\right)$$

Proof. From relations ((4.20)), any pseudoequilibrium of System ((4.5)) must take the form:

$$(W^*, G^*, g^*, w^*) = (W^*, \frac{1}{\tau\mu_G}W^*, \frac{1-\rho}{\rho\tau(\mu_w + \delta(1-\lambda^*))}W^*, \frac{\delta(1-\lambda^*)(1-\rho)}{\mu_g\rho\tau(\mu_w + \delta(1-\lambda^*))}W^*)$$

Recall the value of λ^* in Equation ((4.22))

$$\lambda^* = \frac{\mu_G\mu_g\theta(\delta\tau\rho + 1 - \rho + \mu_w\rho\tau) - (1-\theta)(\delta(\mu_G(1-\rho) + \mu_g\rho) + \mu_g\mu_w\rho)}{\delta(\mu_G\mu_g\rho\tau\theta - (1-\theta)(\mu_G(1-\rho) + \mu_g\rho))} \tag{C.4}$$

First, note that $\lambda^* \in [0,1] \iff \gamma_b \leq \theta \leq \gamma_c$. In fact, the equation for λ^* can be rearranged as a function of θ as

$$\lambda^*(\theta) = \frac{-A + \theta B}{\delta\,(C + \theta D)} \tag{C.5}$$

with

$$A = \delta(\mu_G(1-\rho) + \mu_g\rho) + \mu_g\mu_w\rho$$
$$B = \delta(\mu_G(1-\rho) + \mu_g\rho(1+\mu_G\tau)) + \mu_g(\mu_G(1-\rho) + \mu_w\rho(1+\mu_G\tau))$$
$$C = -\mu_G(1-\rho) + \mu_g\rho$$
$$D = \mu_G(1-\rho) + \mu_g\rho(1+\mu_G\tau).$$

This is a monotonically decreasing hyperbola, since the derivative

$$\frac{\partial \lambda^*}{\partial \theta} = \frac{-\mu_g \mu_G (1-\rho)\left(\mu_G(1-\rho) + \mu_g \rho + \mu_G \mu_w \rho \tau\right)}{\delta^2 \left(-(1-\theta)\mu_g \rho + \mu_G(-(1-\rho) + \theta(1-\rho+\mu_g \rho \tau))\right)^2}$$

is negative for all θ except at the vertical asymptote, where it is undefined. Furthermore, the hyperbola has a horizontal asymptote at

$$1 + \frac{\mu_g \left(\mu_G(1-\rho) + \mu_w \rho(1+\mu_G \tau)\right)}{\delta \left(\mu_G(1-\rho) + \mu_g \rho(1+\mu_G \tau)\right)} > 1.$$

Moreover, $\theta = \gamma_b \implies \lambda^* = 1$ and $\theta = \gamma_c \implies \lambda^* = 0$. Thus,

$$\lambda^* \in [0,1] \iff \gamma_b \leq \theta \leq \gamma_c$$

By substituting the value of λ^* from Equation ((4.22)), we get the form

$$(W^*, G^*, g^*, w^*) = \Bigg(W^*, \frac{1}{\tau \mu_G} W^*, \frac{(1-\theta)(\mu_G(1-\rho) - \mu_g \rho) + \theta \mu_G \mu_g \rho \tau)}{\mu_G \rho \tau (\theta \mu_g + \mu_w(1-\theta))} W^*, \\ \frac{-\mu_w \rho + \theta(\mu_G(1-\rho) + \mu_w \rho(1+\mu_G \tau))}{\mu_G \rho \tau (\theta \mu_g + \mu_w(1-\theta))} W^* \Bigg)$$

Furthermore, the value of W^* must be a root of

$$f(W^*) = W^{*2} - \Lambda \tau \rho W^* + \Big(\frac{b(\mu_w + \delta(1-\lambda^*))\tau}{\frac{1-\rho}{\rho} + (\mu_w + \delta(1-\lambda^*))\tau}\Big)^2$$

with all parameters being positive and finite, and that root must be positive by Theorem 4.3.1. This yields the existence condition

$$C_p : \frac{\Lambda}{2b}\Big(\rho\tau + (1-\rho)\frac{1}{\mu_w + \delta(1-\lambda^*)}\Big) \geq 1$$

Substituting λ^* again from ((4.22)), it follows that there are at most two pseudoequilibria, E_+^p and E_-^p, such that

$$W^*|_{E_\pm^p} = \frac{1}{2}\rho\tau \left(\Lambda \pm \sqrt{\Lambda^2 - \left(\frac{2b\mu_G(\theta\mu_g + (1-\theta)\mu_w)}{(1-\theta)(\mu_G(1-\rho) + \mu_g \rho + \mu_G \mu_w \rho \tau)} \right)^2} \right)$$

Now assume that $\gamma_b \leq \theta < \gamma_c$. We will show that E_+^p and E_-^p lay on the sliding set $\Sigma_s \subseteq \Sigma$. That is, we will demonstrate $\sigma(E_\pm^p) \leq 0$, for the function σ defined in ((4.17)). In fact,

$$\sigma(E_{\pm}^{p}) = \phi \frac{\left(\Lambda \pm \sqrt{\Lambda^2 - \left(\frac{2b\mu_G(\theta(\mu_g - \mu_w) + \mu_w)}{(1-\theta)(\mu_G + \mu_g\rho + \mu_G\rho(-1 + \mu_w\tau)}\right)^2}\right)^2}{4\mu_G^2(\theta(\mu_g - \mu_w) + \mu_w)^2}$$

with

$$\begin{aligned}
\phi := \\
&\theta^2\Big(\delta\rho\mu_g\left(\mu_G + \rho\mu_G\left(\tau\mu_w - 1\right) + \rho\mu_w\right) + \delta\rho\mu_G\left(\tau\mu_g - 1\right)\left(\mu_G + \rho\mu_G\left(\tau\mu_w - 1\right) + \rho\mu_w\right) \\
&\quad + \mu_g\left(\mu_G + \rho\mu_G\left(\tau\mu_w - 1\right) + \rho\mu_w\right)^2 + \delta\mu_G\left(\mu_G + \rho\mu_G\left(\tau\mu_w - 1\right) + \rho\mu_w\right)\Big) \\
&+ \theta\Big(-\delta\rho^2\mu_G\mu_w\left(\tau\mu_g - 1\right) - \delta\rho\mu_g\Big(\mu_G + \rho\mu_G\left(\tau\mu_w - 1\right) + \rho\mu_w\Big) \\
&\quad - 2\rho\mu_g\mu_w\left(\mu_G + \rho\mu_G\left(\tau\mu_w - 1\right) + \rho\mu_w\right) - \delta\rho^2\mu_g\mu_w \\
&\quad + \delta\rho\mu_G\left(\mu_G + \rho\mu_G\left(\tau\mu_w - 1\right) + \rho\mu_w\right) \\
&\quad - \delta\mu_G\left(\mu_G + \rho\mu_G\left(\tau\mu_w - 1\right) + \rho\mu_w\right) - \delta\rho\mu_G\mu_w\Big) \\
&+ \delta\rho^2\mu_g\mu_w + \rho^2\mu_g\mu_w^2 - \delta\rho^2\mu_G\mu_w + \delta\rho\mu_G\mu_w
\end{aligned}$$

It follows that $\sigma(E_{\pm}^{p}) \leq 0 \iff \phi \leq 0$. Therefore, we examine the sign of ϕ. As a function of θ, $\phi(\theta)$ is a parabola with two positive roots γ_b and γ_c. Moreover,

$$\phi(0) = \delta\rho^2\mu_g\mu_w + \rho^2\mu_g\mu_w^2 + \delta\rho\mu_G\mu_w(1-\rho) \geq 0$$

so the parabola has a positive intercept and two positive roots. Then it must be negative between its roots, that is, $\phi(\theta) \leq 0$ for $\gamma_b \leq \theta \leq \gamma_c$. Therefore, E_{-}^{p} and E_{+}^{p} belong to the sliding set Σ_s.

We have shown that E_{-}^{p} and E_{+}^{p} are indeed pseudoequilibria when $\gamma_b \leq \theta \leq \gamma_c$ and condition C_p holds. We can also see that, should any of these conditions fail to hold, there are no pseudoequilibria. In fact, if $\theta < \gamma_b$ or $\theta > \gamma_c$, then $\lambda^* \notin [0,1]$ and E_{-}^{p} and E_{+}^{p} do not lay on the sliding segment Σ_s, and if C_p is false then E_{-}^{p} and E_{+}^{p} are not real values. This completes the proof.

□

C.2.6 Proof of Theorem 4.3.5 (Characterization of the Equilibrium Guard Ratios)

Theorem. *The ratio*

$$\gamma_b = \frac{\rho\mu_w}{\mu_G(1-\rho) + \rho\mu_w(1 + \mu_G\tau)}$$

is monotonically increasing with respect to ρ, while the ratio

$$\gamma_c = \frac{\rho\left(\mu_w + \delta\right) + \mu_G(1-\rho)\frac{\delta}{\mu_g}}{\mu_G(1-\rho)\left(\frac{\delta}{\mu_g}+1\right) + \rho\left(\mu_w+\delta\right)\left(1+\tau\mu_G\right)}$$

is monotonically decreasing with respect to ρ if $\mu_g \leq \delta\tau\mu_G$ and monotonically increasing otherwise

Proof. 1. Consider the derivatives of γ_b and γ_c with respect to ρ:

$$\frac{\partial\gamma_b}{\partial\rho} = \frac{\mu_G\mu_w}{\left(\mu_G(1-\rho)+\rho\mu_w(1+\mu_G\tau)\right)^2} > 0$$

$$\frac{\partial\gamma_c}{\partial\rho} = \frac{\mu_g\mu_G\left(\delta+\mu_w\right)\left(\mu_g-\delta\tau\mu_G\right)}{\left(\mu_G(1-\rho)\left(\frac{\delta}{\mu_g}+1\right)+\rho\left(\mu_w+\delta\right)\left(1+\tau\mu_G\right)\right)^2}$$

$$\implies \begin{cases} \frac{\partial\gamma_c}{\partial\rho} \leq 0\ ,\ \mu_g \leq \delta\tau\mu_G \\ \frac{\partial\gamma_c}{\partial\rho} > 0\ ,\ \text{otherwise} \end{cases}.$$

Thus, both ratios are monotonic functions of ρ.

2. Moreover,

$$\frac{\rho\mu_w}{\mu_G(1-\rho)+\rho\mu_w(1+\mu_G\tau)} \leq \frac{\rho(\mu_w+\delta)+\mu_G(1-\rho)\delta/\mu_g}{\mu_G(1-\rho)(1+\delta/\mu_g)+\rho(\mu_w+\delta)(1+\tau\mu_G)}$$

$$\begin{aligned}\iff &\rho\mu_w\mu_G(1-\rho)(1+\delta/\mu_g)+\mu_w\rho^2(\mu_w+\delta)(1+\mu_G\tau) \\ &\leq (\rho(\mu_w+\delta)+\mu_G(1-\rho)\delta/\mu_g)(\mu_G(1-\rho)+\rho\mu_w(1+\mu_G\tau))\end{aligned}$$

After some manipulation, the last inequality can be reduced to

$$-\rho\mu_w\mu_G\tau\delta/\mu_g - \rho\delta - \mu_G(1-\rho)\delta/\mu_g \leq 0$$

which is always true. Therefore, $\gamma_b \leq \gamma_c$. Therefore, by the conditions on θ from Theorems 4.3.3–4.3.4, it follows that the Full System ((4.5)) can have at most one stable regular equilibrium.

This completes the proof. □

C.3 Parameter values for *T. angustula* stingless bees

General assumptions for stingless bee colonies:

- $\delta >> 1/\tau$: replacement by minors is a fast response mechanism and occurs at a faster rate than the natural maturation of majors into guards
- $\tau < 1/\mu_w$: maturation of majors is shorter than the average lifespan of minors
- $\mu_g > \mu_G$: minors are worst at defense, so they die sooner thank major guards
- $\rho << 1$: majors are the minority of the colony

Specific values found in literature, summarized in Table 4:

- The average guarding duration was estimated to be 5.4 $\pm$ 1.5 days Hammel et al. 2015; Grüter, Kärcher, and Ratnieks 2011
- The average age of guarding workers was 26.3 $\pm$ 3.3 days, and bees started guarding at 20 days of age Hammel et al. 2015
- Replacement guards are observed 5h after removing guards Baudier et al. 2019. That is, replacement occurs within 5 hours (δ is at least 4/day)
- The final age (last day a bee was seen in the hive) between the two size classes (majors: 27.85 $\pm$ 5.6 days; minors: 27.0 $\pm$ 8.4 days) does not differ Hammel et al. 2015. In another study, the average lifespan of bees was estimated to be 21 days Grüter, Kärcher, and Ratnieks 2011
- In a swarming colony estimated to have around 10,000 adults, the recently founded offspring colonies had between 500 and 1000 workers Van Veen and Sommeijer 2000
- The egg-laying rate by the queen was on average 6.41 eggs per hour in an observation period of 18 hours per day. Koedam, Brone, and Van Tienen 1997